

**VICTORIA UNIVERSITY**  
MELBOURNE AUSTRALIA

*Development of microporous substrates of polyamide thin film composite membranes for pressure-driven and osmotically-driven membrane processes: a review*

This is the Accepted version of the following publication

Lau, WJ, Lai, GS, Li, J, Gray, Stephen, Hu, Y, Misdan, N, Goh, PS, Matsuura, T, Azelee, IW and Ismail, AF (2019) Development of microporous substrates of polyamide thin film composite membranes for pressure-driven and osmotically-driven membrane processes: a review. *Journal of Industrial and Engineering Chemistry*, 77. pp. 25-59. ISSN 1226-086X

The publisher's official version can be found at  
<https://www.sciencedirect.com/science/article/pii/S1226086X1930231X>  
Note that access to this version may require subscription.

Downloaded from VU Research Repository <https://vuir.vu.edu.au/39142/>

# Development of Microporous Substrates of Polyamide Thin Film Composite Membranes for Pressure-driven and Osmotically-driven Membrane Processes

Woei-Jye Lau<sup>a,\*</sup>, Gwo-Sung Lai<sup>a</sup>, Jianxin Li<sup>b</sup>, Yunxia Hu<sup>b</sup>, Stephen Gray<sup>c</sup>, Nurasyikin Misdan<sup>d</sup>, Pei-Sean Goh<sup>a</sup>, Ihsan Wan Azelee<sup>a</sup>, Ahmad Fauzi Ismail<sup>a</sup>

<sup>a</sup>Advanced Membrane Technology Research Centre (AMTEC), School of Chemical and Energy Engineering, Universiti Teknologi Malaysia, 81310 Skudai, Johor, Malaysia

<sup>b</sup>State Key Laboratory of Separation Membranes and Membrane Processes, School of Materials Science and Engineering, Tianjin Polytechnic University, Tianjin 300387, China

<sup>c</sup>Institute for Sustainable Industries & Liveable Cities, Victoria University, Werribee Campus, PO Box 14428, Melbourne, VIC 8001, Australia

<sup>d</sup>Faculty of Engineering Technology, Universiti Tun Hussein Onn Malaysia, 86400 Parit Raja, Johor, Malaysia

\*Corresponding author: [lwoeijye@utm.my](mailto:lwoeijye@utm.my); [lau\\_woeijye@yahoo.com](mailto:lau_woeijye@yahoo.com)

## Abstract

Thin film composite (TFC) membranes are state-of-the-art membranes with superior permeability and selectivity and are widely used in various membrane-based processes for desalination, wastewater treatment and other separation applications. These TFC membranes are generally made out of a thin polyamide selective layer that synthesized through interfacial polymerization on the top surface of a microporous substrate. The first commercialized TFC membrane was reported in the 1970s for reverse osmosis (RO) process of seawater desalination. It was later expanded to nanofiltration (NF) process for colour and divalent salts removal in the 1980s. In the early 2000s, the potential use of TFC membrane was explored in the osmotically-driven process including forward osmosis (FO) process and pressure retarded osmosis (PRO) process. Despite the exceptional performance improvement of TFC membrane was achieved, the existing TFC membranes still suffer from several bottlenecks in terms of fouling resistance, productivity as well as durability upon compaction and chemical attack and have the limited overall separation efficiency. Research in the past has focused mainly on the fabrication of polyamide layer that determines the rejection rate and antifouling resistance of the TFC membrane. This strong research interest on the polyamide layer development can be reflected by the large number of relevant articles published in open literature since 1970s (> 3,000 articles). Nevertheless, over the past 15 years, we have seen growing interest among membrane scientists to study the roles of polymeric substrate and perform in-depth analyses on how the changes in the substrate physicochemical properties could affect polyamide layer structure and thus membrane performance. Recent advancements in the new polymeric materials development and nanomaterials synthesis have opened a lot of opportunities for new generation substrate development. Compared to the pressure-driven membrane processes, the substrate of TFC membranes plays a more significant role in osmotically-driven process as the occurrence of internal concentration polarization (ICP) (within the substrate) to reduce the available driving force for osmosis and may be regarded as an artificial source of inefficiency in FO/PRO process. Considering the importance of TFC membranes for industrial separation process, this review will give a high-quality state-of-the-art account of the subject matter by emphasizing the substrates made by different techniques (e.g., Loeb-Sourirajan phase inversion method, double-blade casting, electrospinning, and surface modification technique) and various materials (e.g., new polymeric materials, polymer-polymer composite, polymer-inorganic nanocomposite, etc.). More specifically, the article will review the roles of the developed substrates on the chemical and physical properties of polyamide selective layer and further their influences on

the TFC membrane performances for both pressure-driven (NF/RO) and osmotically-driven (FO/PRO) processes, aiming to stimulate progress in the field. Furthermore, the requirements for fabricating effective substrates will be discussed and future perspectives will be presented.

**Keywords:** *Microporous substrates; thin film composite; membranes; water applications; properties*

## **Content**

### 1.0 Introduction

### 2.0 Brief Description of Microporous Substrate Fabrication Methods

#### 2.1 Phase Inversion Method

#### 2.2 Electrospinning Method

### 3.0 Roles of Microporous Substrates

#### 3.1 Polymer or Polymer/Polymer Blend Substrates

##### 3.1.1 Substrates Made of Single Polymer

##### 3.1.2 Polymer-polymer Blend Substrates

#### 3.2 Polymer/Inorganic Nanocomposite Substrates

##### 3.2.1 Substrates Incorporated with Non-Porous Nanofillers

##### 3.2.2 Substrates Incorporated with Mesoporous Nanofillers

#### 3.3 Surface-modified Substrates

### 4.0 Concluding remarks and future directions

### Acknowledgements

### References

## 1.0 Introduction

Thin film composite (TFC) membranes which were first developed in the 1970s [1] for saline water desalination are currently dominating the water treatment industry worldwide, particularly for the removals of dissolved ions and compounds with molecular weights of several hundreds. Commercially, the flat sheet TFC membranes configured in spiral wound element consist of three important layers, i.e., an ultrathin polyamide selective layer on the top surface, a relatively loose interlayer having ultrafiltration (UF) membrane properties and a nonwoven polyester bottom layer acting as support layer. This membrane configuration has been widely used in industrial processes of nanofiltration (NF) and reverse osmosis (RO) [2–5].

In the early 2000s, the potential use of TFC membrane for osmotically-driven process was documented as an emerging solution to address the high energy consumption of RO process and the severe membrane surface fouling [6]. Forward osmosis (FO) process using TFC membrane could draw the water from brackish/seawater source via salinity gradient between feed and draw solutions, thus requires minimum amount of energy during operation [7]. Meanwhile, the osmotic pressure gradient energy between two solutions can be harvested via pressure retarded osmosis (PRO) process by employing TFC membrane to control the mixing process [8,9]. The energy from PRO process is expected to be new renewable energy since it uses a highly stable energy source instead of a time-dependent energy sources, e.g., solar and wind power. Nevertheless, it must be pointed out that the commercial-scale applications of TFC membranes for FO and PRO process are still under development and only limited number of pilot-scale studies was conducted. Some of the challenges encountered by the TFC membranes for osmotically-driven processes are the presence of internal concentration polarization (ICP) that severely affects the water permeation rate, lack of powerful and easy-to-recover draw solutes, poor membrane mechanical strength that limits the power generation, etc.

Research in the past has focused mainly on the surface of polyamide layer that determines the rejection rate and antifouling resistance of the TFC membrane. The strong research interest on the polyamide layer development can be reflected by the large number of relevant articles published in open literature since 1970s (> 3,000 articles). Nevertheless, over the past 15 years, we have seen growing interest among membrane scientists to study the roles of loose interlayer (*a.k.a.* microporous substrate) and perform in-depth analyses on how the changes in the substrate physicochemical properties could affect polyamide layer structure and thus membrane performance for both pressure-driven and osmotically-driven processes [9–12].

One of the stumbling blocks that hinders the practicability of polyamide layer modification is the negative effects imparted on the integrity of the selective layer. Comparatively, the design and modification of substrate is a more promising strategy to enhance the TFC membrane performance due to the facile approaches that can effectively tailor the properties and functionalities of the substrate. Currently, the microporous substrates made of polysulfone (PSf) and polyethersulfone (PES) via phase inversion technique are the most popular polymeric materials used for manufacturing commercial TFC NF and RO membranes. However, these microporous membranes are not without drawbacks being the support layer. Their hydrophobic characteristics (relatively high water contact angle), low structural porosity and moderate chemical resistances are the main limitations for effective filtration process.

Currently, difference approaches have been applied to fine-tune the substrate properties to suit the purpose of the TFC membranes. These include blending the commonly used substrate materials with hydrophilic polymeric additives [13,14], incorporating advanced nanomaterials with exceptional properties into the substrate matrix [15–17], surface modification of substrates via coating and grafting [18–20], and development of nanofiber-based substrates with extremely high porosity [21,22]. Generally, the modification of NF/RO membrane substrates is aimed to improve the water flux and the mechanical strength without compromising salt rejection while the modification of FO/PRO membrane substrates is mainly focused on achieving smaller structural (S) parameters (correlated to higher structural porosity and lower tortuosity factor) and greater hydrophilicity to counter the negative impacts of ICP and surface fouling, respectively.

As the development of innovative TFC membrane substrates has attracted considerable attention and has been the subject of extensive number of studies over the last decade, this review will give a high-quality state-of-the-art account of the subject matter by emphasizing the substrates made by different techniques (e.g., Loeb-Sourirajan phase inversion method, double-blade casting method, electrospinning method, and surface modification technique) and various materials (e.g., new polymeric materials, polymer-polymer composite, polymer-inorganic nanocomposite, etc.). The fabrication routes of microporous substrates are briefly described, followed by the review on the roles of substrates in enhancing the intrinsic properties and performance of TFC membranes for both pressure-driven (NF/RO) and osmotically-driven (FO/PRO) processes. Finally, the requirements for fabricating effective substrates will be discussed and future perspectives will be presented.

## **2.0 Brief Description of Microporous Substrate Fabrication Methods**

A description on the substrate synthesis will be briefly given in this section to provide readers a quick access to information about the techniques and their synthesis conditions in fabricating microporous substrates for TFC membranes.

### **2.1 Phase Inversion Method**

Nonsolvent induced phase separation (NIPS) is the most popular technique in synthesizing microporous membranes. It was invented by Sidney Loeb and Srinivasa Sourirajan in the 1960s to develop an asymmetric skin-type RO membrane for desalination process [23]. Currently, this technique is adopted by industry to prepare flat sheet microporous substrate for commercial TFC NF and RO membranes. In the commercial membranes, the microporous substrate is cast onto a polyester-based nonwoven for handling strength. Although microporous substrates in hollow fiber configuration could also be made by the phase inversion process, they are limited to the use in the lab-scale TFC membrane studies.

In principle, NIPS process involves the conversion of homogeneous polymeric solution of two or more components into a two-phase system with a solid, polymer-rich phase forming the rigid membrane structure and a liquid, polymer-poor phase forming the membrane pores, using non-solvent (usually water) as medium. To create a smooth film, polymeric solution will be first poured on a clean and dry glass plate. It is followed by casting using an adjustable doctor blade with gap of 50–200  $\mu\text{m}$ . The nascent polymeric film together with glass plate is then immersed in a non-solvent medium so as phase inversion process can take place to form membranes. The mechanisms of forming hollow fiber substrates are very similar to the flat sheet membranes, except spinning machine is required to produce cylindrical fiber with open lumen. Both the inner and outer diameter of the hollow fiber membrane can be manipulated during spinning process to produce desirable wall thickness. Depending on the applications, polyamide selective layer can be formed either on the inner or outer surface of the hollow fiber substrate.

For polymers (e.g., polypropylene (PP) and polytetrafluoroethylene (PTFE)) that cannot dissolve in the common organic solvents, thermally-induced phase separation (TIPS) is the most commonly employed technique. A homogeneous solution can be obtained by mixing the polymer with other components at an elevated temperature with a high boiling point. When the hot solution is cooled in the desired shape, occurrence of solidification will produce microporous substrate.

By comparing between these two techniques, NIPS technique is more popular among membrane scientists in preparing microporous substrates for TFC membranes. This is mainly

because most of the hydrophilic substrates can be produced from this technique. In addition, the NIPS technique is very versatile for tuning the membrane pore size and morphology. A large number of variables can influence the properties of a substrate made via NIPS. These include the characteristics of main membrane forming material (e.g., molecular weight and concentration in polymeric solution), additives (e.g., secondary polymer and inorganic nanofillers), solvent type (e.g., solubility parameter and viscosity), synthesis conditions (e.g., shear rate/take up speed, coagulation medium, evaporation temperature and humidity), and post treatment (e.g., drying method and period) [24]. The variation of these conditions can affect not only the physiochemical characteristics of the substrate (e.g., pore size, porosity, thickness, hydrophilicity) but also its interaction with polyamide layer during interfacial polymerization, leading to production of composite membranes with wide range of properties.

Xu et al. [11] concluded in their recent review article that polymer concentration is the most crucial factor that influences the properties of substrates, mainly because this parameter is critical in controlling types of pores, pore size distribution, porosity, roughness, cross-sectional structure and thickness which subsequently affect the polyamide layer properties. Particular attention should also be paid to the properties of dope solution containing other components in order to optimize the separation performance of TFC membranes.

## **2.2 *Electrospinning method***

Although the first patent related to electrospinning was filed about one century ago, it did not gain substantial attention in industry and academia until the important research activities carried out by Reneker's group in the 1990s [25]. After many years of research and development, electrospun nanofibers have been found useful and practical for various applications, particularly drug delivery, tissue engineering, electronic and photonic devices and sensor technology [26,27].

The advancements of nanofibers production technology have also opened up the possibilities of applying nanofibers as a support for TFC membrane. Compared to the substrate made by the phase inversion process, the nanofiber substrate that is electrospun exhibits amazing characteristics such as very large surface area to volume ratio, superior porosity, and excellent mechanical properties. Most importantly, the surface pore structures are all interconnected throughout the nanofiber, achieving no dead-end pores in the membrane matrix.

Nanofiber substrates can be produced with ease by forcing a polymeric solution through a spinneret with an electrical driving force. The solution contained in a syringe is pumped at a low flow rate to a tube connected to a spinneret. In this process, a high voltage is applied



between two electrodes connected to the spinning solution/melt and to the collector to create an electrically charged jet of polymer solution from a syringe. The electric field is subjected to the tip of the needle containing a droplet of the polymeric solution. Once the surface of the droplet is electrified, the Taylor cone spins down as a fiber to reach collector plate and starts to form fiber mat. In most of the cases, nanofiber is subjected to compression and/or heat treatment before being used as substrate for TFC membrane. A variety of polymers including those routinely used in the NIPS process can be processed via electrospinning. In addition to the properties of polymeric solution, there are many electrospinning parameters that can be considered to alter the characteristics of nanofiber substrates (e.g., morphology, pore size/porosity, thickness and mechanical strength). These include applied voltage, flow rate, humidity, distance between syringe and collector [28].

### **3.0 Roles of Microporous Substrates**

In this section, the impacts of substrates made of different materials (polymers or polymer-inorganic) on the characteristics and filtration performance of TFC membranes for water applications will be reviewed. Generally, two immiscible active monomers – amine and acyl chloride are required during interfacial polymerization process to create a cross-linked polymeric film (polyamide) over the surface of microporous substrate as illustrated in [Figure 1](#). In the laboratory, the polyamide layer is established by pouring the substrate with an aqueous solution containing amine monomer followed by organic solution of acyl chloride monomer. The amines in the aqueous phase would diffuse to the organic phase to react with the acyl chlorides, causing a film growing perpendicularly towards the organic phase. As the interfacial polymerization process is based on the diffusion-controlled mechanism, the increase in the thickness and density of the film would eventually inhibit amine diffusion and terminate the cross-linking process. The properties of substrate are of critically importance to govern the degree of amine impregnation which in turn affects the structure of polyamide layer and thereby the performance of TFC membranes. In order to facilitate better understanding of the roles of microporous substrates, this section is organized into three subtopics, (a) polymer or polymer/polymer blend substrates, (b) polymer/inorganic nanocomposite substrates, and (c) surface-modified substrates.



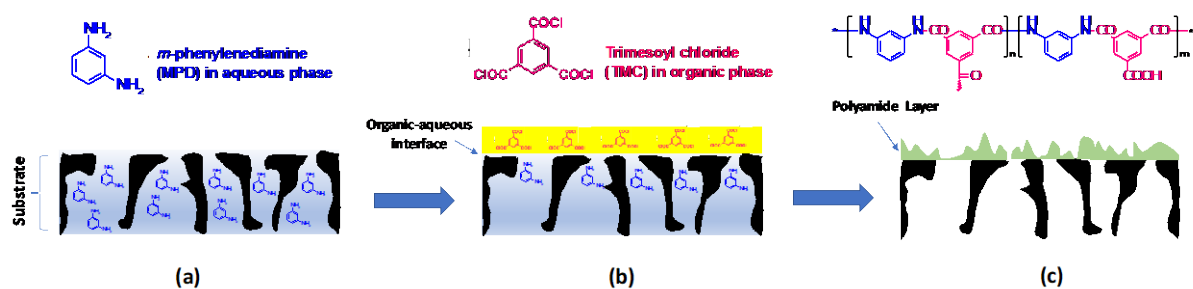


**Figure 1.** Interfacial polymerization on the substrate surface, (a) contact the substrate surface with an aqueous solution of m-phenylenediamine (MPD), (b) contact the substrate surface with an organic solution of trimesoyl chloride (TMC) and (c) formation of polyamide layer over substrate surface as a result of MPD-TMC cross-linking.

### 3.1 Polymer or Polymer/Polymer Blend Substrates

#### 3.1.1 Substrates Made of Single Polymer

Various polymeric materials have been explored in the past for substrates fabrication [12]. Among the materials used, PSf and PES membranes with surface pore sizes in the range of 30–50 kDa are very frequently used as the substrates of TFC membranes [29–31]. These kinds of polymeric substrates offer several advantages including commercially available, reasonable material cost, good mechanical strength, and chlorine resistance. In the early stage of composite membrane development (for RO process), asymmetric cellulose acetate membranes were used as microporous supports [1]. An ultrathin polymeric film produced from float-casting method was laminated to the cellulosic substrate to produce TFC membrane. However, the severe pressure compaction of the cellulosic substrates at high operating pressure was soon recognized as the major issue of application, causing the need to develop noncellulosic substrate membranes.

Although many polymeric materials such as polyacrylonitrile (PAN) [32], PP [33], polyvinylidene fluoride (PVDF) [33,34], PTFE [35], sulfonated polyphenylsulfone (sPPSU) [35], poly(etherimide) (PEI) [36], polyfurane (PF) [37], polyether-polyfurane [37], polyvinylamine [37], polyimide (PI) [38], and polyketone (PK) [39] have been utilized for substrate fabrication over the years and promising lab-scale results were obtained using TFC membranes made of them, PSf still remains a mainstay in the commercial TFC membranes to this day. It is mainly due to the widespread use of PSf as an UF membrane.

Besides acting as mechanical layer for the polyamide film, the intrinsic properties of substrate (e.g., pore size, porosity, roughness and hydrophilicity) could also influence the characteristics of polyamide layer formed. Many studies have been carried out to investigate

the relationship between substrate properties and polyamide layer characteristics in order to produce ideal substrate properties for TFC membrane.

Misdan et al. [40] for instance reported that increasing PSf concentration from 12 to 20 wt.% in the dope solution could result in the production of substrate with reduced pore size (from 84.4 to 11.70 nm) and surface porosity (from ~23% to ~10%) as well as decreased surface hydrophilicity (from ~66° to 71°). This led to formation of thicker polyamide layer with greater water transport resistance (i.e., reduced water permeability). The presence of high polymer concentration in the dope solution is elucidated to increase solution viscosity which delays solvent (NMP) and non-solvent (water) exchange rate during phase inversion process, forming denser membrane structure.

By reducing the PSf substrate pore size from 0.15  $\mu\text{m}$  (Type 2) to 0.07  $\mu\text{m}$  (Type 1), Singh et al. [41] also found that thicker but smoother polyamide layer was formed over the support. They attributed the results to the difficulty of the monomers to penetrate into the smaller pores. Large substrate pores presumably favour penetration of diamine monomer by forming an adsorbed layer of aqueous diamine solution that is ready to react with acid chloride, leading to polyamide formed inside the pores as schematically shown in Figure 2. Because of the thick polyamide layer formed over the substrate of larger pores (~0.35  $\mu\text{m}$ ), it reduces the chances of defects in the selective layer, resulting in low passage of dissolved ions.

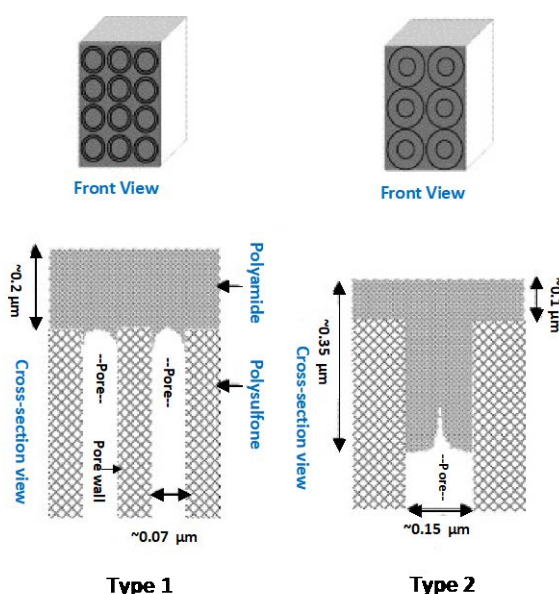


**Figure 2.** Schematic pictures of polyamide-PSf layers from Type 1 and Type 2 TFC membranes.

A comprehensive investigation on the impacts of PSf substrate properties on the polyamide layer has been carried out by Gosh and Hoek [42] by producing a wide range of substrate properties. In order to give clear understanding on the interaction between these layers, conceptual models as shown in Figure 3 were proposed to explain four different scenarios based on the observations from different substrates. The conceptual models however were only applicable to the substrates made of PSf with pore size in the range of 30–70 nm, RMS roughness of 5–10 nm and water contact angle of 60°–80°. It is noticed that polyamide layers with different water permeability and morphology were possibly produced through a variation in structure and chemistry of PSf-based substrate. In general, hydrophilic substrate with larger pore produced less permeable and intermediate rough composite membranes because of the formation of more polyamide within substrate pores. High permeable TFC membrane meanwhile could be produced using hydrophobic substrate with larger surface pore. The formation of less polyamide within the pores reduced the transport resistance of water molecules.

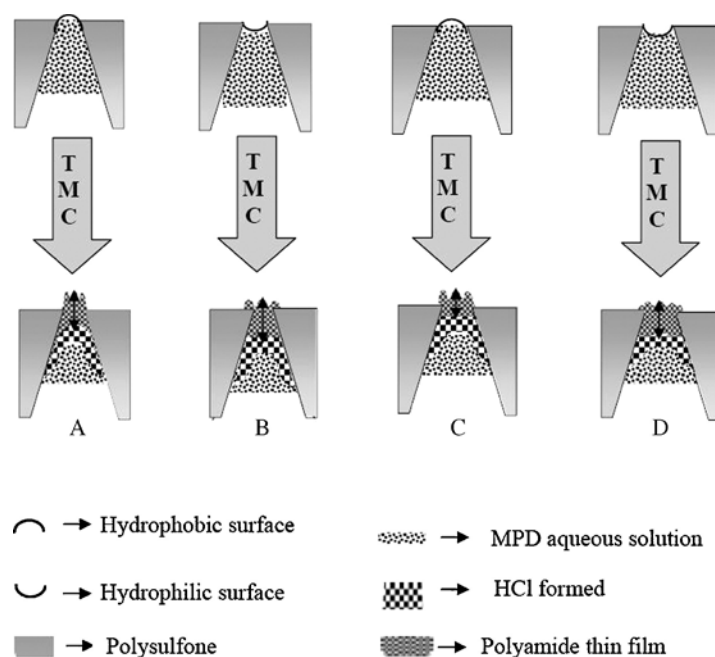


**Figure 3.** The impacts of PSf support structure and chemistry in producing TFC membrane with (a) greater permeability and rougher surface (using hydrophobic substrate), (b) relatively impermeability and intermediate surface roughness (using hydrophilic substrate), (c) the most permeability and the highest roughness (using hydrophobic substrate with larger pore), and (d) the least permeability and intermediate surface roughness (using hydrophilic substrate with larger pore) [42].

As polyamide layer thickness usually has a certain deviation in different spots, artefacts might often be introduced by electron microscope methods. Zhang et al. [43] utilized profilometer to precisely verify the selective layer of TFC membranes fabricated on five types of PSf substrates with different pore size. The selective layer of TFC membrane was obtained after the PSf substrate was dissolved in the organic solvents. The remaining selective layer was then individually loaded in silicon wafer by monolayer followed by characterization. The polyamide layer was found to be quite different in which its thickness gradually decreased from ~200 to ~85 nm by reducing substrate pore size from ~40 to 20 nm. They also experienced that the selective layer fabricated on the largest substrate pore size tended to delaminate from the support owing to its higher degree of water swelling coupled with lower cross-linking degree. As the maximum substrate pore size used in this work (~200 nm) is significantly higher than the substrate pore size reported in the work of Misdan et al. [40] (up to 84 nm) and Singh et al. [41] (~150 nm), there is a reason to believe that the very large substrate pore size could not make the polyamide adhered firmly which in turn responsible for inferior separation performance of TFC membrane.

Contradictory to the aforementioned studies, Huang et al. [44] found that the thickness of the polyamide selective layer was independent of the substrate pore size. It was reported that TFC membranes with very similar polyamide layer thickness (average of ~100 nm) were obtained regardless of the pore size of nylon 6,6 substrate (i.e., 25, 100, 200 and 450 nm). Nevertheless, the polyamide cross-linking degree decreased from 0.69 to 0.37 with increasing substrate pore size from 25 to 450 nm. In other words, the TFC membrane separation efficiency was negatively affected when large-pore size substrate was used. As can be seen from these works, the morphology of the polyamide layer is not easy to predict as contradictory results are always reported on the substrates. In addition to pore size, there are other factors contributing to the different outcomes. The simultaneous changes in the other parameters such as pore size distribution, porosity, roughness, and hydrophilicity, when pore size is changed, make the polyamide layer characteristics even more difficult to predict.

In addition to the PSf substrate, Misdan et al. [45] compared the performance of the TFC membrane with two other TFC membranes made of PES and PEI-based substrates. It was reported that the fluxes of both pure water and salt solution decreased in the order of PEI-based TFC > PES-based TFC  $\geq$  PSf-based TFC. Characterization results confirmed that the physical and chemical properties of poly(piperazine-amide) layer were obviously altered depending on the properties (hydrophilicity and pore size) of the substrates. Apparently, the effect of the hydrophilicity governs the polyamide formation more strongly than the substrate pore structure.

XPS analysis revealed that the polyamide layer prepared over PSf substrate produced a highly cross-linked structure due to increased substrate hydrophilicity. Whereas, the PES-based TFC and PEI-based TFC membrane are close to that of the linear structure. Thus, selection of polymer type should be given particular attention for the substrate fabrication in order to optimize the separation properties of TFC membranes.

It is interesting to note that when PSf and PES were separately used to produce nanofiber support for flat-sheet TFC membrane synthesis [21], only the PSf nanofiber could demonstrate strong adhesion with the polyamide layer. PES nanofiber meanwhile showed poor adhesion with selective layer, causing polyamide film to delaminate (Figure 4). The authors explained that the presence of additional bisphenol A (BPA) moiety in the PSf structure is the main factor contributing to good adhesion between substrate and polyamide derived from MPD and TMC through a specific chemical interaction as illustrated in Figure 5. The electrons from  $-CH_3$  groups of BPA moiety can be donated to the two aromatic rings, activating them toward electrophilic attack. Because of this, the electrophilic will replace a hydrogen atom at the ortho site of the aromatic ring via electrophilic aromatic substitution mechanism. The presence of byproduct (HCl) during interfacial polymerization process and the use of high temperature ( $95^\circ$ ) for TFC membrane post-treatment in this work are also likely to catalyze this mechanism.

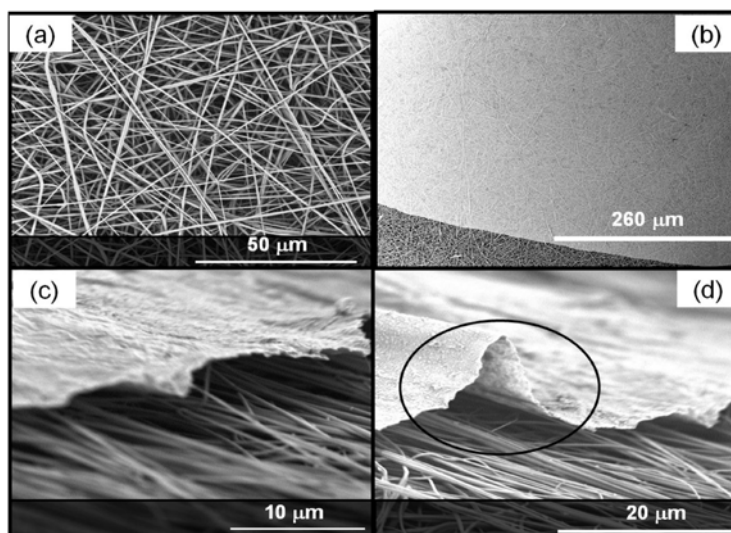


**Figure 4.** SEM images of (a) electrospun PES and (b–d) PES-based TFC polyamide membranes at different magnifications. Images (c) and (d) show poor adhesion between polyamide and PES nanofiber support.

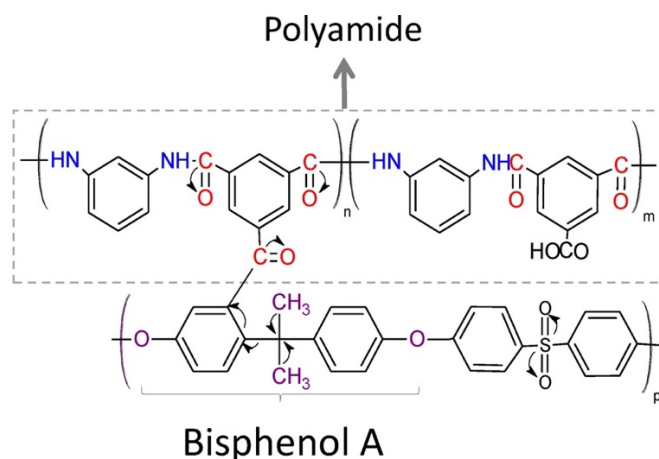
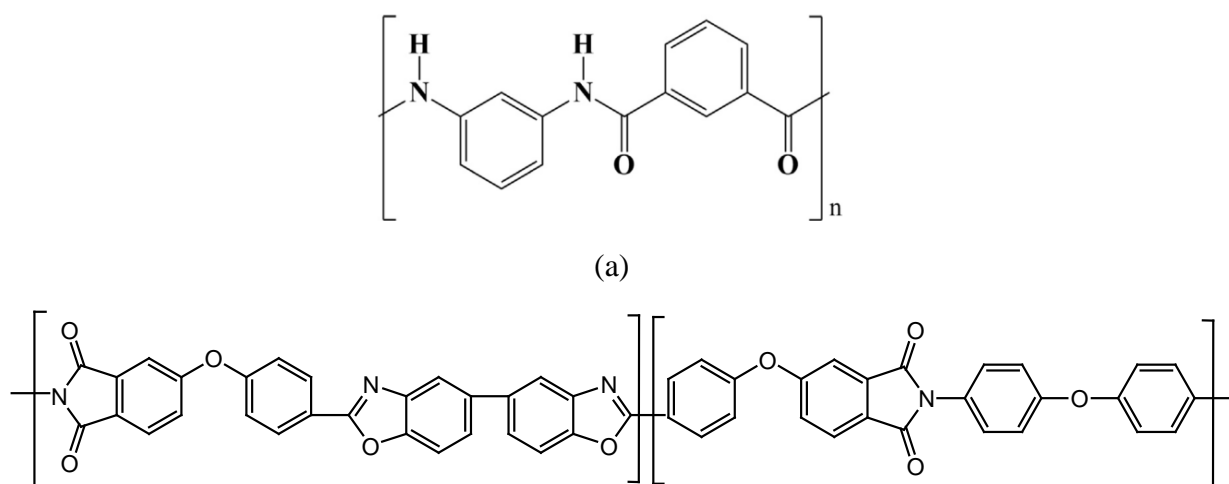


**Figure 5.** Proposed cross-linking interaction between polyamide and the bisphenol A group of PSf nanofiber support. (Note: Arrows indicate the proposed reaction mechanism).

Although PSf- and PES-based substrates are widely used for commercial and lab-scale TFC membrane fabrication, the main limitation of these substrates is their relatively poor thermal stability in handling hot solution (above 50°C) and organic solvents. This has brought towards the development of new type of polymers. Chen et al. [46] fabricated thermally stable TFC NF membrane using poly(m-phenyleneisophthalamide) (PMIA) as shown in Figure 6(a). The meta-type benzene amide linkages in the skeletal chains and hydrogen bonding network of PMIA contribute outstanding thermal stability, superior mechanical properties and hydrophilic properties. The resultant TFC membrane was reported to be stable for operating temperature up to 90°C. Its Na<sub>2</sub>SO<sub>4</sub> rejections were remained stable at more than 95% regarding of operating temperature, even though the water flux of PMIA-supported TFC membrane was significantly increased due to reduced solution viscosity at high temperature. More significantly, the newly developed PMIA-supported TFC membrane exhibited almost three-fold higher water flux than the PSf-supported TFC membrane.





(b)

**Figure 6.** The organic structure of (a) poly(m-phenyleneisophthalamide) (PMIA) and (b) polybenzoxazole-co-imide (PBOI) for making substrate with improved properties.

Using a novel synthesized poly(phthalazinone ether amide) (PPEA) as substrate material, a thermally stable composite membrane was successfully fabricated by Wu et al. [47]. The resultant composite membrane has shown superior performance in removing dyes from a dye-salt mixed solution at 1.0 MPa, 80°C. The relative stability of the flux and dye rejection during a 5-h experiment at 80°C testified to the thermal stability of the PPEA-based composite membrane. A new series of polymeric materials manufactured by Dalian New Polymer Material Co. Ltd. (China) have also been examined as possible materials to fabricate a thermal-resistant substrate. Among these new materials, poly(phthalazinone ether sulfone ketone) (PPESK) was reported as exhibiting a higher upper temperature limit and better thermal stability than that of the PSf-based substrate [48]. Even being operated at a temperature greater than 80°C, there was no significant sign of pore expansion on the PPESK-based substrate, proving its extraordinary resistance against thermal attack.

To make the TFC membrane more resistance to organic solvents, Kim et al. [49] fabricated thermally rearranged substrate made of polybenzoxazole-co-imide (PBOI) (see Figure 6(b)) for the TFC NF membrane. PBOI substrate was synthesized through furnace of hydroxyl polyimide nanofiber membrane at 400°C for 2 h under an argon atmosphere. The developed TFC membrane was able to achieve good results not only at high operating temperature (up to 90°C) but also in non-aqueous solution (i.e., dimethylformamide (DMF)) without experiencing aging phenomena. To most of the commercial TFC membranes that used conventional polymeric substrates, the use of DMF could cause the polymeric materials to age easily. However, the newly developed TFC membrane could consistently maintain >94% NaCl rejection even after exposing to DMF for 140 h.

A TFC RO membrane having high permselectivity and excellent mechanical/chemical durability was developed by Park et al. [35] using a polyethylene (PE)-based substrate. The PE-based substrate possesses uniform pores and high surface porosity which are beneficial for enhancing membrane separation rate, but its intrinsic hydrophobicity makes the fabrication of a polyamide selective layer challenging. An oxygen plasma treatment on the PE substrate was thus carried out to enhance its water wettability before interfacial polymerization was initiated. The resultant PE-supported TFC membrane showed ~30% higher water flux compared to a commercial RO membrane with NaCl rejection remained unchanged. Such TFC membrane also



exhibited superior mechanical properties and organic solvent resistance which is attributed to the excellent mechanical and chemical stability of the PE material. The authors explained that the improved properties of PE substrate could expand the application of TFC membranes to harsh operating environments involving organic solvents. Currently, the development and commercialization of solvent-resistant NF membranes are in high demand for applications in pharmaceutical and oil refining industries [50].

Recent developments in nanofibers production technology have opened up the possibilities of applying nanofibers for various process improvements, including as a support for TFC membrane. Compared to the substrate made via the phase inversion process, the nanofiber substrate that is electrospun exhibits fascinating features such as superior porosity (up to 90%), very large surface area to volume ratio, and excellent mechanical properties. Most importantly, the highly porous structure of nanofibers can mitigate ICP effect in the osmotically-driven membrane processes. In addition to the typical external concentration polarization (ECP) that takes place as a result of solute buildup at the membrane active layer surface, osmotically-driven membrane suffers from ICP that occurs within the membrane structure.

Depending on the membrane orientation, two phenomena - concentrative ICP and (b) dilutive ICP can occur. As illustrated in Figure 7, if the substrate of TFC membrane faces the feed solution, as in PRO, a polarized layer is established along the inside of the polyamide layer as water and dissolved solutes propagate the substrate layer. Oppositely, if the polyamide layer faces the feed solution and the substrate faces the draw solution, the water permeating through polyamide layer would dilute draw solution within porous substructure, causing dilutive ICP. As the effective osmotic pressure driving force ( $\Delta\pi_{\text{eff}}$ ) in the PRO orientation is higher than the FO orientation, relatively higher water permeability can be produced from PRO process. Nevertheless, it must be pointed out that the ICP cannot be avoided in the substrate of the TFC membrane during engineered osmosis process. Thus, developing a novel nanofiber substrate that exhibits low structural parameter ( $S$  value = thickness  $\times$  tortuosity/porosity) is highly preferable.

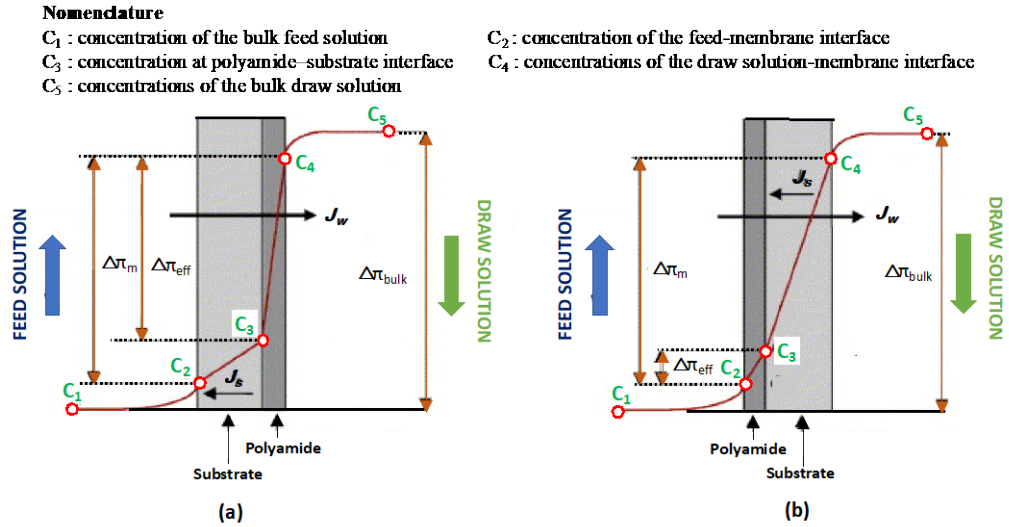


**Figure 7.** Internal concentration polarization profile across TFC membranes, (a) Concentrative ICP (PRO process) and (b) dilutive ICP (FO process).

One of the earliest research studies examining the potential of nanofiber as alternative substrate to fabricate polyamide TFC membrane was carried out by Yoon et al. in 2009 [51]. In this work, the authors fabricated TFC membranes using PAN substrates made via phase inversion and electrospinning method. The electrospun substrate ( $>3500 \text{ L/m}^2\cdot\text{h}\cdot\text{psi}$ ) exhibited remarkably higher water flux than that of the conventional substrate ( $\sim 50 \text{ L/m}^2\cdot\text{h}\cdot\text{psi}$ ) and possessed about 85% porosity. It was also reported that the nanofiber-supported TFC membrane demonstrated 2.5 times more water flux than the conventional TFC membrane, while maintaining similar  $\text{MgSO}_4$  rejection at  $\sim 98\%$ . The improved water flux of newly developed membrane was possibly due to the large open pore structure and low hydraulic resistance of nanofiber substrate.

Using nanofiber substrate made of PI, Chi et al. [52] developed a novel TFC membrane with the aim of alleviating ICP and enhancing membrane water flux during engineered osmosis process. The average pore size of the nanofiber substrate is much bigger than the commonly used substrates, which is intentionally designed to minimize the membrane permeability resistance. When tested under RO mode, the resultant membrane made of optimized interfacial polymerization process achieved as high as  $15.9 \text{ L/m}^2\cdot\text{h}\cdot\text{bar}$  pure water flux. Although the authors reported the same membrane could attain low  $J_s/J_v$  value during FO test, the poor  $\text{NaCl}$  rejection of the membrane (34.7–49.8%) obtained from RO mode raised question if the resultant TFC membrane was suitable for engineered osmosis process.

On the other hand, Park et al. [53] employed hydrophobic PVDF nanofiber for TFC FO membrane preparation. Prior to interfacial polymerization process, the PVDF nanofiber was modified with polyvinyl alcohol (PVA) via dip coating to enhance its surface hydrophilicity. Using the PVA-modified substrate, the resultant TFC membranes showed improved hydrophilicity, porosity, and mechanical strength. With respect to FO performance, the membrane achieved water flux of 34.2 L/m<sup>2</sup>.h when tested with 1 M NaCl and DI water as draw and feed solution, respectively.

In a recent study, Liang et al. [54] developed a vertically oriented porous substrates (VOPSs) as the supports for TFC membranes to address ICP problems during FO process. The structure of VOPS as shown in Figure 8 was prepared via bidirectional freezing of PVDF/dimethyl sulfone (DMSO<sub>2</sub>) solution using oriented DMSO<sub>2</sub> crystal as templates before interfacial polymerization was carried out on the surface for TFC membrane fabrication. The SEM images revealed that both the top and bottom substrate surfaces exhibited an open porous structure, indicating that the vertical pores were throughout the entire substrate matrix. This highly porous substrate (porosity of ~74%) endowed the TFC membrane with very low tortuosity, offering direct paths for fast water permeation. The VOPSs-supported TFC membrane demonstrated an unprecedented water flux up to 93.6 L/m<sup>2</sup>.h in the FO mode using a draw solution of 2.0 M NaCl with reverse solute flux recorded at ~10.5 g/m<sup>2</sup>.h.

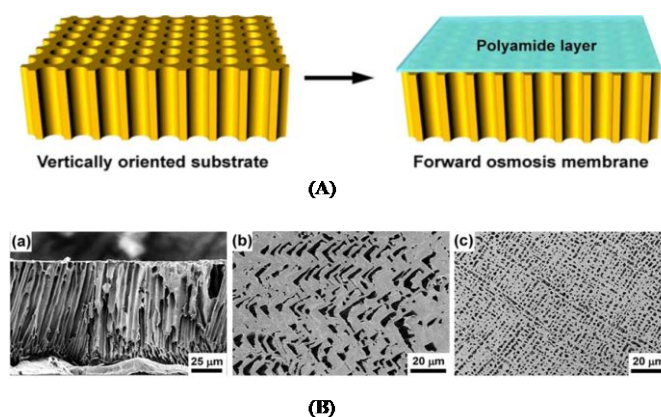


**Figure 8.** (A) Schematic representation of fabrication of VOPS-supported TFC membrane. (B) SEM images of PVDF-based VOPS, (a) cross-section, (b) top surface and (c) bottom surface.

Concerted efforts devoted to the FO membranes development over the last decade have also opened up new perspectives for the rapid progress of PRO membranes. Generally, TFC hollow fiber membranes that possess unique characteristics of high membrane surface area per module, easy of fabrication and self-mechanical support are particularly well-suited for

harvesting energy from osmotic pressure gradient based on PRO technology. Since this membrane configuration requires no feed spacer during operation, the potential energy loss from the membrane-spacer interface could be avoided, leading to improved power density.

Zhang et al. [55] highlighted that a hollow fiber support membrane consisting of a dense and thick inner skin layer supported by fully porous structure is essential to produce high performance TFC membranes for PRO process. They have molecularly engineered PES-based hollow fiber membrane and produced supports comprising different cross-section morphologies (from macrovoids to sponge-like structure) by altering water content in the polymeric dope solutions. Using the support membrane with best properties (mean pore diameter: 8.7 nm; porosity: 75.3%; maximum tensile stress: 4.69 MPa and burst pressure: 22 bar), the resultant TFC membrane was able to produce a maximum power density of 24.3 W/m<sup>2</sup> at 20 bar using pure water as the feed and 1 M NaCl as the concentrated brine. In order for the PRO process to be commercially viable, Skilhagen et al. [56] emphasized a target power density of 5.0 W/m<sup>2</sup> is required.

As reported in most of the research studies, polyamide skin layer is formed on the inner surface of hollow fiber membranes. It is mainly because of the difficulties of establishing uniform polyamide layer on the outer surface, even though outer-selective hollow fiber membrane offers higher surface area per module and exhibits lower pressure drop in the brine solution. To enable the resultant TFC membrane to exhibit enhanced mechanical properties, Chou et al. [57] utilized robust polymeric material - polyetherimide (PEI) to fabricate hollow fiber support membrane. The tensile modulus of PEI support was reported to be 243 MPa, i.e., significantly higher than those of PES-based supports (81–96.6 MPa) reported in other studies [58,59]. By optimizing the synthesis conditions, a sponge-like hollow fiber membrane with porosity of 72% and burst pressure of 16.5 bar was successfully produced and used as support for making a novel TFC membrane with robust mechanical strength. Figure 9 shows that the polyamide layer only experienced small changes after high pressure compaction as the leaf-like polyamide layer could still be clearly seen on the inner surface of the hollow fiber membrane. Experimental results indicated that the newly developed TFC membrane was able to achieve a power density of 20.9 W/m<sup>2</sup> with minimum specific reverse salt flux ( $J_s/J_w$  of 0.03 mol/L) at 15.1 bar using 1 mM NaCl and 1 M NaCl as the feed and brine water, respectively. Shibuya et al. [60] meanwhile reported that an optimum hollow fiber diameter did exist by taking into consideration the pressure resistance and water flux of membrane during engineered osmosis process. Their results revealed that the TFC membrane made of small-lumen size hollow fiber (ID/OD: 347/480  $\mu$ m) offered higher pressure resistance than that of membrane made of larger

lumen size (ID/OD: 609/893  $\mu\text{m}$ ). The maximum burst pressure ( $P_{\text{max}}$ ) of the first membrane against hydraulic pressure force on the shell side was about 10 bar which is two times higher than the value shown by the second membrane.

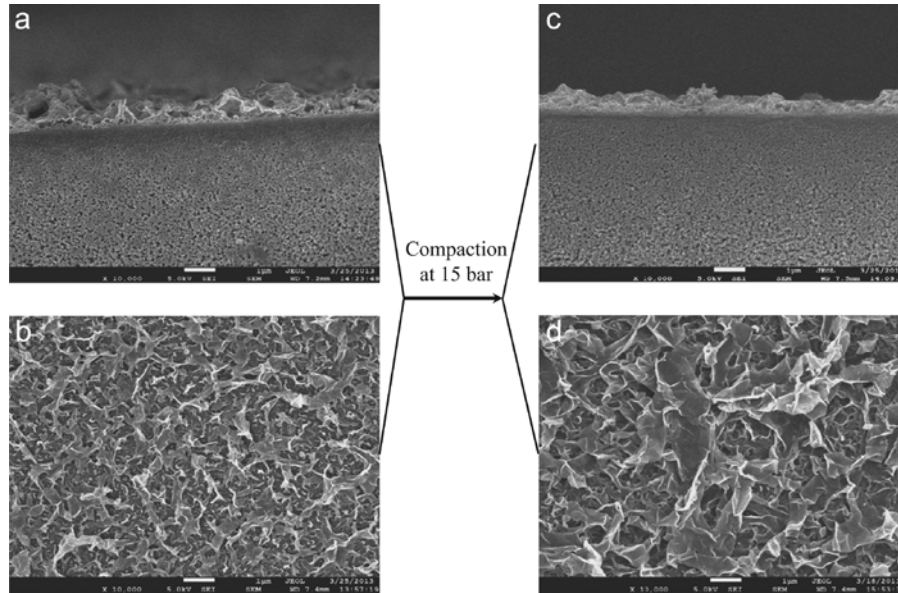


**Figure 9.** SEM image of TFC-PEI membranes, (a,b) cross-section near the inner surface (top) and inner surface of membrane (bottom) before compaction and (c,d) cross-section near the inner surface (top) and inner surface of membrane (bottom) after compaction at 15 bar.

Separately, Chung's research team evaluated the impacts of using hollow fiber membrane made of co-polyimide (P84) [61] and PI (Matrimid<sup>®</sup> 5218) [62] on the performance of TFC membrane for osmotic power generation. The best performing TFC membrane made of optimized PI support exhibited a power density of 16.5 W/m<sup>2</sup> and a very low  $J_s/J_w$  of 0.015 mol/L at 15 bar using 10 mM NaCl as the feed and 1 M NaCl as the brine water. As a comparison, the TFC membrane made of co-polyimide hollow fiber support only exhibited maximum power density of 12 W/m<sup>2</sup> when tested at hydraulic pressure of 21 bar using 1 M NaCl as draw solution. One of the main reasons contributing to the better performance of TFC membrane made of PI (Matrimid<sup>®</sup> 5218) is due to its larger pore size (~150 kDa) that led to significantly higher pure water permeability (284 L/m<sup>2</sup>.h.bar). The TFC co-polyimide hollow fiber membrane meanwhile demonstrated pore size and pure water permeability of 26 kDa and 150-170 L/m<sup>2</sup>.h.bar, respectively.

In 2018, Kim et al. [49] developed a robust TFC membrane incorporating thermally rearranged nanofiber substrate that could achieve remarkably high-power density through PRO

process using a concentrated brine. The thinness, high porosity (62%) and excellent mechanical property (tensile strength of 39 MPa) of polybenzoxazole-*co*-imide (PBOI) nanofiber make it particularly suitable as the TFC membrane substrate for power generation. A solvent activation using 50% DMF aqueous solution on the polyamide layer of the TFC membrane could significantly enhance water flux with slight reduction in salt rejection. This post treatment process further improved TFC membrane performance during PRO application, recording power density as high as 40 W/m<sup>2</sup> at 18 bar using pure water and 3 M NaCl solution as feed and draw solution, respectively. Most importantly, this newly developed membrane demonstrated long-term performance stability over 75 h under high operating pressure without any significant damage on its structure.

Compared to the inner-selective TFC hollow fiber membranes, the outer-selective membranes provide additional benefits such as easier membrane surface cleaning, larger surface area per module and less pressure drop because pressurized draw solution flows through the module shell side. Nevertheless, the development of outer-selective TFC hollow fiber membranes is much slower mainly due to the difficulty of forming defect-free selective layer on the fiber outer surface. Hollow fibers tend to stick together during interfacial polymerization process, making the formation of defect-free polyamide layer difficult [9]. To address the technical challenge, Cheng et al. [63] first designed a low-packing density hollow fiber module (~2.1%) before recirculating several chemical solutions through the module shell side to initiate interfacial polymerization process. The properties of the hollow fiber substrate used for TFC membrane fabrication were optimized by manipulating the water content in the PES dope solution. A low water content (2 wt%) tended to induce an open-cell porous substrate with enhanced mechanical strength and lower tortuosity value. High water content (5.6 wt%) meanwhile yielded a partial close-cell substrate that was more brittle and had higher tortuosity value. The best performing TFC membrane has a maximum power density of approximately 10 W/m<sup>2</sup> at 22 bar using pure water as the feed and 1 M NaCl as the draw solution. Such value is the highest power density ever achieved by the outer-selective TFC hollow fiber membranes in the literature.

### **3.1.2 Polymer-polymer Blend Substrates**

Achieving new property of polymeric solution by blending it with another polymer is always an efficient method to outperform the property of single polymer [64]. In particular, incorporating hydrophilic polymers into the substrates have been proved to be effective yet



simple to alter membrane physical and chemical characteristics to achieve desired separation properties of TFC membranes.

Polyether glycol (PEG) and polyvinylpyrrolidone (PVP) are perhaps the most popular additives used to modify microporous substrates. Depending on the concentration and molecular weight of the additives, the substrates with different physical morphologies and wide range of pure water flux (from as low as 30–50 L/m<sup>2</sup>.h.bar to several hundreds of L/m<sup>2</sup>.h.bar) could be produced. Nevertheless, it must be noted that variability exists in researching the impacts of these two hydrophilic additives incorporation. Xu et al. [11] in their review article reported that contradictory results on the changes of pore dimension, porosity, and cross-sectional morphology have always been found upon incorporation of PEG and PVP.

Boom et al. [65] experienced that the introduction of PVP could suppress macrovoids formation of substrate in the PES/NMP/PVP solution, while the results were contradictory to the findings of Yoo et al. [66] where PVP was added in the PSf/DMF dope solution. Using PEG as secondary additive, Fathizadeh et al. [67] were able to produce PES substrate with reduced pore size, but this result is opposite compared to the work of Idris et al. [68] during which PEG addition increased the substrate pore size. The varying effects of PEG and PVP incorporation can be attributed to several factors including molecular weight of the additive selected, additive concentration used in dope solution as well as conditions of substrate synthesis and post-treatment.

Blending the substrates with other hydrophilic additives (e.g., PAN and polyaniline (PANI)) and sulfonated polymers (e.g., sulfonated polysulfone (SPSf), sulfonated poly(ether ether ketone) (SPEEK), sPPSU and sulfonated poly(phenylene oxide) (SPPO)) seem to be more effective compared to the PEG and PVP in improving the hydrophilicity. This is because PEG and PVP are highly soluble in water and may get washed away from substrate matrix during phase inversion process. A large amount of additives could be removed together with solvent in water coagulation bath, leaving only a small amount of additives in the substrate.

To develop a TFC NF membrane with enhanced water flux and salt rejection, Zhu et al. [69] blended PES substrate with polyaniline (PANI). The reason of utilizing PANI is due to its capability to act as both pore forming agent and hydrophilic modifier [70,71]. Upon addition of 0.2 wt.% PANI into PES sublayer, the resultant TFC membrane attained water flux of 95.3 L/m<sup>2</sup>h and MgSO<sub>4</sub> rejection of 94.9% when tested at 0.6 MPa. Compared to the performance of the TFC control membrane (made of pure PES substrate), the results were enhanced by 101% and 5.1%, respectively. Figure 10 compares the performance of the TFC membranes made of a series of PAN-modified PES substrates (by varying PANI concentration) with respect to water



flux and salt rejection. The optimum performance of PA/PES/PANI-0.2 membrane may be ascribed to the formation of the thinnest polyamide layer coupled with highest cross-linked degree.

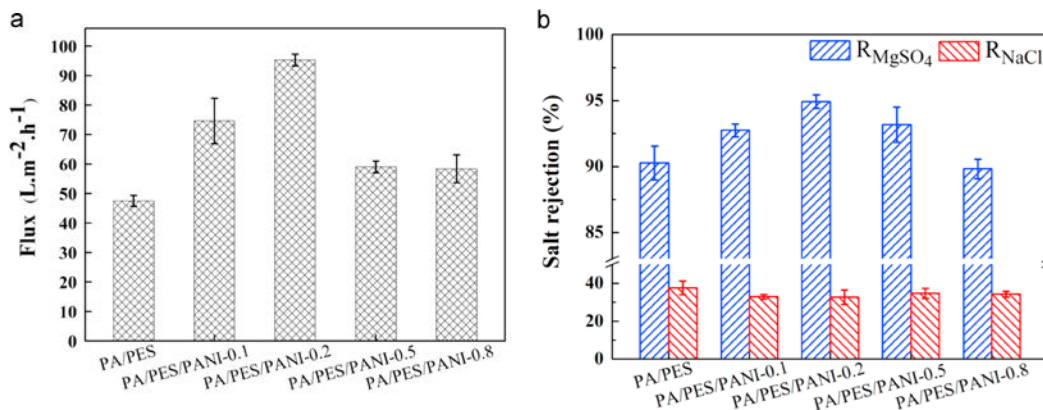


**Figure 10.** Separation performance of the TFC NF membranes made over different substrates, (a) water flux and (b) salt rejections at 6 bar, 1000 ppm single salt solution (Note: *The number in the membrane designation corresponded to the PANI content used in the substrate preparation*).

Peyravi et al. [72] improved the solvent resistance properties of the PSf substrate by introducing sulfonated poly(ether sulphide sulfone) (SPESS) as a secondary polymer during dope preparation. The swelling degree of the PSf/SPESS-supported TFC membrane in methanol solution was significantly lower than that of the PSf-based TFC membrane. The improvement in the modified PSf with respect to solvent resistance as explained by the authors is mainly due to the formation of rigid ionic domain of SPESS in the PSf matrix, hindering the polymer chains to fluctuate freely in methanol.

The incorporation of sulfonated polymers in the substrate showed greater impacts on the osmotically-driven membrane process as the substrate of TFC membrane is directly contacted with aqueous solution during filtration process. Zhang et al. [73] improved the PSf-based substrate by blending it with disulfonated poly(arylene ether sulfone) hydrophilic-hydrophobic multiblock copolymer (BPSH100-BPS0) (Figure 11) and utilized the substrates for TFC membrane fabrication for engineered osmosis application. Although incorporation of 25 wt% of BPSH100-BPS0 in the PSf substrate led to reduced tensile strength, the FO performance of the TFC membrane was significantly improved. The pure water flux of the membrane was recorded at 40.5 and 74.4  $\text{L/m}^2.\text{h}$  when tested under FO and PRO mode that used 2M NaCl as draw solution, respectively. The results were almost one-fold higher than the

TFC membrane without addition of BPSH100-BPS0. Such membrane also showed promising results for desalination process that used model seawater (3.5 wt% NaCl) as the feed solution and 2M NaCl as draw solution. The results showed that the water fluxes of 18.6 and 29.06 L/m<sup>2</sup>.h were achieved under FO and PRO mode, respectively.

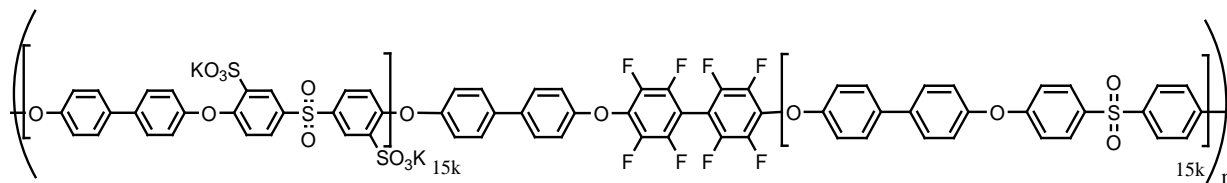


**Figure 11.** The molecular formula of BPSH100-BPS0 [73].

By blending PSf with PAN, Shokrollahzadeh et al. [64] produced a new type of nanofiber substrate for TFC membrane and compared its performance with the conventional PSf/PAN-supported TFC membrane. They observed the improvement in the nanofiber-based TFC membrane was significant compared to the typical TFC membrane. Besides exhibiting 3.54-fold tensile strength, the newly developed TFC membrane also exhibited 1.5 times more water permeability coupled with about 10% reduction in reverse salt flux (from 11.6 to 10.1 g/m<sup>2</sup>.h). More importantly, the *S* parameter value of the nanofiber-supported TFC membrane decreased considerably which correlated with the reduced ICP during FO process. The *S* values of the nanofiber-supported TFC membrane and typical TFC membrane were 0.34 and 1.23 mm, respectively.

A novel TFC membrane composed of hydrophobic/hydrophilic interpenetrating network composite nanofibers (HH-IPN-CNF) was designed by Tian et al. [74] and used for engineered osmosis process. The hydrophobic polyethylene terephthalate (PET) and hydrophilic PVA composite nanofibers were fabricated in single-step by electrospinning. When tested using DI water as feed solution and 0.5 M NaCl solution as draw solution under PRO mode, the resultant membrane made of optimized PET/PVA nanofiber achieved the highest water flux (47.2 L/m<sup>2</sup>.h) and low salt leakage (9.5 g/m<sup>2</sup>.h). The promising membrane performance was attributed to the increased wetting performance of nanofiber substrate and its water-transferring function which led to reduced ICP.

Recently, Shibuya et al. [13] introduced a novel nanofiber substrate for TFC membrane fabrication via coaxial electrospinning. The nanofiber substrate consisted of a PVDF as core layer and a CA as sheath layer (cover layer) was able to address the poor wettability of the PVDF-based substrate. A hydrophilic sheath layer formed on the surface of PVDF nanofiber have potential to offer a synergistic effect of both polymeric materials. Besides exhibiting

mechanical property similar to the pure PVDF nanofiber, the TFC membrane made of coaxial electrospun CA/PVDF nanofiber could produce significantly higher FO flux with lower reverse solute flux as a result of improved substrate hydrophilicity that mitigated ICP effects during filtration process.

As nanofiber substrate is of highly porous, it could make the resultant TFC membrane intolerant to pressure during PRO process. High operating pressure is likely to compact the highly porous support layer, causing substantial increase in mass transfer resistance and further a decrease in power density in long run. In order to address the problem, Huang et al. [75] tailor-made a substrate layer that was integrated with nonwoven scrim. Two casting solutions containing nylon 6,6 were used to form supporting zone and buffer zone on each side of nonwoven scrim, producing pore size of 0.04 and 0.1  $\mu\text{m}$ , respectively. Polyamide selective layer was later formed over the surface of 0.04  $\mu\text{m}$  pore size. Figure 12 illustrates the changes in the structure of the conventional TFC membrane and the tailored-made nylon 6,6 supported TFC membrane before and after pressure compaction. As can be seen from the illustration, most of the pores in the conventional TFC membrane were experienced deformation upon compression. However, the newly developed TFC membrane only suffered compression on its supporting zone. Its buffer zone was resistant to compression due to the reinforcement from the rigid scrim. Using the reinforced substrate, the TFC membrane could capture up to 82% of its theoretical power. Conventional TFC membrane meanwhile could only achieve half of its theoretical power under same testing conditions. Although the newly developed substrate could potentially minimize TFC membrane performance loss from compaction, its power densities (2.8–3.5  $\text{W}/\text{m}^2$ ) were significantly lower than most of the novel membranes reported earlier. This relatively low membrane performance is attributed to the high S parameter value of spongy pores in the substrate which led to higher tortuosity in comparison to the macrovoids or dendritic pores. Further optimization of the multi-zoned nylon 6,6 substrate is worthy of investigation.

Table 1 highlights the important findings of several works that utilized polymer-polymer blend substrates for TFC membranes for both pressure-driven and osmotically-driven process. As can be seen, the TFC membranes made of modified substrates (with best properties) always demonstrated enhanced filtration performances compared to the conventional TFC membranes.

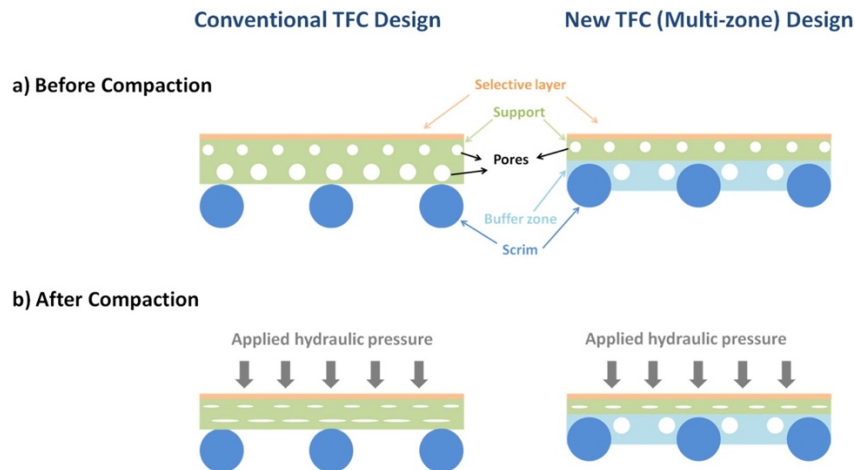


**Figure 12.** Comparison on the structure of conventional TFC and newly designed TFC membrane before and after compaction.

**Table 1.** The impacts of secondary hydrophilic polymer on the microporous substrate properties and the resultant TFC membrane performance.

<sup>a</sup> Substrate	Structure	Changes in Substrate Properties	Application	Membrane Performance	Ref.
PES/PANI	Asymmetric (NIPS)	Pore size, porosity and hydrophilicity of PES substrate were increased upon addition of PANI. This led improved water permeability.	NF	<b>TFC (PES/PANI-0.2):</b> 15.9 L/m <sup>2</sup> .h.bar; 95% MgSO <sub>4</sub> rejection; 33% NaCl rejection  <b>Control TFC (PES):</b> 7.8 L/m <sup>2</sup> .h.bar; 91% MgSO <sub>4</sub> rejection; 38% NaCl rejection	[69]
PET/PVA	Nanofiber (Electrospinning)	PET/PVA (1/4) nanofiber exhibited water contact angle of <40° in compared to the pure PET nanofiber that showed 134.8°. Both nanofibers possessed same thickness (57 μm).	FO/PRO	<b><sup>b</sup>TFC (PET/PVA):</b> Water flux: 47.2 L/m <sup>2</sup> .h; Reverse salt flux: 9.5 g/m <sup>2</sup> .h  <b>Control TFC (PET):</b> Water flux: 7.4 L/m <sup>2</sup> .h; Reverse salt flux: 15.0 g/m <sup>2</sup> .h	[74]
CA (sheath side)/PVDF (core layer)	Nanofiber (Coaxial-electrospinning)	CA (17 wt%)/PVDF (15 wt%) nanofiber possessed mean pore size of 2.4 μm, porosity of 89.1% and contact angle of 136.7°. Control PVDF nanofiber meanwhile showed 3.7 μm, 86.5% and 147.2°, respectively.	FO	<b><sup>c</sup>TFC (CA/PVDF):</b> Water flux: 31.3 L/m <sup>2</sup> .h; Reverse salt flux: 0.8 g/m <sup>2</sup> .h  <b>Control TFC (PVDF):</b> Water flux: 18.5 L/m <sup>2</sup> .h; Reverse salt flux: 2.7 g/m <sup>2</sup> .h	[13]
PSf/BPSH100-BPS0	Asymmetric (NIPS)	Introduction of copolymer into PSf substrate improved hydrophilicity, porosity and water flux, but affected its mechanical properties by 23%.	FO/PRO	<b><sup>d</sup>TFC (PSf/BPSH100-BPS0):</b> Water flux: 40.9 (FO)/74.4 (PRO) L/m <sup>2</sup> .h; Reverse solute flux: 9.32 (FO) / 11.88 (PRO) g/m <sup>2</sup> .h  <b>TFC (PSf):</b>	[73]

				Water flux: 25.5 (FO)/34 (PRO) L/m <sup>2</sup> .h; Reverse solute flux: 3.5 (FO) / 4.9 (PRO) g/m <sup>2</sup> .h	
PSf/PAN	Nanofiber (Electrospinning)	Porosity and tensile strength of PSf/PAN nanofiber were much higher compared to the PSf/PAN substrate made of NIPS method. Besides, PSf/PAN nanofiber also exhibited lower water contact angle with slightly thicker layer.	RO/FO	<b>TFC (PSf/PAN nanofiber):</b> 3.68 L/m <sup>2</sup> .h.bar, 97.12% NaCl rejection; 0.34 nm S value  <b>TFC (PSf/PAN conventional):</b> 3.59 L/m <sup>2</sup> .h.bar, 95.35% NaCl rejection; 1.23 nm S value	[64]
PSf/SPEK	Asymmetric (NIPS)	Introduction of SPEK (up to 50 wt%) into PSf substrate improved membrane surface hydrophilicity and its ductility. The substrate thickness was reduced and sponge-like structure was formed.	FO/PRO	<b><sup>e</sup>TFC (PSf/SPEK-50 wt%):</b> Water flux: 35 (FO)/50 (PRO) L/m <sup>2</sup> .h; Reverse solute flux: 7 (FO) / 9 (PRO) g/m <sup>2</sup> .h  <b>Control TFC (PSf):</b> Water flux: 23 (FO)/38 (PRO) L/m <sup>2</sup> .h; Reverse solute flux: 4 (FO) / 6 (PRO) g/m <sup>2</sup> .h	[14]
PES/SPSf	Asymmetric (NIPS)	Water flux of PES/SPSf substrate (505 L/m <sup>2</sup> .h.bar) is higher than the PES substrate (411 L/m <sup>2</sup> .h.bar), mainly due to the greater mean pore size coupled with higher porosity.	FO/PRO	<b><sup>f</sup>TFC (PES/SPSf):</b> Water flux: 26 L/m <sup>2</sup> .h; Reverse salt flux: 8.3 g/m <sup>2</sup> .h  <b>HTI (Commercial):</b> Water flux: 13 L/m <sup>2</sup> .h; Reverse salt flux: 10.5 g/m <sup>2</sup> .h	[76]
PES/PESU-co-sPPSU11	Asymmetric (NIPS)	PES substrate blended with 50 wt% copolymer exhibited a fully sponge-like structure compared to the control PES substrate that showed finger-like structure. The blended substrate also showed higher porosity and larger surface pores.	FO/PRO	<b><sup>g</sup>TFC (PES/PESU-co-sPPSU11-50 wt%):</b> Water flux: 21 (FO)/33 (PRO) L/m <sup>2</sup> .h; Reverse solute flux: 2.2 (FO) / 2.8 (PRO) g/m <sup>2</sup> .h  <b>Control TFC (PES):</b> Water flux: 10.5 (FO)/13.5 (PRO) L/m <sup>2</sup> .h; Reverse solute flux: 3.1 (FO) / 3.7 (PRO) g/m <sup>2</sup> .h	[77]

<sup>a</sup> SPEK: Sulfonated poly(ether ketone); PESU-co-sPPSU11: sulfonated copolymer made of PES and sulfonated polyphenylsulfone;

<sup>b</sup> Testing conditions - Feed solution: pure water; Draw solution: 0.5 M NaCl; Orientation: PRO; Volumetric flow rate for feed and draw solution: 184 mL/min

<sup>c</sup> Testing conditions - Feed solution: pure water; Draw solution: 0.5 M NaCl; Orientation: FO; Velocity for feed and draw solution: 13.88 cm/s.

<sup>d</sup> Testing conditions – Feed solution: pure water; Draw solution: 2.0 M NaCl; Orientation: FO & PRO; Velocity for feed and draw solution: 8.5 cm/s. Power density was not shown as the PRO test was carried out without hydraulic pressure.

<sup>e</sup> Testing conditions - Feed solution: pure water; Draw solution: 2.0 M NaCl; Orientation: FO & PRO; Velocity for feed and draw solution: 0.2 L/min. Power density was not shown as the PRO test was carried out without hydraulic pressure.

<sup>f</sup> Testing conditions - Feed solution: pure water; Draw solution: 2.0 M NaCl; Orientation: FO; Velocity for feed and draw solution: 8.3 cm/s

<sup>g</sup> Testing conditions - Feed solution: pure water; Draw solution: 2.0 M NaCl; Orientation: FO & PRO; Velocity for feed and draw solution: 8.33 cm/s. Power density was not shown as the PRO test was carried out without hydraulic pressure.

### 3.2 *Polymer/Inorganic Nanocomposite Substrates*

Another strategy to improve the substrate properties of composite membrane is by introducing hydrophilic nanofillers (solid or mesoporous) into microporous substrates. This section will review the roles of two types of nanofillers (solid and mesoporous) on the substrate properties and how the changes in the nanocomposite substrates led to improved TFC membrane performance for water applications.

#### 3.2.1 *Substrates Incorporated with Non-Porous Nanofillers*

Table 2 compares some of the relevant works studied the impacts of solid nanofillers on substrate characteristics that might affect TFC membrane performance for different water applications. Although the substrate of the TFC membrane for the NF and RO process does not seem to play key role in improving antifouling properties, it does to certain extent affect the characteristics of polyamide layer formed and alter membrane water flux and rejection. Any modification done on the substrate tends to influence the amine and acyl chloride monomers reaction, forming polyamide layer with different cross-linking degree, thickness, surface roughness, pore size, etc. It has also been reported that the incorporation of charge nanoparticles into the substrate matrix could induce higher polyamide charge density, leading to improved salt rejection and better antifouling characteristics [78]. As the polyamide layer is of several hundreds of nanometers, it is less likely that the charge property is induced by the substrate. Instead, it is more likely that the substrate affects the degree of polyamide cross-linking which further alters the surface charge properties.

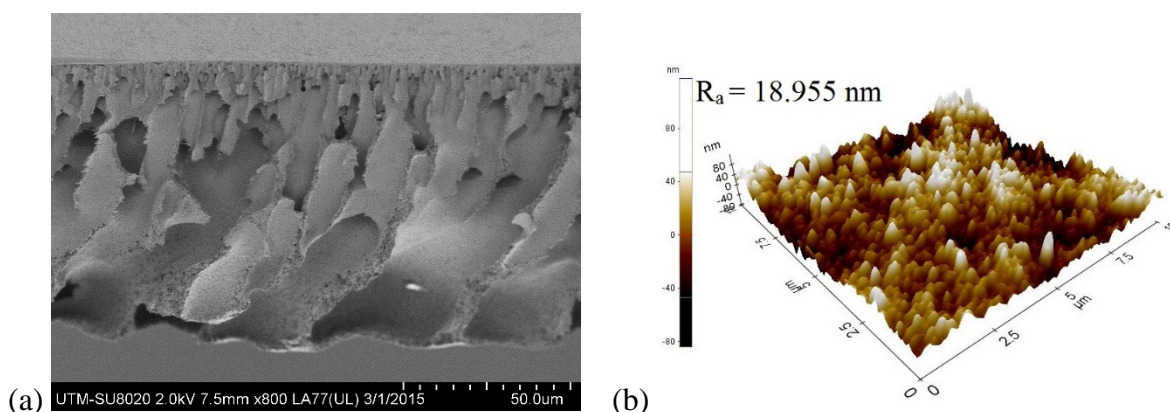
Among the nanoparticles used to modify the polymeric substrates, titanium dioxide ( $\text{TiO}_2$ ) perhaps is the most famous nanomaterials reported in the literature. Its impacts have been evaluated for microporous substrates (UF membranes) made of a wide of polymeric materials [79–83]. Mollahosseini and Rahimpour [84] studied the effect of  $\text{TiO}_2$  loading (0.1, 0.3 and 0.5 wt%) on the PSf substrate and its impacts on the TFC NF membranes morphology and performance. They reported that by incorporating 0.5 wt%  $\text{TiO}_2$ , a smoother and defect-less polyamide surface can be formed. The high-water affinity of  $\text{TiO}_2$  significantly increased the membrane flux due to its polar groups. In addition to enhanced salt rejections, the  $\text{TiO}_2$ -modified TFC membranes also induced greater resistance against organic foulants and exhibited antibacterial effect against *E. coli* growth.

Promising results were also reported by Emadzadeh et al. [16] in which PSf- $\text{TiO}_2$  substrates with varying nanoparticle content (0.5, 0.75 and 1.0 wt%) were used for TFC RO membrane fabrication. The  $\text{TiO}_2$ -modified substrates showed significant enhancement in water



flux which is mainly attributed by the improved surface hydrophilicity (lower water contact angle) coupled with higher porosity. The substrate incorporating 1.0 wt%  $\text{TiO}_2$  demonstrated  $855 \text{ L/m}^2\cdot\text{h}$  (tested at 2.5 bar) water flux,  $58^\circ$  contact angle and 81% porosity in comparison to  $163 \text{ L/m}^2\cdot\text{h}$ ,  $71^\circ$  and 71%, respectively shown by the pristine substrate. Nevertheless, this modified substrate (incorporated with highest  $\text{TiO}_2$  quantity) tended to produce TFC membrane with reduced separation efficiency ( $<75\%$  NaCl rejection) owing to the formation of reduced cross-linked polyamide layer caused by localized defects spotted on the substrate surface. In order to produce TFC membrane with good balance performance, the authors found that 0.5%  $\text{TiO}_2$  is the optimum loading to modify substrate properties, producing TFC membrane that could overcome trade-off effect of water flux and rejection encountered by TFC membrane made of pristine substrates.

In recent years, special efforts were devoted to develop new type of TFC membranes using substrates embedded with graphene oxide (GO). GO is of superior hydrophilicity and possesses high level of negative charge resulted from abundant oxygen functional groups such as epoxy, carboxyl and hydroxyl groups. Lai et al. [17] incorporated 0.3 wt% GO (optimum loading) into the PSf substrate and found the substrate exhibited larger microvoids (higher porosity) and rougher surface upon nanomaterials incorporation (see Figure 13), in addition to improved surface hydrophilicity (contact angle reduced from  $78.2^\circ$  to  $69.8^\circ$ ). Using the optimized GO-PSf nanocomposite substrate, the resultant TFC NF membrane exhibited 50.9% higher water flux ( $2.43 \text{ L/m}^2\cdot\text{h}\cdot\text{bar}$ ) compared to the control TFC membrane ( $1.61 \text{ L/m}^2\cdot\text{h}\cdot\text{bar}$ ) without compromising the salt rejection. From zeta potential measurements, the GO-modified substrate was able to increase the TFC membrane surface charge, leading to promising salt rejection towards multivalent salts (95.2% and 91.1% rejection for  $\text{Na}_2\text{SO}_4$  and  $\text{MgSO}_4$ , respectively).





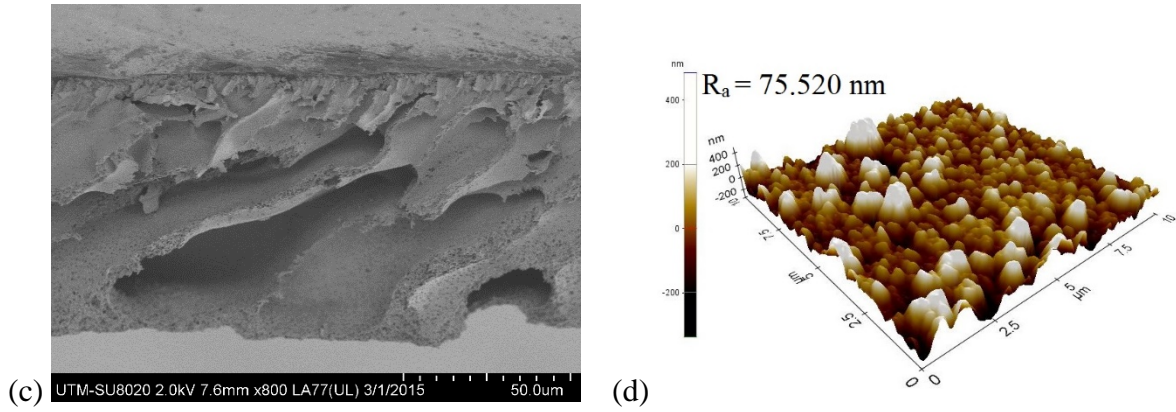
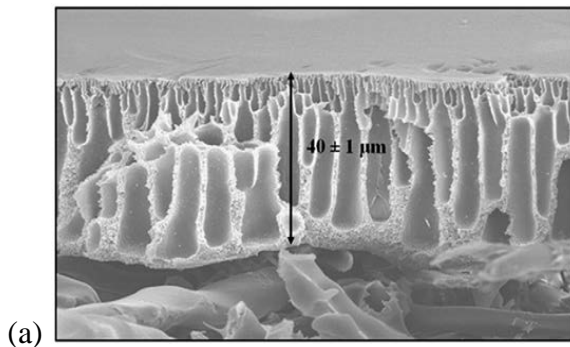


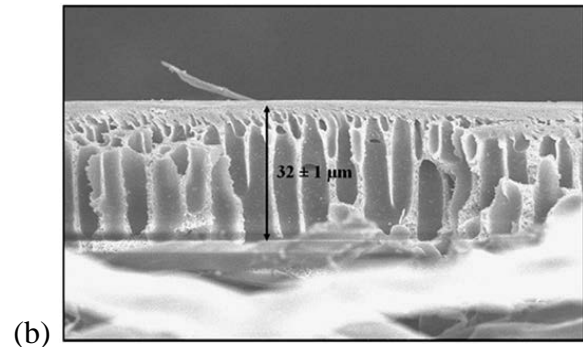
**Figure 13.** FESEM cross-sectional images (left) and AFM surface images (right) for (a,b) PSf substrate and (c,d) PSf substrate modified by 0.3 wt% GO [17].

As RO process typically requires high operating pressure to overcome the osmotic pressure of feed solution, the mechanical property of TFC RO membrane is particularly important for long term stability. The work carried out by Pendergast et al. [85] in 2010 was the first to study the effects of nanofillers on the membrane compaction behavior during RO process. Silica ( $\text{SiO}_2$ ) nanoparticles were embedded into the PSf substrate, which was then used in the interfacial polymerization process to prepare TFC membranes. In addition the flux enhancement, the  $\text{SiO}_2$ -modified TFC membrane also experienced lower flux decline ( $\sim 28\%$ ) than that of unmodified membrane ( $\sim 32\%$ ) when both membranes were compacted at 250 psi for  $> 400$  min. The existence of nanofillers was believed to have provided necessary mechanical support to mitigate the porous structure collapse by preventing thin layer from reduction upon high-pressure operation as shown in Figure 14.

#### Before compaction



#### After compaction



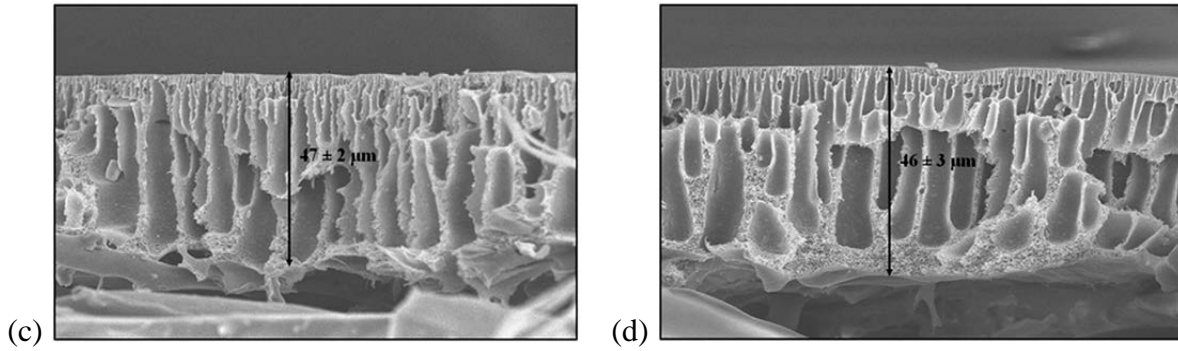


**Figure 14.** SEM cross-sectional images of (a,b) unmodified TFC and (c,d) SiO<sub>2</sub>-modified TFC membrane (labeled as ST50-TFC in the work) before and after compaction at 250 psi [85].

Compared to the substrates of TFC membranes applied for NF/RO process, research has shown that modified substrate plays a more significant role in the engineered osmosis process that directly deals with aqueous solution either in FO or PRO mode. In FO mode, the substrate of TFC membrane will contact with draw solution in which the substrate with smaller *S* parameter value tends to have lower ICP effect and higher water flux. For PRO mode, it will contact with feed solution (solution wanted to be treated) and the high hydrophilicity of it enables better antifouling properties and is more sustainable for long run.

Emadzadeh et al. [16,86,87] explored the possibility of using TiO<sub>2</sub>-modified substrates to prepare TFC membranes, aiming to achieve small *S* parameter value to minimize ICP effect during FO/PRO process. As reported, the membrane water flux when tested at FO and PRO mode was improved by 86–93% using the substrates incorporating appropriate TiO<sub>2</sub> quantity. The use of 0.5 wt% TiO<sub>2</sub>-modified substrate could produce TFC membrane with water flux of 17.1 (FO) and 31.2 L/m<sup>2</sup>.h (PRO) when tested using 10 mM NaCl as feed solution and 0.5 M NaCl as draw solution [88]. Their reverse draw solute fluxes were recorded at 2.9 and 6.7 g/m<sup>2</sup>.h, respectively under the same testing conditions. The authors explained that the decrease in *S* parameter value was a direct result of the formation of more hydrophilic substrate with more finger-like macrovoids, higher porosity and pore size which in turn, reduced the tortuosity. However, the use of high loading TiO<sub>2</sub> nanoparticles (0.75 and 1 wt%) was not advisable as it tended to increase reverse solute flux due to formation of a less cross-linked polyamide layer.

Park et al. [89] fabricated a series of TFC membranes using PSf substrate incorporated with various GO loadings (0.1 to 1.0 wt%). From Figure 15, the TFC membrane made of 0.25 wt% GO-modified substrate (labelled as GOT-0.25) exhibited the highest *J<sub>v</sub>* and moderate *J<sub>s</sub>* among all the membranes studied. The improvement in membrane water permeability is mainly due to reduced *S* parameter of substrate layer (191 μm) as well as improved substrate

hydrophilicity (contact angle of 62°). Similar to TiO<sub>2</sub>, excessive use of GO (> 0.5 and 1.0 wt% in dope solution) tended to negatively affect TFC membrane performance (as shown in GOT-0.5 and GOT-1.0 membranes) owing to severe nanoparticle agglomeration, leading to increased  $J_s$  value and reduced  $J_v/J_s$  selectivity.

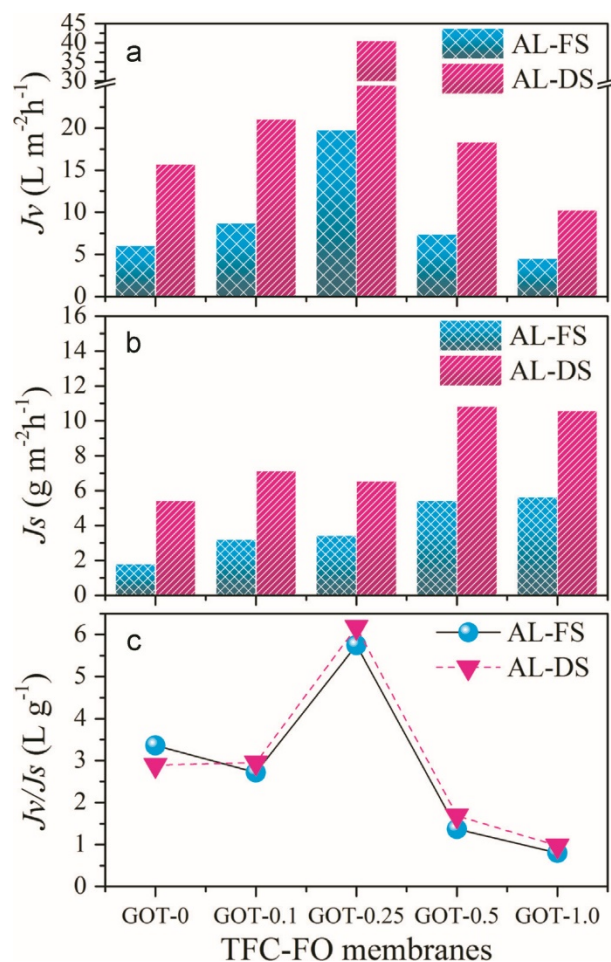


**Figure 15.** Effect of GO loading on the substrate for TFC membrane performance, (a) water flux,  $J_v$ , (b) reverse salt flux,  $J_s$  and (c)  $J_v/J_s$  selectivity [89].

A new approach was presented by Lim et al. [90] to fabricate dual-layered GO-incorporated substrate using two casting blades in which both top and bottom layer contained same amount of GO (0.25 wt%) but different PSf concentration (15 and 7 wt%, respectively) as illustrated in Figure 16. Lower polymer concentration was used for the bottom layer in order to maximize porosity and mitigate ICP. As GO was incorporated into both layers, the TFC FO membrane with improved S parameter value (130  $\mu m$ ) and hydrophilic properties were produced, achieving FO water flux of 33.8  $L/m^2.h$  and  $J_v/J_s$  selectivity of 0.19 using DI water as feed and 1 M NaCl as draw solution. These results were better compared to the membrane

with single-layered substrate ( $20.0 \text{ L/m}^2\cdot\text{h}$  and  $0.39$ ) and dual-layered substrate without GO incorporation ( $30.3 \text{ L/m}^2\cdot\text{h}$  and  $0.32$ ).

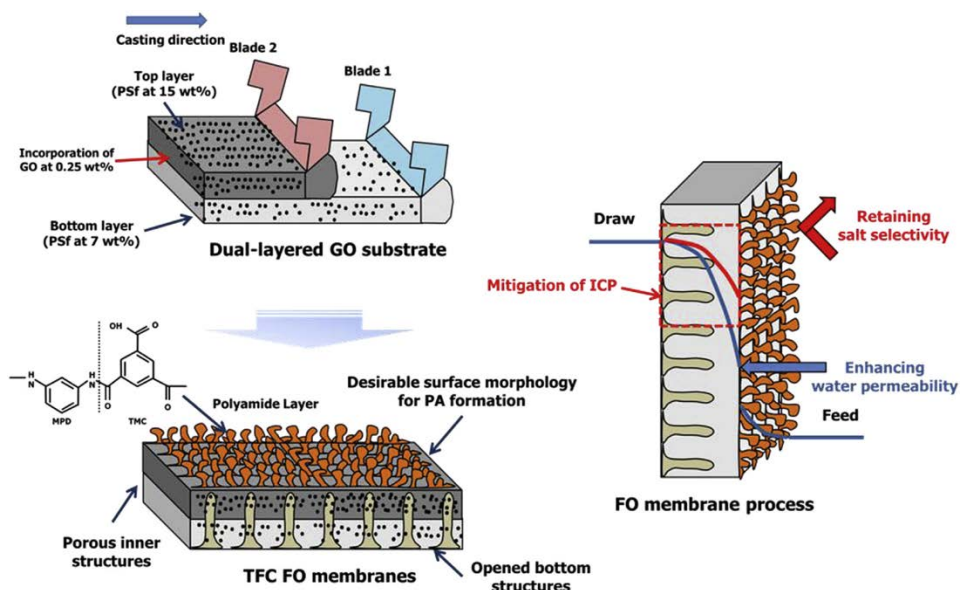


**Figure 16.** Approach of fabricating dual-layered GO-incorporated PSf substrate for TFC FO membrane [90].

In addition to the substrate made of single type of nanofiller, Sirinupong et al. [91] modified the TFC membrane using substrate incorporating  $\text{TiO}_2/\text{GO}$  mixture and compared the membrane performance with substrates made of  $\text{TiO}_2$  and GO, respectively. Both the surface hydrophilicity and roughness of pristine substrates were reported to increase upon incorporation of nanomaterials. However, substrates with long finger-like voids extended from the top to the bottom could only be developed using either  $\text{TiO}_2$  or  $\text{TiO}_2/\text{GO}$  mixture. The improved surface hydrophilicity and favorable structure formed in these two substrates are the main factors leading to higher water flux of TFC membranes. More importantly, there were no significant increase in reverse draw solute flux in FO and PRO process in comparison to the control TFC membrane.

Using hybrid nanomaterial - graphene oxide modified graphitic carbon nitride (CN-rGO), Li et al. [92] produced a series of substrates with varying properties by manipulating the nanomaterial concentration in the range of 0.2–1.0 wt%. It has been shown that the optimal pore structure and enhanced wettability of modified substrate (0.5 wt% CN-rGO) could contribute to lower S parameter value, making the TFC membrane to achieve  $26.3 \text{ L/m}^2\cdot\text{h}$  water flux in FO mode using DI water as feed and 2 M NaCl as draw solution. Such result was 20% higher than that of control TFC membrane.

Rastgar et al. [93] dispersed 0.1–2.0 wt% zinc oxide (ZnO)-SiO<sub>2</sub> core-shell nanoparticles within PES substrate in order to improve sublayer properties of TFC FO membrane. All the ZnO-SiO<sub>2</sub>-incorporated substrates exhibited lower contact angle than the neat substrate, mainly due to the presence of hydrophilic nanoparticles that improved surface affinity towards water. ZnO-SiO<sub>2</sub> was also potential to develop substrate with long finger-like structures following the enhanced exchange rate between solvent and non-solvent during phase inversion. Such finger-like microvoids possessed low tortuosity to facilitate water flowing through the substrate. A good balance between water flux and reverse draw solute flux of membrane could be attained with the use of substrate incorporated with 1.0 wt% ZnO-SiO<sub>2</sub>. This membrane recorded the highest water fluxes of 33.5 (FO mode) and 50.1 L/m<sup>2</sup>.h (PRO mode) compared to the unmodified TFC membrane that showed 15.4 and 26.0 L/m<sup>2</sup>.h, respectively.

Similar to the approach adopted by Lim et al. [90], Liu and Ng [94] also fabricated double-layer flat sheet substrate for TFC membrane, but only the bottom layer of substrate was embedded with nanomaterials (SiO<sub>2</sub>), as illustrated in Figure 17. Compared to the conventional single-blade casted PSf-SiO<sub>2</sub> substrate, the double-layer substrate exhibited a smooth surface (top layer) that is beneficial for formation of a defect-free polyamide layer. Besides achieving greater salt rejection and water flux, the resultant TFC membrane made of double-layer substrate could retain a relatively low reverse salt flux (7.4 and 16.0 g/m<sup>2</sup>.h in FO and PRO mode, respectively) compared to the conventional membrane (10.1 and 16.7 g/m<sup>2</sup>.h, respectively) when tested with 1 M NaCl as draw solution and DI water as feed solution.

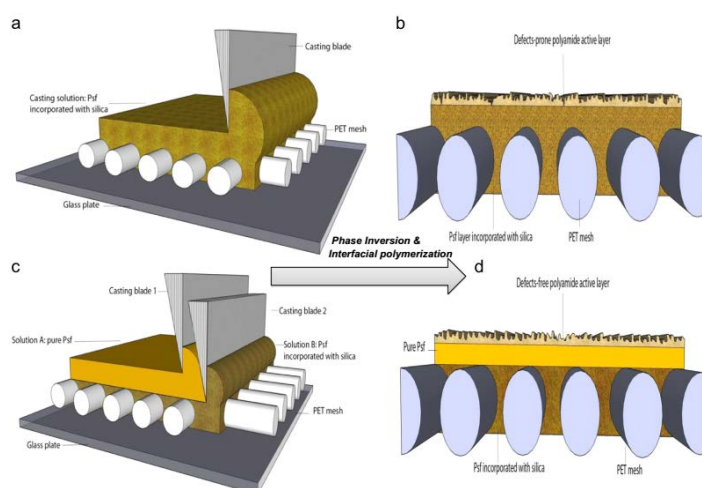


**Figure 17.** Schematic diagram of (a,b) single-blade and (c,d) double-blade casting in fabricating nanocomposite substrate for TFC membrane [94].



Attempt has also been made to evaluate the potential of layered double hydroxide (LDH) nanoparticles for TFC membrane fabrication owing to the unique features of LDH that contain  $Mg^{2+}$ ,  $Al^{3+}$  and water molecules in its interlayer space. In 2016, Lu et al. [95] firstly reported on TFC membranes made of LDH-modified substrates for FO application. The addition of LDH not only improved the substrate morphologies with respect to porosity, hydrophilicity and surface pore, but also its mechanical strength and thermal stability as presented in Figure 18. Results indicated that the TFC FO membrane made of 2 wt% LDH-modified substrate could attain promising water flux of 18.1 (FO mode) and 34.6  $L/m^2.h$  (PRO mode) when tested using DI water as feed solution and 1 M NaCl as draw solution. This is attributed to the lower S parameter value and improved substrate hydrophilicity. Pardeshi et al. [96] on the other hand also experienced similar improvement in the substrate properties upon addition of LDH into the PVC substrate. Incorporating 2 wt% LDH into substrate was potential to reduce S parameter value from 699  $\mu m$  in the control TFC membrane to 303  $\mu m$ , resulting in higher water fluxes for FO (37.5  $L/m^2.h$ ) and PRO (50.9  $L/m^2.h$ ) process when tested with DI water (feed solution) and 1 M NaCl (draw solution).

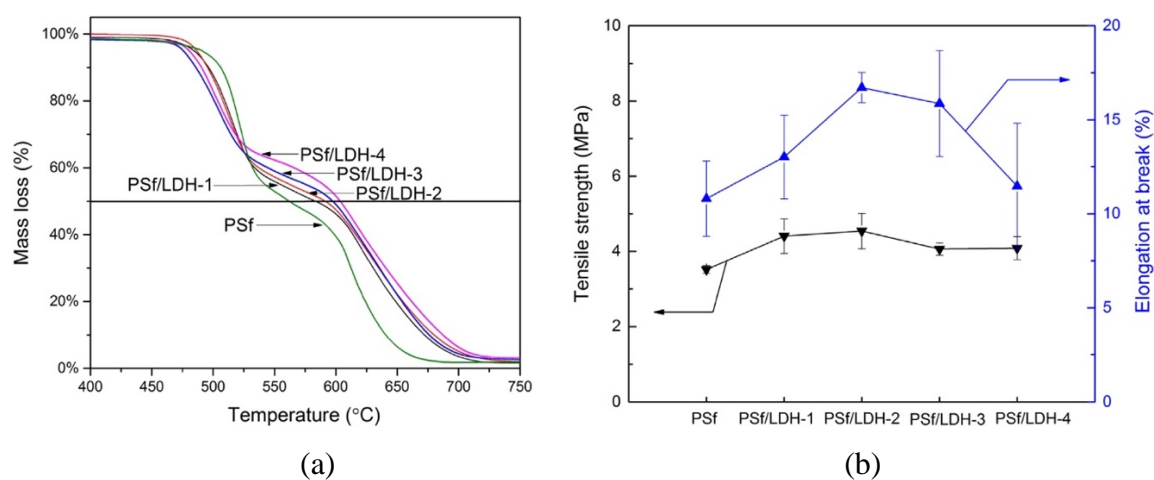


**Figure 18.** (a) TGA curves and (b) mechanical strength of PSf substrate with and without LDH nanoparticles modification. (Note: The number in the membrane designation indicated the loading of LDH nanoparticles in wt%) [95].

The potential of  $SiO_2$  was also evaluated in the nanofiber substrate in which Tian et al. [97] reported that an improved PEI-based nanofiber that exhibited less thermal compaction and porosity reduction during heat-press treatment could be obtained upon  $SiO_2$  incorporation. EDX mapping indicated that the  $SiO_2$  was uniformly distributed throughout the nanofibrous substrates regardless of nanofiller quantity (0.16, 0.8 and 1.6 wt%). Particularly for the substrate

incorporating 1.6 wt% SiO<sub>2</sub>, promising characteristics were achieved, leading to as high as 85% porosity and low S parameter value of 174 μm. The unique structural properties were reported to be able to facilitate faster water transfer during engineered osmosis process which resulted in high water flux of 42 L/m<sup>2</sup>.h in FO mode and 73 L/m<sup>2</sup>.h in PRO mode with DI water as feed and 1 M NaCl as draw solution. Similar flux enhancement on TFC membrane was also reported by Zhang et al. [98] when TiO<sub>2</sub> was incorporated into PSf nanofiber substrates.



**Table 2.** Summary of non-porous nanofillers used in modifying microporous substrates of TFC membranes.

Nanofiller	Properties	Substrate polymer	Filler loading	Performance of modified substrate and its impact on TFC membrane (compared to control substrate and TFC membrane)
TiO <sub>2</sub>	Structure: Spherical particles Size: < 21 nm Charge: 30 to –15 mV at pH 5-8 BET specific surface area: 35–65 g/m <sup>2</sup>	PSf (flat sheet)	0.1–0.5 wt% [84]	NF <ul style="list-style-type: none"> <li>• Smoother membrane surface and thicker polyamide layer</li> <li>• Improved membrane wettability and water flux</li> <li>• Better antifouling and antibacterial resistance</li> <li>• Best findings (0.5 wt% TiO<sub>2</sub>): Pure water flux: 49 L/m<sup>2</sup>.h; NaCl rejection: 84% (Control: 12 L/m<sup>2</sup>.h; 70%)</li> </ul>
			0.5–1.0 wt% [16]	FO <ul style="list-style-type: none"> <li>• Higher substrate hydrophilicity and porosity</li> <li>• Decrease in S parameter value and lower ICP</li> <li>• Best findings (0.5 wt% TiO<sub>2</sub>): J<sub>s</sub>/J<sub>w</sub>: 0.17 g/L in FO mode and 0.21 g/L in PRO mode (Control: 0.24 g/L in FO mode and 0.27 g/L in PRO mode)</li> <li>*Testing solutions: FS: 10 mM NaCl; DS: 0.5 M NaCl</li> </ul>
			0.1–0.9 wt% [86]	FO <ul style="list-style-type: none"> <li>• More finger-like macrovoids formed</li> <li>• Lower S parameter value and reduced ICP</li> <li>• Best findings (0.6 wt% TiO<sub>2</sub>): J<sub>s</sub>/J<sub>v</sub>: 0.39 g/L in FO mode &amp; 0.30 g/L in PRO mode (Control: 0.33 g/L in FO mode and 0.38 g/L in PRO mode)</li> <li>* Testing solutions: FS: DI water; DS: 0.5 M NaCl</li> </ul>
			0.5 wt% [87]	FO <ul style="list-style-type: none"> <li>• Greater water flux due to reduced ICP</li> <li>• Reduced BSA fouling tendency</li> <li>• Higher flux recovery rate (&gt; 92%) with simple water washing</li> </ul>
		PSf (nanofiber)	0.25–0.75 wt% [98]	FO <ul style="list-style-type: none"> <li>• Increased substrate hydrophilicity, porosity and pore size with additional of TiO<sub>2</sub></li> <li>• Best findings (0.25 wt% TiO<sub>2</sub>): J<sub>s</sub>/J<sub>v</sub>: 0.21 g/L in FO mode &amp; 0.23 g/L in PRO mode (Control: 0.24 g/L in FO mode &amp; 0.25 g/L in PRO mode)</li> <li>* Testing solutions: FS: DI water; DS: 1 M NaCl</li> </ul>
GO	Structure: Single to few-layer sheets Lateral size: < 21 μm Thickness: 0.9–1.0 nm	PSf (flat sheet)	0.1–0.5 wt% [17]	NF <ul style="list-style-type: none"> <li>• Improved substrate hydrophilicity which led to higher water flux</li> <li>• Higher polyamide charge properties</li> <li>• Best findings (0.3 wt% GO): PWF: 2.43 L/m<sup>2</sup>.h·bar &amp; Na<sub>2</sub>SO<sub>4</sub> rejection: 95.2%</li> </ul>

	Charge: −30 to −58 mV at pH 5–8			(Control: 2.43 L/m <sup>2</sup> ·h·bar & 94%)
			0.1–1.0 wt% [89]	FO <ul style="list-style-type: none"> <li>• Higher substrate porosity and larger pore sizes</li> <li>• Improved substrate hydrophilicity and reduced S parameter value</li> <li>• Best findings (0.25 wt% GO): J<sub>s</sub>/J<sub>v</sub>: 0.17 g/L in FO mode &amp; 0.16 g/L in PRO mode (Control: 0.30 g/L in FO mode &amp; 0.34 g/L in PRO mode)</li> </ul> <i>* Testing solutions: FS: DI water; DS: 0.5 M NaCl</i>
		PSf (dual-layered flat sheet)	0.25 wt% in both layers [90]	FO <ul style="list-style-type: none"> <li>• Substrate with highly porous bottom structure and dense top layer is formed via dual-blade casting</li> <li>• Modified membrane exhibited higher water permeability and ion selectivity owing to well-dispersed hydrophilic GO</li> <li>• GO-incorporated TFC membrane showed lowest J<sub>s</sub>/J<sub>v</sub>, i.e., 0.19 g/L in FO mode and 0.18 g/L in PRO mode (Control: 0.32 g/L in FO mode and 0.31 g/L in PRO mode)</li> </ul> <i>* Testing solutions: FS: DI water; DS: 1 M NaCl</i>
TiO <sub>2</sub> /GO	Mixing of TiO <sub>2</sub> (P25 Degussa) nanoparticles and GO nanosheets	PSf (flat sheet)	0.5 wt% (TiO <sub>2</sub> :GO ratio of 1:0, 0.5:0.5 or 0:1) [91]	FO <ul style="list-style-type: none"> <li>• More finger-like voids in substrate was resulted</li> <li>• Improved substrate surface hydrophilicity</li> <li>• Higher water flux in PRO and FO mode with minimal reverse draw solute flux</li> <li>• TFC membrane made of TiO<sub>2</sub>/GO mixture exhibited the optimal FO performance with J<sub>s</sub>/J<sub>v</sub> of 0.09 g/L in FO mode and 0.14 g/L in PRO mode (Control: 0.12 g/L in FO mode and 0.07 g/L in PRO mode)</li> </ul> <i>* Testing solutions: FS: DI water; DS: 0.5 M NaCl</i>
CN-rGO	Structure: Stacked nanosheets consists of CN and GO sheets	PES (flat sheet)	0.2–1.0 wt% [92]	FO <ul style="list-style-type: none"> <li>• Substrate with thinner upper layer thicker macrovoids sublayer was resulted</li> <li>• Enhanced substrate surface hydrophilicity which led to reduced ICP</li> <li>• Modified membrane (0.5 wt% CN/rGO) offered 20% greater flux compared to the control membrane</li> </ul> <i>* Testing solutions: FS: DI water; DS: 2 M NaCl</i>
SiO <sub>2</sub>	Structure: Spherical particles Size: 34–130 nm	PSf (flat sheet)	3.76 wt% [85]	RO <ul style="list-style-type: none"> <li>• Increased mechanical stability but decrease in physical compaction</li> </ul>

				<ul style="list-style-type: none"> <li>Higher water permeability was achieved along with promising salt rejection under high operating pressure</li> </ul>
	Structure: Spherical particles Size: 160–240 nm	PSf (dual-layered flat sheet)	1–4 wt% in bottom layer <a href="#">[94]</a>	FO/PRO <ul style="list-style-type: none"> <li>SiO<sub>2</sub>-impregnated porous bottom layer (with pure PSf as top layer) offered ideal interface for polyamide layer formation</li> <li>Improved substrate hydrophilicity and structure that reduced ICP</li> <li>Best water fluxes were recorded at 31.0 L/m<sup>2</sup>.h (FO) and 60.5 L/m<sup>2</sup>.h (PRO) with reverse solute flux in the range of 7.4–16 g/m<sup>2</sup>.h</li> </ul> <i>* Testing solutions: FS: DI water; DS: 1 M NaCl</i>
	Structure: Spherical particles Size: 5–15 nm	PEI (nanofiber)	0.16–1.6 wt% <a href="#">[97]</a>	FO/PRO <ul style="list-style-type: none"> <li>Increased substrate pore size and porosity</li> <li>Better resistance against thermal compaction</li> <li>Best findings (1.6 wt% SiO<sub>2</sub>): J<sub>s</sub>/J<sub>v</sub>: 0.12 g/L in FO mode and 0.10 g/L in PRO mode (Control: 0.26 g/L in FO mode and 0.21 g/L in PRO mode)</li> </ul> <i>* Testing solutions: FS: DI water; DS: 1 M NaCl</i>
ZnO-SiO <sub>2</sub>	Structure: Core-shell particles Size: 30–50 nm BET surface area: 1.46 m <sup>2</sup> /g Total pore volume: 5.09 cm <sup>3</sup> /g Mean pore diameter: 1.393 nm	PES (flat sheet)	0.1–2.0 wt% <a href="#">[93]</a>	FO/PRO <ul style="list-style-type: none"> <li>Substrate became more hydrophilic and porous</li> <li>Improved membrane surface hydrophilicity coupled with greater porosity led to higher permeate flux</li> <li>Best findings (0.5 wt% ZnO-SiO<sub>2</sub>): J<sub>s</sub>/J<sub>v</sub>: 0.43 g/L in FO mode and 0.34 g/L in PRO mode (Control: 0.40 g/L in FO mode; 0.41 g/L in PRO mode)</li> </ul> <i>* Testing solutions: FS: DI water; DS: 1 M NaCl</i>
LDH	Structure: Spherical particles Size: 20–30 nm Surface charge: 0.04 e Å <sup>-2</sup>	PSf (flat sheet)	1–4 wt% <a href="#">[95]</a>	FO/PRO <ul style="list-style-type: none"> <li>Increased substrate porosity and hydrophilicity</li> <li>Improved thermal and mechanical properties</li> <li>Decreased S parameter value due to formation of more finger-like macrovoids</li> <li>Best findings (2 wt% LDH): 18.1 L/m<sup>2</sup>.h in FO mode and 34.6 L/m<sup>2</sup>.h in PRO mode (Control: 12.7 L/m<sup>2</sup>.h in FO mode and 27.7 L/m<sup>2</sup>.h in PRO mode)</li> </ul> <i>* Testing solutions: FS: DI water; DS: 2 M NaCl</i>

	Structure: Spherical particles Size: 0.7–2.0 $\mu\text{m}$	PVC (flat sheet)	0.5–3 wt% <a href="#">[96]</a>	FO/PRO <ul style="list-style-type: none"> <li>▪ Increase in substrate surface hydrophilicity, pore size and porosity</li> <li>▪ Decrease in structural parameter resulted in lower ICP</li> <li>▪ Best findings (2 wt% LDH): <math>J_s/J_v</math>: 0.10 g/L in FO mode and 0.26 g/L in PRO mode            (Control: 0.17 g/L in FO mode and 0.36 g/L in PRO mode)</li> </ul> <i>* Testing solutions: FS: DI water; DS: 1 M NaCl</i>
--	---	---------------------	-----------------------------------	--

### 3.2.2 Substrates Incorporated with Mesoporous Nanofillers

In comparison to the solid nanofillers aforementioned, mesoporous nanofillers with unique structures (e.g., existence of pores/channels and larger surface area) hold a privileged position to act as modifier in preparing substrate of TFC membranes. Various hydrophilic nanotubes such as carbon nanotubes (CNTs), halloysite nanotubes (HNTs) and titania nanotubes (TNTs) have been evaluated for their potential in modifying microporous substrates in an attempt to render not only surface hydrophilicity and charge properties but also to achieve greater water permeability following the existence of additional water channels in the membrane matrix. This section will review the potential uses of different types of mesoporous nanofillers in substrate layer of composite membranes for enhanced water separation processes.

In 2013, Pendergast et al. [99] reported that by adding zeolite A nanoparticles into the substrate, the resultant membrane possessed higher initial flux and experienced less flux decline during high operating pressure process. The improved water stability could be attributed to the enhanced mechanical stability of substrate that resisted compaction and minimized the reduction in PSf substrate thickness as shown in Figure 19. As a result, the zeolite A-incorporated TFC membrane exhibited higher normalized water flux of 0.54 compared to 0.30 shown by the control TFC after being compacted at 225 psi for 4 h.

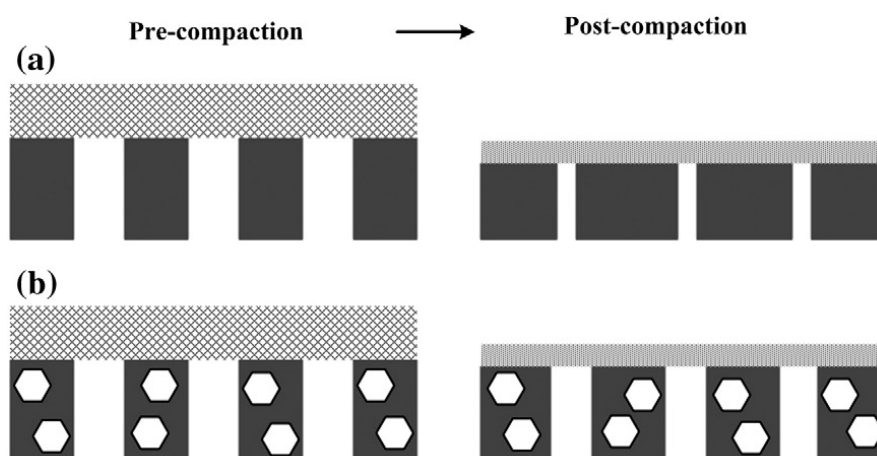


**Figure 19.** Schematic drawings showing physical changes to substrate during compaction in (a) TFC and (b) zeolite A-incorporated TFC membrane [99].

Separately, Son et al. [100] introduced 0.5 wt% carboxylated MWCNTs into substrate, aiming to increase RO membrane performance. In addition to the increased membrane hydrophilicity caused by the hydrophilic nanomaterials embedded, the presence of nanopores in the MWCNTs as shown in Figure 20 could act as water channels that contributed to 44%

flux enhancement in the TFN membrane, recording 1.21 L/m<sup>2</sup>.h.bar. High NaCl rejection (~96.1%) and better antifouling were also resulted following an increase in the membrane surface charge density that led to better repulsion towards anions. The improved surface charge was mainly due to oxygen-containing functional groups present in the MWCNTs.

Similar work was also conducted by Kim et al. [101] in which 5.0 wt% carboxylated MWCNTs were introduced into the PSf substrate of TFC membrane. The TEM image in Figure 21 clearly shows the winding linear arrangement of chemically-modified CNTs that are well-dispersed within the substrate. The filtration results further revealed that the water permeability of modified TFC membrane was increased by 23% due to the diffusive effect of nanopores in MWCNTs without compensating NaCl (88.4%) and Na<sub>2</sub>SO<sub>4</sub> (94.7%) rejection.

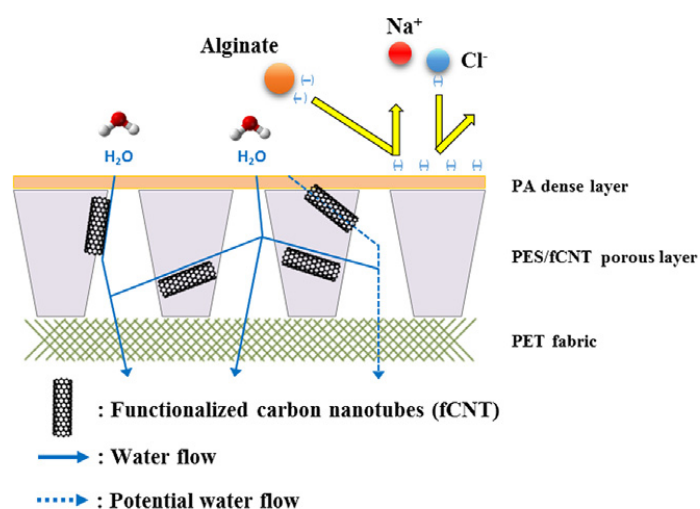


**Figure 20.** Transport mechanism of water molecules through MWCNTs incorporated nanocomposite TFN membrane [100].

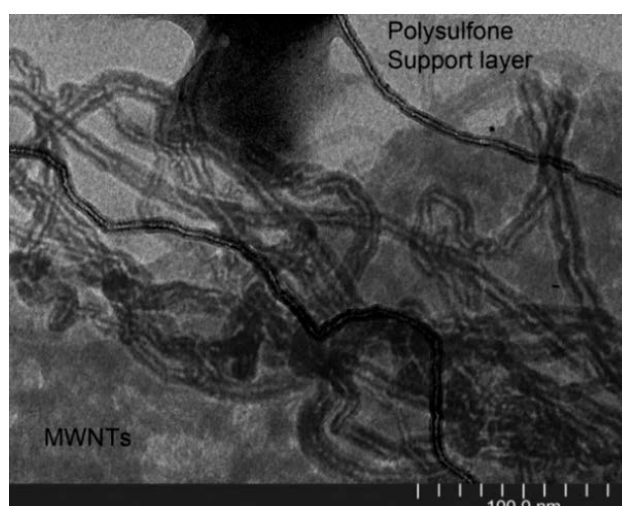


**Figure 21.** TEM image of PSf substrate embedded 5.0 wt% MWCNTs [101].



To fabricate a new type of TFC FO membrane, Tian et al. [102] incorporated hydrophilic f-CNTs into the PEI-based nanofiber substrate before subjecting the substrate to the interfacial polymerization. It is proven that the presence of f-CNTs was able to preserve the substrate porosity during heat-press treatment, maintaining the structural integrity. With respect to the separation performance, the addition of only 0.048 wt% f-CNTs in the substrate could reduce the value of S parameter of TFC membrane from 674 to 468  $\mu\text{m}$  (30% reduction), resulting in remarkable reduction in ICP effect during FO process. As a consequence, the modified TFC membrane achieved higher water flux of 22.1 (FO mode) and 45.0  $\text{L}/\text{m}^2\cdot\text{h}$  (PRO mode) using DI water as feed and 1 M NaCl as draw solution.

Using PAN nanofiber substrates modified by mesoporous  $\text{SiO}_2$ , Bui and McCutcheon [103] produced a series of TFC FO membranes for water applications. Figure 22 compares the PAN nanofibers modified by different quantity of mesoporous  $\text{SiO}_2$ . Nanoparticles were shown to be successfully embedded either within or at the surface of nanofibers, but the appearance of  $\text{SiO}_2$  nanoparticles clusters were more pronounced at higher silica loadings (10 and 15 wt%). Nevertheless, the mechanical strength tests indicated that even at the highest loading of nanoparticles, the mechanical integrity of the membranes was maintained. The use of extremely large surface area of mesoporous  $\text{SiO}_2$  ( $672.7 \text{ m}^2/\text{g}$ ) was the key factor causing the specific surface area of nanofiber substrate to be increased by a factor of 75. The positive features introduced by mesoporous  $\text{SiO}_2$  have resulted the TFC membrane to exhibit a remarkable 7-fold and 3.5-fold enhancements in osmotic water permeability and water/sodium chloride selectivity, respectively, compared to standard commercial FO membrane (HTI-CTA).

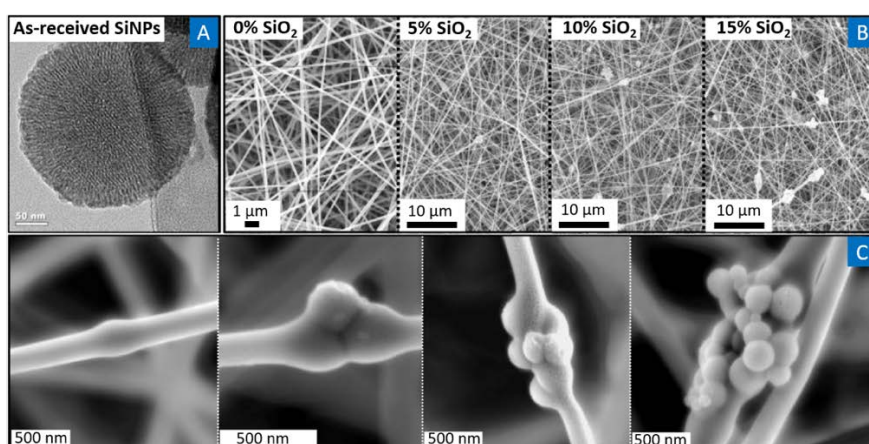


**Figure 22.** TEM images of (a) mesoporous  $\text{SiO}_2$ , (b) nanoparticles-embedded PAN nanofibers at different  $\text{SiO}_2$  loading and (c) zoom-in images showing  $\text{SiO}_2$  dispersion in nanofiber [103].

Similar to Pendergast et al. [99], Ma et al. [104] also utilized zeolite A in modifying the substrate of composite membranes. However, the membranes were developed specifically for FO/PRO process. With the embedment of 0.5 wt% zeolite, the PSf substrate showed improved surface porosity and hydrophilicity (contact angle reduced from 53° to 50°). The improved substrate properties have led the TFC membrane to exhibit higher pure water permeability than the conventional TFC membrane with NaCl rejection maintained at >90%. The significant reduction in the S parameter value of modified TFC membrane (from 0.96 nm in the control TFC to 0.34 nm) has lowered the ICP effect of engineered osmosis membranes, improving the membrane water flux in both PRO and FO process as shown in Figure 23.

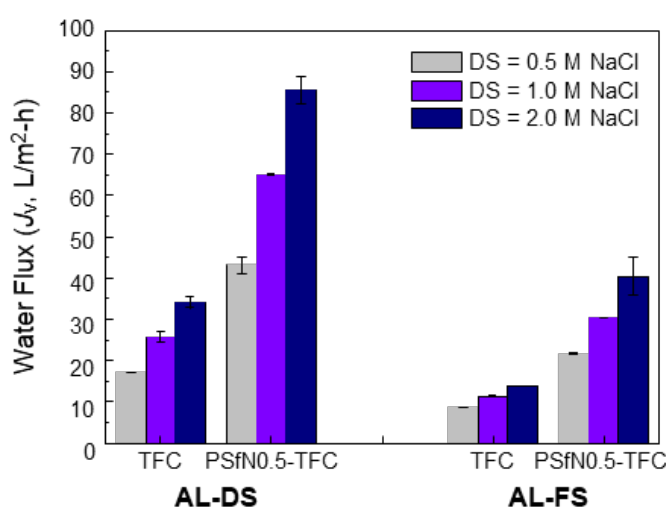


**Figure 23.** Filtration performance of TFC and modified TFC membrane during PRO (AL-DS) and FO (AL-FS) process using different concentration of draw solution (DS) [104] .

On the other hand, Ghanbari et al. [105] incorporated a much cheaper and easy harvested nanomaterials - HNTs into microporous substrate. With geometry similar to CNTs, HNTs are of highly hydrophilic in nature owing to the presence of abundant hydroxyl groups. The researchers found out that with only 0.5 wt% HNTs embedded in the PSf substrate, the overall substrate porosity, mean pore size and hydrophilicity were increased. This contributed to lower S parameter value (~40% lower than the control membrane) and reduced ICP effect. The nanochannels provided by HNTs were likely to improve water flux during FO as claimed by the authors. However, when the high HNTs loading was used (1.0 wt%), the polyamide cross-linking degree was negatively affected which led to lower NaCl rejection. In 2017, Pan et al. [106] synthesized 100–200 nm long INTs with inner diameter of approximately 1 nm (Figure 24) and used the nanotubular aluminosilicate to fabricate nanocomposite substrate. Comparing

to CNTs, INTs show outstanding hydrophilicity due the existence of large amounts of hydroxyl groups not only on their outer wall, but also inner structure. When INTs were dispersed in the PSf substrate, the surface hydrophilicity and porosity were improved, resulting in higher water flux and smaller S parameter value in the TFC membranes. As reported, this newly developed membranes could overcome the severe ICP effect encountered by typical TFC membranes, offering higher water permeability during FO process.

Despite the significantly greater advantages offered by the mesoporous nanofillers (e.g., larger surface area and existence of narrow channel), it is still scientifically unclear if the mesoporous nanofillers do offer a relatively less resistance pathway for water molecules to pass through when they are embedded within the polymeric matrix, leading to water flux improvement. Additional research needs to be conducted to verify the water and ion transport mechanism for these membranes, as improved flux has also been demonstrated for non-porous nanoparticles.

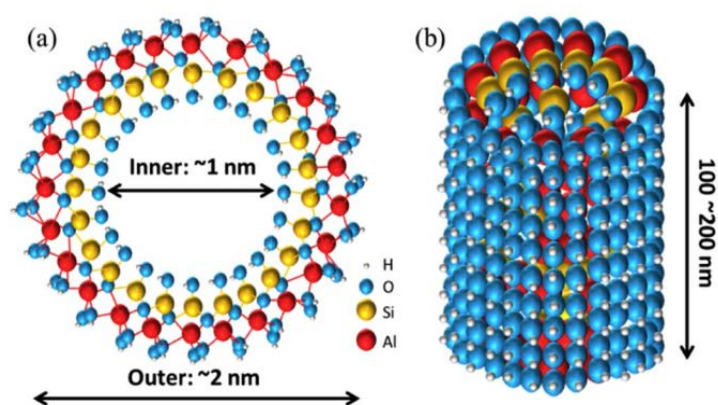


**Figure 24.** Atomic structure of nanotubular aluminosilicate - imogolite nanotubes (INTs) [106].

**Table 3.** Summary of mesoporous nanofillers used in modifying microporous substrates of TFC membranes.

Nanofiller	Properties	Substrate polymer	Filler loading	Performance of modified substrate and its impact on TFC membrane (compared to control substrate and TFC membrane)
Mesoporous SiO <sub>2</sub>	Structure: Mesoporous spherical particles Size: 200 nm Pore size: 4 nm Specific surface area: 672.7 m <sup>2</sup> /g	PAN (nanofiber)	5–15 wt% [103]	FO <ul style="list-style-type: none"> <li>• Mechanical integrity of nanofibers was enhanced with mesoporous SiO<sub>2</sub>, in addition to improved water flux.</li> <li>• Best performing modified membrane showed reduced S parameter value and exhibited 7-time higher osmotic water permeability.</li> </ul>
Zeolite A	Structure: Mesoporous irregular spherical particles Size: 250–300 nm Zeta potential: –13 to –15 mV	PSf (flat sheet)	3.76 wt% [99]	RO <ul style="list-style-type: none"> <li>• Compaction resistance of substrate was improved along with better hydrophilicity.</li> <li>• Irreversible flux decline was enhanced due to better compaction resistance.</li> <li>• Modified TFC membrane showed improvement in both water permeability (~12.5 µm/MPa.s) and NaCl rejection (93%). (Control: ~2.0 µm/MPa.s; 85%)</li> </ul>
	Structure: Mesoporous irregular spherical particles Size: 40–150 nm		0.1–1.0 wt% [104]	FO/PRO <ul style="list-style-type: none"> <li>• Improved substrate hydrophilicity and porosity reduced water transport resistance and enhanced water flux.</li> <li>• Lower S parameter value of modified substrate improved TFC membrane performance, recording J<sub>v</sub> of 31.1 L/m<sup>2</sup>.h in FO mode and 64.8 L/m<sup>2</sup>.h in PRO mode. (Control: 12.1 L/m<sup>2</sup>.h in FO mode and 26.2 L/m<sup>2</sup>.h in PRO mode)</li> </ul> <p>* Testing solutions: FS: DI water; DS: 1 M NaCl</p>
MWCNTs	Structure: Cylindrical multiwalled tube Average diameter: 5–10 nm Length: 10–30 µm Specific surface area: >200 m <sup>2</sup> /g	PSf (flat sheet)	1.0–5.0 wt% [101]	NF <ul style="list-style-type: none"> <li>• Substrate hydrophilicity was improved upon incorporation of MWCNTs that contained hydrophilic functional groups.</li> <li>• The presence of MWCNTs in substrate also offered nanopores for better water diffusion and increased TFC membrane permeability.</li> <li>• Using substrate incorporated with 5 wt% MWCNTs, the TFC membrane showed 23% higher water flux than the control TFC membrane.</li> </ul>
	Structure: Cylindrical multiwalled tube	PES (flat sheet)	0.5 wt% [100]	RO <ul style="list-style-type: none"> <li>• Increased substrate hydrophilicity, average pore size, total pore area and porosity upon addition of MWCNTs.</li> </ul>

	Outer diameter: 10–15 nm Inner diameter: 5 nm Length: 500 nm			<ul style="list-style-type: none"> <li>• The presence of MWCNTs also rendered substrate to become more negatively charged, resulted in better antifouling properties.</li> <li>• Modified TFC membrane showed enhancement on water flux, achieving water permeability of 1.21 L/m<sup>2</sup>.h.bar and NaCl rejection of 96.1%. (Control: 0.84 L/m<sup>2</sup>.h.bar; 95%) <i>* Testing conditions: 2000 ppm NaCl at 20 bar</i></li> </ul>
	Structure: Cylindrical multiwalled tube Outer diameter: ~11 nm Length: 10 µm	PEI (nanofiber)	0.048 wt% [102]	FO/PRO <ul style="list-style-type: none"> <li>• Better mechanical strength of modified substrate</li> <li>• Higher porosity coupled with larger substrate pore size resulted in lower ICP effect.</li> <li>• FO water flux of modified TFC membrane is improved by at least 2 times.</li> <li>• Modified TFC membrane offered lower J<sub>s</sub>/J<sub>v</sub> in FO (0.39 g/L) and PRO (0.10 g/L) mode. (Control: 0.42 g/L in FO mode; 0.22 g/L in PRO mode) <i>* Testing solutions: FS: DI water; DS: 1 M NaCl</i></li> </ul>
	Structure: Cylindrical multiwalled tube Outer diameter: 10–20 nm Length: 1–5 µm	PES (flat sheet)	0.5–2.5 wt% [107]	FO/PRO <ul style="list-style-type: none"> <li>• Improved surface chemistry and structural properties of modified substrate led to reduced S parameter value and enhanced water flux of TFC membrane without compromising J<sub>s</sub>/J<sub>v</sub> selectivity.</li> </ul>
HNTs	Structure: Cylindrical tubes Inner tube diameter: 5–15 nm	PSf (flat sheet)	0.2–1.0 wt% [105]	FO/PRO <ul style="list-style-type: none"> <li>• Improved substrate hydrophilicity coupled with additional hollow nanotubular channels offered greater water transport rate.</li> <li>• At optimum loading (0.5 wt% HNTs), the resultant TFC membrane exhibited promising water flux and low reverse solute flux. Its J<sub>v</sub> at FO and PRO mode was recorded at 27.7 and 42.3 L/m<sup>2</sup>.h, respectively. (Control: 13.3 L/m<sup>2</sup>.h in FO mode and 26.0 L/m<sup>2</sup>.h in PRO mode) <i>* Testing solutions: FS: 10 mM NaCl; DS: 2 M NaCl</i></li> </ul>
INTs	Structure: Cylindrical tube Outer diameter: 2 nm Inner diameter: 1 nm Length: 100–200 nm	PSf (flat sheet)	0.33–1.0 wt% [106]	FO/PRO <ul style="list-style-type: none"> <li>• Hydrophilicity, porosity and roughness of substrate were increased upon incorporation of INTs.</li> <li>• The presence of INTs could reduce S parameter value, but optimal INTs loading (0.66 wt%) is important to achieve</li> </ul>

				<p>good balance between water flux and reverse draw solute flux. Its <math>J_v</math> at FO and PRO mode was recorded at 7.6 L/m<sup>2</sup>.h and 9.8 L/m<sup>2</sup>.h, respectively.            (Control: 1.0 L/m<sup>2</sup>.h in FO mode and 1.13 L/m<sup>2</sup>.h in PRO mode)  <i>* Testing solutions: FS: DI water; DS: 1 M NaCl</i></p>
--	--	--	--	---



### 3.3 *Surface-modified Substrates*

Unlike bulk modification methods, surface modifications based on coating, cross-linking and UV-grafting approach are able to maintain the structural integrity of substrates without compromising their mechanical properties. Although many studies have found that the surface-modified substrates could improve the antifouling properties of the TFC membranes for NF and RO process [108], the findings are not very convincing as the surface fouling of the TFC membranes is mainly governed by the physical and chemical properties of polyamide selective layer rather than the substrate properties. Nevertheless, the changes in substrate properties upon modification that affect the morphology and cross-linking degree of polyamide are highly possible to influence TFC membrane performances including antifouling propensity.

In the past, attention has been paid to tailor the substrate pore structures (e.g., porosity, pore-size distribution, and substructure resistance) and its surface wettability as it is believed that the changes in these parameters tend to influence the formation of polyamide layer and thus separation performance [109,110]. Nevertheless, efforts have also been devoted to hydrophilize the substrate by surface coating with the hydrophilic interlayer prior to interfacial polymerization process, aiming to improve characteristics of polyamide layer formed [109,111].

Zhang et al. [109] conducted coating process on the PSf substrate surface using polyphenol synthesized by co-deposition of tannic acid (TA) and diethylenetriamine (DETA) prior to interfacial polymerization. The procedure of the substrate surface modification for TFC NF membrane fabrication is schematically shown in Figure 25. The as-prepared TFC membranes with a co-deposition time of 50 min exhibited nearly triple fold of water flux ( $63 \text{ L/m}^2\text{.h}$ ) compared to the control TFC membrane ( $26 \text{ L/m}^2\text{.h}$ ) made of pristine PSf substrate when tested with 2000 ppm  $\text{Na}_2\text{SO}_4$  feed solution at 0.6 MPa. The salt rejection of the modified membrane meanwhile maintained at  $>98\%$  due to formation of a thin and defect-free polyamide selective layer. The polyphenol interlayers rendered the substrates easier to be wetted by the aqueous diamine solution and help to promote the diffusivity rate of PIP from the TA/DETA-PSf substrates to the oil phase.

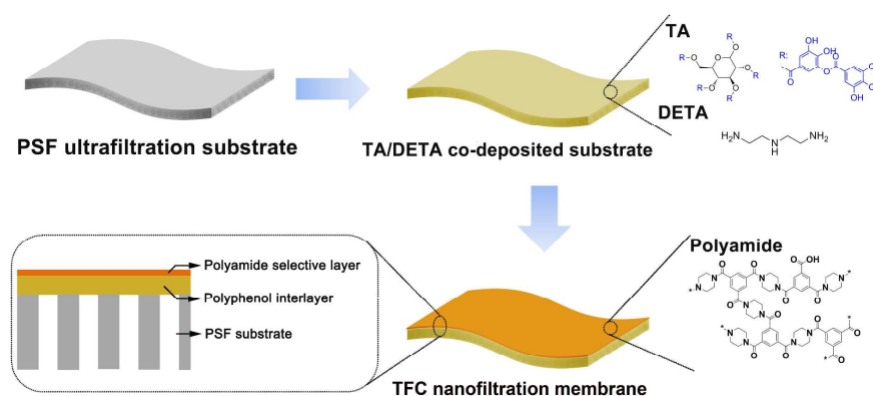


**Figure 25.** Schematic diagram for fabricating TFC NF with a polyphenol interlayer [109].

Separately, Li et al. [112] deposited polydopamine (PDA) on the PES substrate surface before initiating interfacial polymerization between PIP and TMC. The resultant TFC membrane prepared under optimal conditions was able to achieve water flux of 22.8 L/m<sup>2</sup>.h and Na<sub>2</sub>SO<sub>4</sub> rejection of 93.5% when tested at 0.2 MPa. Through a rapid Cu<sup>2+</sup>/H<sub>2</sub>O<sub>2</sub>-induced co-deposition of PDA/PIP on top of the surface of PAN substrate, Zhu et al. [113] successfully fabricated a thin, smooth and hydrophilic polyamide layer as shown in Figure 26. With the assistance of rapid PDA co-deposition, PIP monomers were tightly immobilized to the substrate via strong covalent bonding with PDA and thus, could effectively interact with TMC monomers. The optimum synthesis conditions for the TFC membrane were reported to be at 2:1 ration of PIP/PDA, 5-min co-deposition, 0.1% w/v TMC and 30-s reaction time. Such optimized TFC membrane exhibited superior water permeability of 14.5 L/m<sup>2</sup>.h.bar with promising monovalent/bivalent selectivity (NaCl/Na<sub>2</sub>SO<sub>4</sub>) of 24.1.

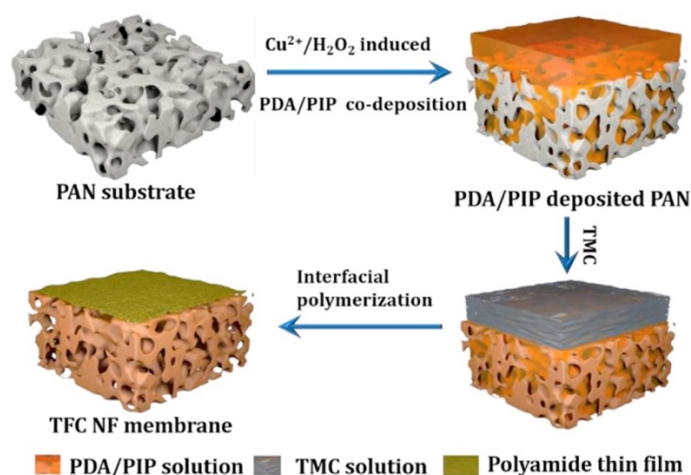


**Figure 26.** Schematic illustration of the TFC NF membranes mediated by a rapid Cu<sup>2+</sup>/H<sub>2</sub>O<sub>2</sub>-induced co-deposition of PDA/PIP [113].

As the TFC membranes used in the engineered osmosis applications are associated with the adverse influence of ICP which results in a sharp concentration gradient formed within the porous substrate layer [111,114,115], one of the strategies to address the problem is to improve the substrate hydrophilicity via surface modification. Surface modification using PDA is able to improve substrate characteristics by increasing its hydrophilicity and narrowing pore size distribution so as it exhibits better interaction with TMC during interfacial polymerization process [18,111]. Using the PDA coated-substrate, Han et al. [111] experienced the resultant TFC membrane was able to achieve better water flux and salt rejection. Its  $J_v/J_s$  ratio was reported to be  $\sim 20$  when tested with pure water as feed solution and 2 M NaCl as draw solution in the PRO orientation. Saraf et al. [116] also found that when the substrate surface was coated with hydrophilic PVA, it improved substrate pores wetting which in turn reduced ICP effect of TFC membranes.

The fabrication of double-skinned TFC membranes has also been proposed by researchers in an effort to reduce the adverse influence of ICP within the porous substrate layer as well as to mitigate fouling during engineered osmosis process. Figure 27 compares the structure of double-skinned TFC membrane with the typical TFC membrane. Wang et al. [114] were the first to introduce the double-skinned cellulose acetate membrane for engineered osmosis process in 2010 and found that the newly developed membrane could attain water flux of 48.4 L/m<sup>2</sup>.h and reverse salt flux of 6.5 g/m<sup>2</sup>.h when tested with DI water as the feed solution and 5.0 M MgCl<sub>2</sub> as the draw solution in PRO mode. Although some might argue that the formation of a second skin layer in the TFC membrane has the tendency of inducing additional water transport resistance and decreasing water flux, the adverse effect of the ICP could be potentially mitigated.

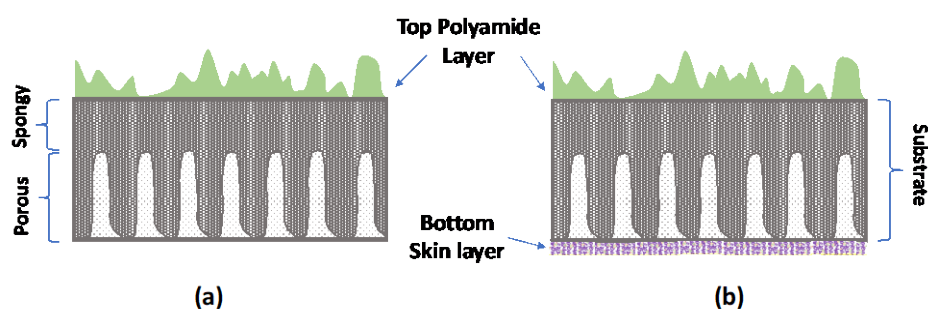


**Figure 27.** Structural of (a) typical TFC membrane with single selective layer and (b) TFC membranes with double skin layers.

Duong et al. [117] also fabricated a double-skinned TFC membrane consisting a PAN substrate with a polyamide selective layer on top of the PAN substrate, followed by the formation of hydrophilic Nexar copolymer layer on the bottom of the PAN substrate in an attempt to improve membrane performance during FO process. The resultant double-skinned membrane exhibited a high-water flux of 17.2 L/m<sup>2</sup>.h and a low reverse salt transport of 4.85 g/m<sup>2</sup>.h using 0.5 M NaCl as draw solution and DI water as the feed. Similarly, Ong et al. [118] modified the bottom surface of TFC membrane using hydrophilic zwitterionic polymer but used for the membrane particularly for oily wastewater treatment. The structure of the double-skinned FO membrane is illustrated in Figure 28. It was reported that the deposition of poly(3-N-2-methacryloxyethyl-N,N-dimethyl) ammonatopropanesultone (PMAPS) could act as an antifouling layer to prevent the internal fouling and reduce the ICP effect, leading to higher water flux and enhanced water recovery rate. The obtained results showed that double-skinned FO membrane displayed a water flux of 13.6 L/m<sup>2</sup>.h and reverse salt transport of 1.6 g/m<sup>2</sup>.h under FO mode using 10,000 ppm emulsified oily solution as the feed and 2 M NaCl as the draw solution.

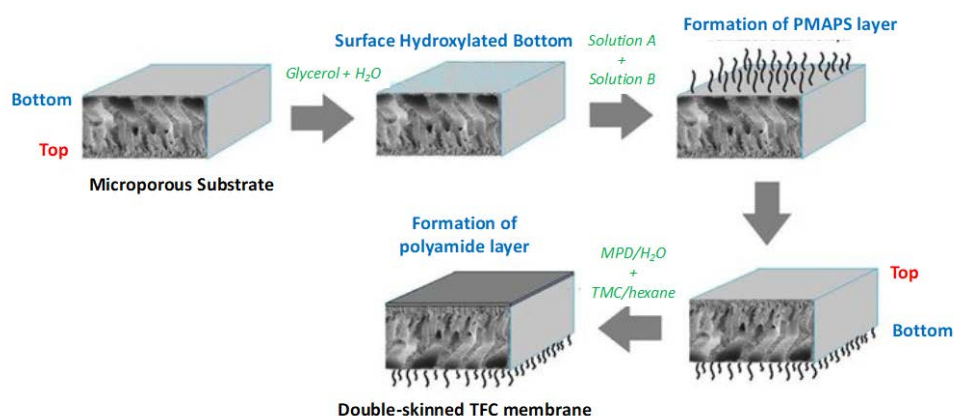


**Figure 28.** Fabrication procedure of double-skinned TFC flat sheet membrane for oily wastewater treatment [118].

In an attempt to ameliorate the internal fouling, Liu et al. [119] deposited PDA on the bottom surface of the mesh-incorporated substrate prior to the formation of TFC FO membrane. As shown in Figure 29, the TFC FO membrane was prepared via three steps - (1) fabrication of PSf substrate with embedded mesh via phase inversion method, (2) deposition of PDA onto the bottom surface of the substrate; and (3) formation of polyamide layer on the top surface of PSf substrate via interfacial polymerization technique. A remarkable reduction on the contact angle of substrate (from 82.2° to 37.4°) was observed with increasing the PDA deposition time from zero to 6 h. This strongly indicated that the PDA deposition efficaciously enhanced the

hydrophilicity of the bottom surface of the prepared TFC FO membrane. The improved hydrophilicity however was associated with lower water permeability as a result of reduced mean pore size of the substrate. Owing to the PDA hydrophilization of the bottom substrate, the modified double-skinned membrane demonstrated more than 93% of water flux recovery in the PRO process after combined fouling, surpassing the performance of control TFC membrane (61.7%) and unmodified double-skinned TFC membrane (81.7%) under the same testing conditions.

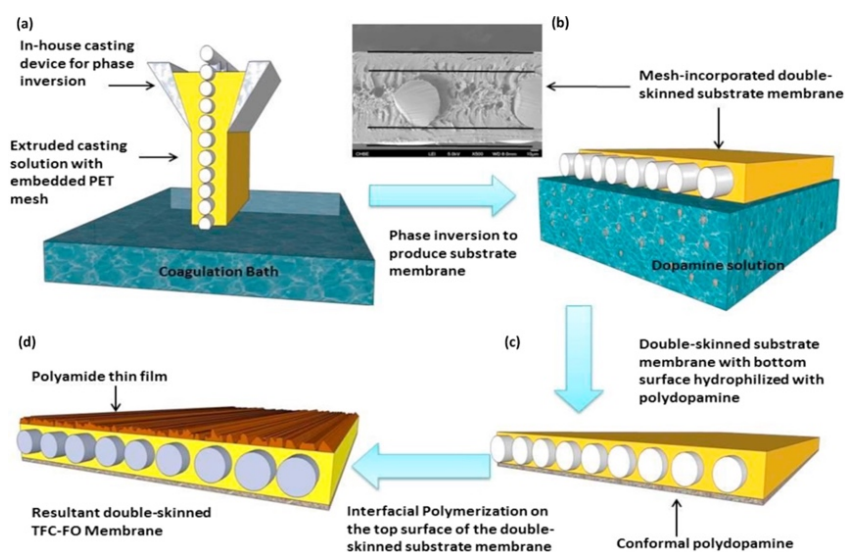


**Figure 29.** Schematics of double-skinned TFC FO membrane preparation, (a) phase inversion of substrate with embedded PET mesh, (b) dopamine deposition on the bottom surface of substrate, (c) substrate with bottom surface coated with PDA, and (d) resultant TFC membrane with polyamide formed on the substrate top surface [119].

Instead of using flat substrate, Fang et al. [120] utilized PAI-based hollow fiber substrate to develop double-skinned TFC membrane having polyamide RO-like inner skin and positively charge NF-like outer skin as shown in Figure 30. The reason for having a RO-like skin layer in the lumen of the fiber was due to that the experimental procedures were more controllable in this situation. Such double-skinned membrane was reported to be able to produce promising water permeability ( $2.05 \text{ L/m}^2\cdot\text{h}$ ) with reasonably high NaCl rejection (85%) even at extremely low operating pressure (0.1 MPa). With respect to its engineered osmosis performance, it attained superior PRO water flux of  $41.3 \text{ L/m}^2\cdot\text{h}$  and low  $J_s/J_v$  of 0.126 g/L when using DI water and 2.0 M NaCl as feed and draw solution, respectively. Compared to the flat sheet membrane, hollow fiber membrane is more advantageous as it is mechanically self-supported and does not require feed spacer during operation.

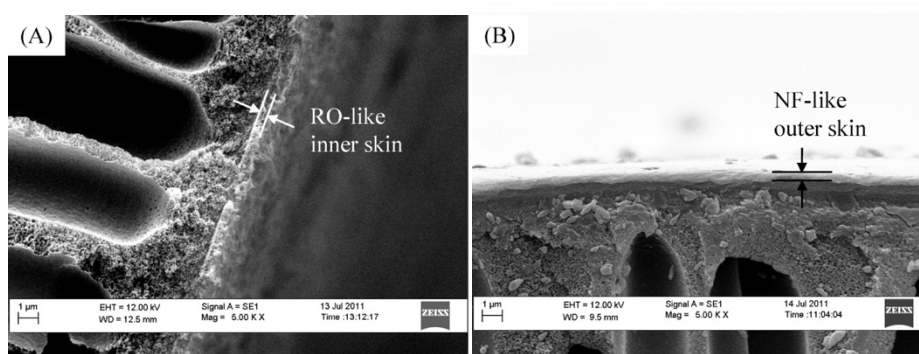


**Figure 30.** Cross-section morphology (at magnification of 5,000 $\times$ ) of double-skinned TFC hollow fiber membrane, (A) RO-like inner skin and (B) NF-like outer skin [120].

Fouling on the PRO membranes must also be mitigated in order to sustain high performance of osmotic power generation. Li et al. [19] molecularly designed antifouling PRO TFC membranes by grafting hyperbranched polyglycerol (HFG) on the outer surface of PES hollow fiber substrate with the aid of PDA. In high-pressure PRO tests, HFG-grafted TFC membrane demonstrated enhanced power density of 6.7 W/m<sup>2</sup> (using pure water as feed and 0.6 M NaCl as draw solution) due to higher water flux induced by HPG grafting than that of control TFC membrane. In addition to better flux recovery rate and greater hydraulic pressure impulsion, the HFG-grafted TFC membrane also showed excellent resistance against *E-coli* adhesion, *S. aureus* attachment and BSA adsorption.

Lower degree of flux decline was also demonstrated in other studies in which zwitterions were coated on the surface of TFC hollow fiber membrane [121,122]. The water flux of the zwitterions-modified TFC membrane was able to recover by 68–75% after being used to treat municipal wastewater for 3 cycles (each cycle lasted for 3 h) [121]. As a comparison, the control TFC membrane showed <50% flux recovery rate under the same testing conditions. It is also important to mention that the modified TFC membrane could achieve as high as 7.7 W/m<sup>2</sup> during 3-h PRO test using wastewater from municipal recycle plant as the feed solution and 0.81 M NaCl as the draw solution at an operating pressure of 1.5 MPa.

The formation of polyamide layer is of significantly controlled by the diffusion rate of diamine monomer from the substrate pores to the organic phase. Thus, the growth of the polyamide layer is generally known as a self-limiting diffusion-controlled process [123,124]. Due to poorly controllable of the interfacial polymerization process, fabrication of a very thin and defect-free polyamide layer is always challenging, particularly in the lab-scale study.



Strategies to form a uniform, ultra-thin and defect-free polyamide layer with robust performance have been proposed by developing an interlayer between the polyamide layer and the substrate. The interlayer is reported to act as a “storage” for the aqueous diamine monomer and facilitate the following interfacial polymerization process [69,110,125,126]. Such interlayer typically has small and uniform surface pores, high surface porosity and hydrophilic surfaces that could provide a homogenous surface to uniformly distribute diamine monomer and thus to uniformly initiate the interfacial polymerization for the controlled formation of a ultra-thin and defect-free polyamide selective layer. Livingston and co-workers [125] had made a significant breakthrough in the fabrication of an ultrathin polyamide selective layer with a thickness less than 10 nm on a cadmium hydroxide ( $\text{Cd}(\text{OH})_2$ ) nanostrands interlayer. The sacrificial  $\text{Cd}(\text{OH})_2$  interlayer was prepared on top of substrates (either porous alumina or cross-linked polyimide), followed by interfacial polymerization of diamine (MPD/PIP) and TMC onto the modified substrate surface. The nanostrand interlayer layer was, subsequently, removed by acid dissolution, resulting in a free-standing nanofilm that was attached to the substrate. Although the resultant TFC membrane was reported to exhibit ultrafast molecular transport specifically for organic solvents, the nanostrands-based layer suffered from chemically instability and environmentally harm.

In 2017, Wang et al. [110] fabricated triple-layered TFC NF membrane by having a hydrophilic cellulose nanocrystal (CNC) interlayer between the polyamide and the microporous substrate. The CNC-coated substrate was firstly prepared by vacuum filtrating CNC suspension onto the PES-based microporous membrane. Besides playing a crucial role in the modifying the substrate surface properties, the CNC interlayer was reported to be able to store aqueous diamine solution, creating a polyamide layer with relative low cross-linking degree. The optimized TFC membrane showed a promising performance for both water flux ( $204 \text{ L/m}^2\cdot\text{h}$ ) and  $\text{Na}_2\text{SO}_4$  rejection (97%) when tested at 0.6 MPa using 1000 ppm salt solution. The enhanced filtration efficiency was mainly attributed to the CNC interlayer that facilitated the water permeation through a “dragging” effect.

Many other materials such as CNTs [127], mussel-inspired material [128] and tannic acid/ $\text{Fe}^{3+}$  nanoscaffolds [129] have also been utilized as an interlayer to fabricate the highly permeable TFC NF membranes, which exhibited high water permeability and rejection of large molecules (e.g., organic dyes and divalent ions) but very low rejection of NaCl. Zhou et al. [20] found that the ultrathin nanofibrous CNT interlayer could prevent the formation of a thick PA inside the substrate pores and facilitate the formation of a highly permeable and selective PA layer with large effective surface area for high flux water transport. In addition, the

incorporation of a CNT interlayer was found to decrease the structure parameter of the resulting TFC membranes and to suppress ICP significantly in the FO process.

A hydrophilic mineral material – calcium carbonate ( $\text{CaCO}_3$ ) has also been used to modify the bottom surface of PES/polyacrylic acid (PAA) substrate in order to develop a new type of TFC membrane that could minimize ICP effect during FO process [130,131]. Compared to the cellulose-based TFC membrane, the newly developed  $\text{CaCO}_3$ -coated PES/PAA-based TFC membrane could show improved water flux without experiencing mechanical fragility [130]. Considering membrane fouling is a major obstacle impeding the performance of FO membranes, Liu and co-workers [131] developed a new approach to fabricate TFC membrane using substrate having a dual-functional (Ag/AgCl) property. PES substrate was firstly blended with PAA followed by polyamide layer formation. Alternative soaking process was then applied on the bottom layer of PES/PAA substrate to establish AgCl layer. To partially convert AgCl to *n*-Ag, light irradiation was performed. With respect to antibacterial properties, the developed TFC membrane exhibited superior performance arising from the combined effect of the direct contact between *n*-Ag on the membrane exterior surface and the bacterial cells, and the biocidal action of  $\text{Ag}^+$  ion released from the nanocomposite substrate. Furthermore, such developed TFC membrane also showed nearly 250% increase in water flux when compared with the PES-based TFC membranes.

In addition to the aforementioned surface modification techniques, plasma-based method has also been used to improve the surface properties of hydrophobic substrates made of PVDF and PP prior to TFC membrane fabrication [132–134]. Kim et al. [134] reported that the water contact angle of PVDF substrate was dramatically reduced from  $119^\circ$  to  $52^\circ$  after subjecting to 60-s plasma exposure of oxygen/methane mixture. The decrease in water contact angle was attributed by the formation of hydrophilic moieties on the substrate surface upon plasma treatment. Similarly, Park et al. [35] used plasma treatment to modify PE-based substrate by creating oxygen-containing polar functional groups for enhanced hydrophilicity. Such substrate was chosen mainly because of the excellent mechanical and chemical durability of PE. The plasma-treated PE substrate was then immersed in the MPD aqueous solution with the aid of sodium dodecyl sulfate (SDS) surfactant before soaking in the TMC solution and post-treated at  $70^\circ\text{C}$  to produce TFC membrane. The fabricated PE-supported TFC membrane exhibited ~30% higher water flux than that of a commercial RO membrane upon optimization of membrane fabrication parameters, i.e., plasma treatment, monomer and SDS compositions as well as post-heat treatment.

Based on oxidation method, Korikov et al. [135] hydrophilized the PP-based hollow fiber and flat substrate surfaces with a hot chromic acid solution. The findings indicated that the surface modification could provide greater adhesion between polyamide layer and the substrate membrane, leading to improved separation efficiency. Among a number of factors which hold the key to a successful TFC membrane fabrication are hydrophilization of different surfaces of PP substrates, order of introduction of the monomer-containing solutions, exposure of the nascent film to reduced shear conditions, and heat treatment for the polyamide layer.

Partial hydrolysis method, on the other hand, was also considered for the modification of PAN-based substrates. Oh et al. [136] altered the surface chemistry of the PAN substrate using NaOH solution so as it created stronger chemical interaction with polyamide active layer. The  $-\text{CN}$  groups of PAN were converted into  $-\text{COOH}$  groups upon NaOH modification, forming ionic and covalent bonds with amine compounds as shown in Figure 31. Such chemical bonding with the PA active layer was found to be able to increase chemical and physical stability of the resultant TFC membrane [136]. Pérez-Manríquez et al. [137,138] meanwhile cross-linked PAN substrate with hydrazine hydrate in which the reaction process was performed at 85 °C for 6 h. Figure 32 presents the organic structure of PAN substrate cross-linked with hydrazine hydrate. Using the cross-linked substrate, the resultant TFC membrane demonstrated excellent solvent stability toward DMF with a permeance of 1.7 L/m<sup>2</sup>.h.bar and possessed molecular weight cut-off of less than 600 Da [137]. Unfortunately, no demonstration was carried out on the membrane for water application.

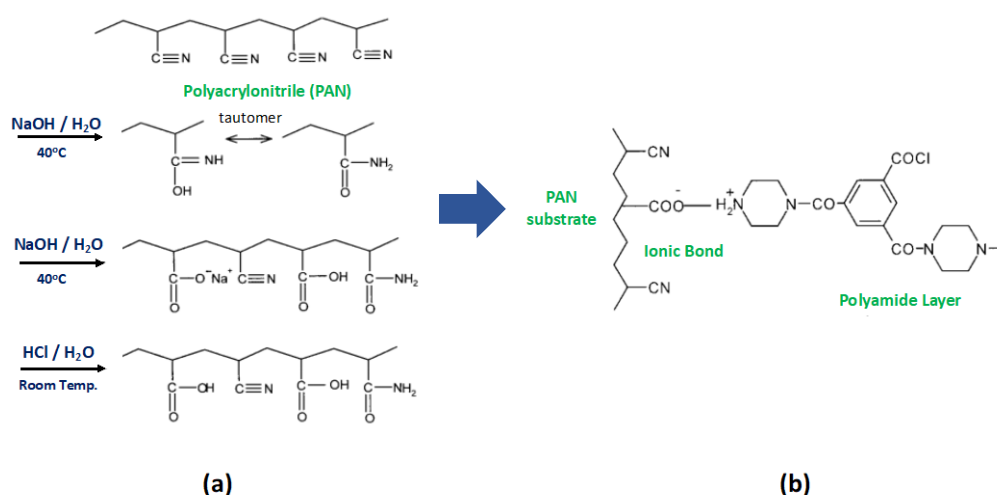


**Figure 31.** (a) Reaction mechanism of PAN substrate with NaOH solution and (b) schematic representation of the ionic bond formation between the  $-\text{COOH}$  on the PAN support and PIP of polyamide layer [136].

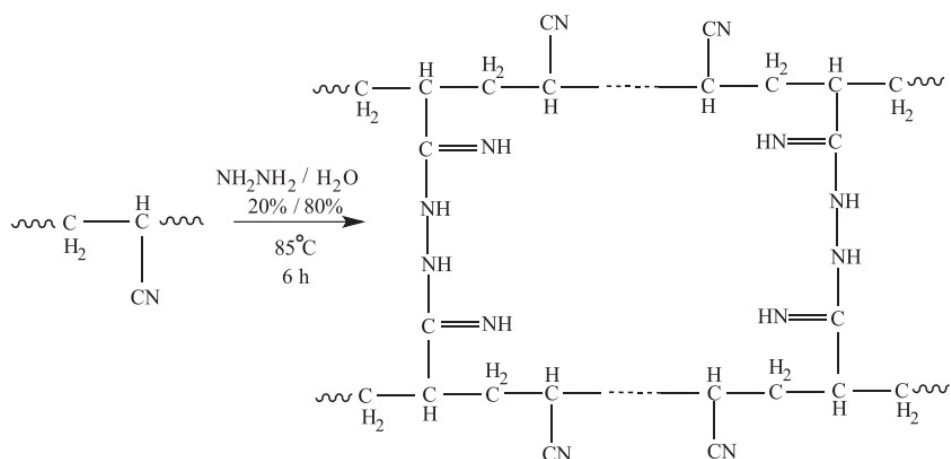


**Figure 32.** Crosslinking reaction of PAN substrate with hydrazine hydrate [137].

A new technique in fabricating a surface-patterned TFC NF/RO membrane was first introduced by Maruf et al. [139] in 2014 as an alternative approach for fouling mitigation. Several studies have reported a two-step fabrication process in which PES substrate was initially nanoimprinted before forming a thin polyamide layer on top of the nanoimprinted substrate [139–141]. Figure 33 shows the topographical images of the nano-imprinted and non-imprinted PES substrate and their respective TFC membrane [139]. The formation of unique surface patterns is believed to change the mass transfer in the vicinity of the membrane surface, enhancing back diffusion to the bulk. The authors believed that the unique surface patterns could induce hydrodynamic secondary flows at the membrane-feed interface and play key role in reducing concentration polarization and decreasing scaling effects [139].

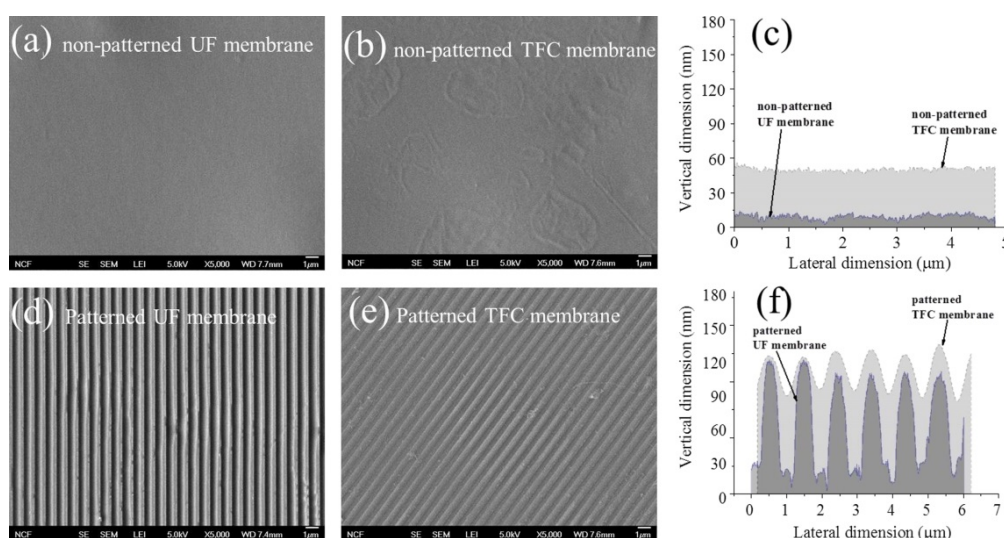


**Figure 33.** Morphological images of nanoimprinted and non-imprinted PES UF substrate membranes and TFC membranes. Representative top-surface SEM images of (a) non-imprinted

PES substrate, (b) non-imprinted TFC membrane, (d) nanoimprinted PES substrate, and (e) nanoimprinted TFC membrane. Images (c) and (f) are representative cross-sectional profiles for non-imprinted and nanoimprinted TFC membranes obtained from AFM scans [139].

Maruf et al. [140] further carried out the research to study the influence of patterned substrate and interfacial polymerization conditions on the morphology of the resultant TFC membranes and reported that the surface topography of the resultant TFC membranes, measured by the height of the patterns, appeared independent to the interfacial polymerization reaction time. It was further suggested that the rate of protein deposition might be reduced on the patterned TFC membrane in comparison to the non-patterned TFC membrane due to improved local hydrodynamics caused by the regular surface patterning [142].

A more reliable fabrication technique has been developed by ElSherbiny et al. [141] to produce a high performance micro-patterned TFC membrane. The PES substrate was first micro-patterned using two different micro-fabrication methods, namely micro-moulding ( $\mu\text{M}$ ) and micro-imprinting lithography (MIL). The pattern-supported TFC membranes exhibited superior water permeability up to 2 folds than that of flat TFC membranes with NaCl rejection remained at >96%. This is mainly attributed to enhanced membrane active surface area of about ~70% in the TFC\_P $\mu\text{M}$  coupled with the increased membrane surface roughness upon substrate surface micro-patterning as shown in Figure 34. Even though the membrane orientation appeared insignificantly to the water permeability, it apparently affected the filtration performance of pattern-supported TFC membranes to some extent. At high feed concentrations, for instance, the “parallel” orientation of the micro-patterned channels to the direction of feed flow is always favorable than that in a perpendicular orientation. The “parallel” orientation is likely to promote flow circulation towards efficient surface-induced mixing effects, minimizing the concentration polarization [141]. Although there is a surge in the number of research articles related to the use of surface-modified substrate for TFC membranes in recent years, the sustainability of the membrane in long run remains largely unknown.



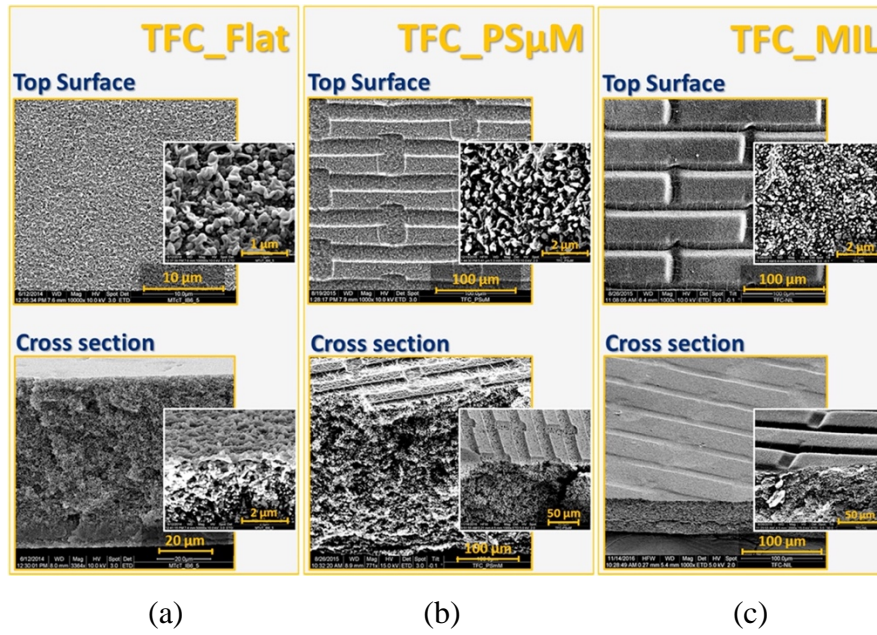


**Figure 34.** SEM micrographs of top surface and cross-section morphology of TFC membranes, (a) TFC\_Flat (note: conventional TFC membrane), (b) TFC\_PSμM (made of micro-moulding) and (c) TFC\_MIL (made of micro-imprinting lithography) [141].

Over the past decade, nanofiber substrate produced by electrospinning method has become prominent method for the fabrication of new generation TFC membrane due to its highly porous characteristic with inter-connected void network structures [51]. The potential use of polymeric materials incorporating with or without nanofillers for nanofiber substrate fabrication has been reviewed in the previous section as a promising supporting layer to enhance performance of TFC membranes for various water applications. Nevertheless, the relatively weak interactions between the nanofiber substrate (made of certain polymers) and the active layer have motivated researchers to further improve the surface properties of nanofiber substrate.

To improve the chemical interaction of hydrophobic PVDF nanofiber with the polyamide layer, Tian et al. [143] pre-wetted the PVDF nanofiber substrate with alcohol for 2 h, followed by DI water washing for several times before using it for TFC membrane fabrication. Two nanofiber substrates with different mean pore sizes (0.28 and 0.41 μm) were synthesized and the results showed that it was easier to form polyamide layer with higher cross-linking degree on the substrate with smaller pore sizes. Such TFC membrane exhibited higher salt rejection but lower water flux than the counterpart of bigger pore size substrate. With respect to FO/PRO performance, the best performing membrane could achieve water flux of 11.6/30.4 L/m<sup>2</sup>.h with  $J_s/J_v$  of 0.21–0.30 using when tested using 1.0 M NaCl as the draw



solution and DI water as the feed solution. In a recent study, Park et al. [53] improved the surface wettability of hydrophobic PVDF nanofiber by dip coating it with hydrophilic PVA. The PVA-coated PVDF nanofiber was subsequently crosslinked using glutaraldehyde (GA) before subjecting to heat treatment at 100 °C for 10 min. Owing to the thin polyamide layer formed over the PVA-coated substrate, the shapes and patterns of the electrospun nanofibers were clearly imprinted under the selective layer as observed from the FESEM images. The authors claimed that the presence of PVA coating layer could significantly enhance membrane hydrophilicity, resulting in the remarkable reduction in the ICP effects and, thus achieving FO water flux of 34.2 L/m<sup>2</sup>.h when tested using DI water and 1 M NaCl solution.

Son et al. [144] developed a new thermal-rolling technique that could continuously pre-treat the surface of nanofiber at high temperature (150 °C) prior to the polyamide layer synthesis, as illustrated in Figure 35. The thermally pre-treated nanofiber substrate possessed a smoother surface and exhibited narrow pore size and average fiber diameter of about 0.4 μm and 292 nm, respectively. The modified TFC membrane exhibited promising water permeability up to 30 L/m<sup>2</sup>.h using 1 M NaCl as draw solution and DI water as feed solution during FO process. Nevertheless, it must be noted that the maximum power density (~2.0 W/m<sup>2</sup>) that could be generated by this modified membrane is far below the target power density (5.0 W/m<sup>2</sup>) required by the PRO process for industrial implementation. Although the construction of nanofiber-supported TFC membranes could certainly address the ICP problems to some extent and improve the water permeation as well, the fabrication of nanofiber substrate may often be associated with some technical limitations. Its relatively large surface pore size makes the formation of defect-free polyamide layer very challenging.

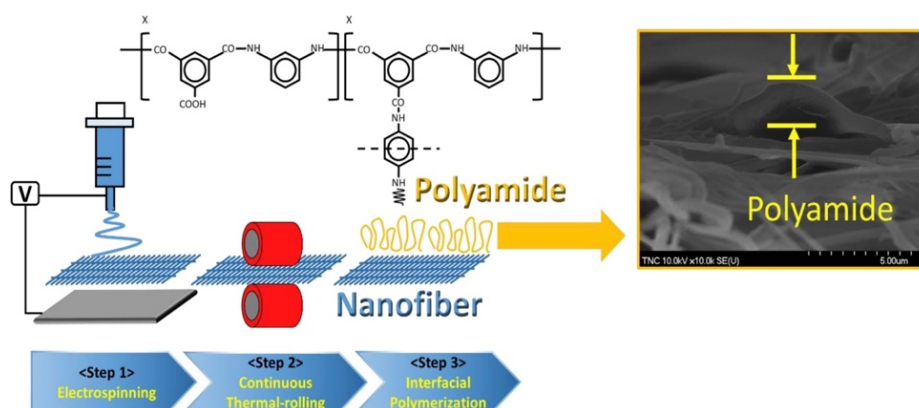


**Figure 35.** Schematic of three-step used to synthesize nanofiber-supported TFC membrane, (1) electrospinning, (2) thermal-rolling, and (3) interfacial polymerization. Cross-section SEM image showing polyamide layer attached onto the heat-treated nanofiber substrate [144].

#### 4.0 Concluding remarks and future directions

Interfacial polymerization technique is a mature technology which has existed in the literature for more than 50 years for thin polymeric film synthesis. It is also the industrial manufacturing method for the fabrication of commercial TFC NF and RO membranes for water and wastewater treatment. The interfacial polymerization technique is generally acknowledged as the scientific breakthrough in the membrane research that is equivalent to the historic announcement of Loeb–Sourirajan asymmetric membrane in the nineteen sixty. The establishment of ultrathin polyamide selective is the decisive factor to produce a modern membrane with good balance of water flux and solute rejection.

Although the characteristics of polyamide layer are the keys to govern the membrane filtration performance, its establishment is strongly dependent on the substrate properties. Without the polymeric substrates, the polyamide layer alone does not able to be used for water filtration, mainly due to its poor mechanical strength. We have seen a significant increase of the publications involving substrate development over the past 15 years in the literature. A comprehensive as well as state-of-art review on the substrate development has thus been made in this paper.

As substrate membranes can be prepared from various materials (e.g., polymers or polymer-inorganic nanocomposites) and in different formats (e.g., flat sheet, hollow fiber, and nanofiber) using different fabrication techniques, the selection of a substrate for TFC membrane preparation is, therefore, dependent on the area of industrial application as well as the manufacturing and material cost. Nevertheless, advances in the development of stable substrate with lower manufacturing cost will definitely offer more opportunities to expand the application area particularly to industries where there are harsh conditions, for example, the petrochemical and pharmaceutical industries.

The impacts of three main substrate materials, i.e., (a) polymer or polymer/polymer blend substrates, (b) polymer/inorganic nanocomposite substrates, and (c) surface-modified substrates on the characteristics and filtration performance of TFC membranes for water applications are comprehensively reviewed in this paper. Some further remarks are given as follows.

Although substrates made of thermally- or solvent-enhanced materials, e.g., PVDF, PP and PE are generally able to exhibit better results compared to the commonly used PSf and PES-based substrates, their hydrophobic characteristics require surface modification to improve their compatibility with the polyamide layer. Even though the hydrophobic substrates upon

modification could be used for TFC membranes fabrication, they are only suitable for NF or RO process as only the polyamide layer is in contact with feed solution. Such substrates are not recommended for FO and PRO processes as severe fouling could take place easily within the hydrophobic substrate materials. In view of this, substrates made of hydrophilic polymeric materials, e.g., PAN and sulfonated polymers are more practical and feasible.

So far, most of the TFC membranes made of polymer/polymer blend substrates are only assessed at operating pressure much lower than the real NF/RO process and thus their long-term mechanical stability against high pressure operation remains unclear. The issues of polymer-polymer compatibility that affect the structural integrity of the substrates are the main concerns for the TFC membrane performance, particularly in the cases where high quantity of secondary polymer is introduced to the existing polymeric substrates to render them highly hydrophilic. This is an issue worthy of further investigation.

Practical applications of nanofiber substrates are rather limited so far for water applications, although such materials exhibit amazing characteristics such as very large surface area to volume ratio and superior porosity which are not able to be seen in the typical substrates made of phase inversion technique. One of the biggest challenges is the difficulty of forming good integrity polyamide layer over its highly porous structure. Fine-tuning the electrospinning conditions and heat-press treatment are always very crucial in order to produce a nanofiber with suitable surface pore size and porosity for better interaction with the monomer-containing solutions. Furthermore, compared to the substrates made of famous NIPS technique, it is still very time-consuming to produce nanofiber substrates even with the use of latest needle-free electrospinning technology. In spite of that, it must be pointed out that the very porous structure of nanofiber substrates could significantly reduce ICP effects in the FO/PRO process and deserve further investigation to ascertain their potential benefits.

The TFC membranes made of polymer-inorganic nanocomposite substrates (whether in asymmetric or nanofiber structure) on the other hand are associated with several technical challenges, although laboratory-scale studies always yielded promising results. One major issue is the uneven distribution of the nanomaterials in the polymeric matrix particularly when the amount of nanomaterials added is beyond a trade-off. This is likely to affect structural integrity and mechanical properties of resultant substrates. Also, the possible nanomaterials leaching from the substrate during operation raises a safety concern on the treated water quality. Improved nanomaterials distribution in the polymeric matrix have been successfully demonstrated in many recent studies by subjecting the nanomaterials to mild surface

modification prior to use for polymeric solution preparation. Nevertheless, more research work is still needed before they can reach the commercialization level.

It has been previously reported that instead of using hydrophilic nonporous nanoparticles, embedding substrates with hydrophilic mesoporous nanomaterials could create a preferential pathway for water molecules, leading to an improvement in water flux of TFC membrane. Nonetheless, the orientation of the mesoporous nanomaterials within the substrate is not possible to be horizontally arranged via the conventional blending method. This contradicts to the claim of many researchers that water flows through vertically aligned channels. In spite of that, randomly arranged nanotubes have to certain extent created a relatively less resistant pathway for water molecules to pass through, leading to flux improvement. Additional research is needed to verify the water transport mechanism for these membranes as enhanced flux has also been demonstrated for the substrates incorporated with nonporous nanoparticles. Other challenge of nanocomposite substrates is the use of expensive nanomaterials (e.g., CNTs and GO) in enhancing substrate properties. This is the main barrier to its commercialization.

Surface modification of the existing polymeric substrates (either top or bottom surface) perhaps is the easiest way to alter the properties of TFC membrane without affecting the structural integrity of substrates. It specifically alters the substrate surface chemistry so as it can have better interaction with the polyamide layer (for top surface modification) and exhibit reduced ICP effect and enhanced antifouling resistance (for bottom surface modification) during FO/PRO operation. Nevertheless, how much the bottom surface modification can contribute to the fouling mitigation remains largely unclear. Some researchers have observed that the TFC membranes upon bottom surface modification could indeed reduce membrane fouling, but their experiments were carried out using dilute solution and/or demonstration was shown only in the initial stage of separation. Once the deposition of foulants has fully taken place, the surface modification is no longer effective to address fouling. Thus, future work should also study how effective the modified surface of TFC membrane in retrieving water flux after cleaning process.

Despite the significant progresses that have been made, more research is still required. One obvious trend in the microporous substrate development is its rapid movement beyond the fields of NF and RO. The TFC membranes are now also the main research domain for the applications of osmotically-driven processes, i.e., FO and PRO. The subject of microporous substrates development is a multi-disciplinary study that requires researchers with different backgrounds (chemistry, materials science, physics and engineering) to work together. We hope

this review article could provide insights to researchers in fabricating effective substrates for TFC membranes for enhanced water treatment processes.

## Acknowledgements

The corresponding author would like to thank the Ministry of Education Malaysia for the research grants provided under Fundamental Research Grant Scheme (FRGS) (Vot no. 3235) and Translational Research Grant Scheme (TRGS) (Vot no 4536). Co-author – N. Misdan from UTHM also wishes to acknowledge the Ministry of Education Malaysia for the financial support given under FRGS (Vot. no. 1617).

## References

- [1] R.J. Petersen, Composite reverse osmosis and nanofiltration membranes, *J. Memb. Sci.* 83 (1993) 81–150.
- [2] W.J. Lau, A.F. Ismail, P.S. Goh, N. Hilal, B.S. Ooi, Characterization methods of thin film composite nanofiltration membranes, *Sep. Purif. Rev.* 44 (2015) 135–156.
- [3] N. Ahmad, P. Goh, Z. Abdul Karim, A. Ismail, Thin Film Composite Membrane for Oily Waste Water Treatment: Recent Advances and Challenges, *Membranes (Basel)*. 8 (2018) 86.
- [4] W.J. Lau, A.F. Ismail, *Nanofiltration Membranes: Synthesis, Characterization, and Applications*, CRC Press, 2016.
- [5] J. Kucera, *Reverse Osmosis: Industrial Processes and Applications*, John Wiley & Sons, 2015.
- [6] T.Y. Cath, A.E. Childress, M. Elimelech, Forward osmosis: Principles, applications, and recent developments, *J. Memb. Sci.* 281 (2006) 70–87.
- [7] N. Akther, A. Sodiq, A. Giwa, S. Daer, H.A. Arafat, S.W. Hasan, Recent advancements in forward osmosis desalination: A review, *Chem. Eng. J.* 281 (2015) 502–522.
- [8] M. Kurihara, H. Takeuchi, Earth-Friendly Seawater Desalination System Required in the 21st Century, *Chem. Eng. Technol.* 41 (2018) 401–412.
- [9] G. Han, S. Zhang, X. Li, T.S. Chung, Progress in pressure retarded osmosis (PRO) membranes for osmotic power generation, *Prog. Polym. Sci.* 51 (2014) 1–27.
- [10] J. Li, M. Wei, Y. Wang, Substrate matters: The influences of substrate layers on the performances of thin-film composite reverse osmosis membranes, *Chinese J. Chem. Eng.* 25 (2017) 1676–1684.
- [11] G.R. Xu, J.M. Xu, H.J. Feng, H.L. Zhao, S.B. Wu, Tailoring structures and performance of polyamide thin film composite (PA-TFC) desalination membranes via sublayers adjustment-a review, *Desalination*. 417 (2017) 19–35.
- [12] W.J. Lau, A.F. Ismail, N. Misdan, M.A. Kassim, A recent progress in thin film composite membrane: A review, *Desalination*. 287 (2012).
- [13] M. Shibuya, M.J. Park, S. Lim, S. Phuntsho, H. Matsuyama, H.K. Shon, Novel CA/PVDF nanofiber supports strategically designed via coaxial electrospinning for high performance thin-film composite forward osmosis membranes for desalination, *Desalination*. 445 (2018) 63–74.
- [14] G. Han, T.-S. Chung, M. Toriida, S. Tamai, Thin-film composite forward osmosis membranes with novel hydrophilic supports for desalination, *J. Memb. Sci.* 423 (2012)

- 543–555.
- [15] M. Rezaei-DashtArzhandi, M.H. Sarrafzadeh, P.S. Goh, W.J. Lau, A.F. Ismail, M.A. Mohamed, Development of novel thin film nanocomposite forward osmosis membranes containing halloysite/graphitic carbon nitride nanoparticles towards enhanced desalination performance, *Desalination*. 447 (2018) 18–28.
  - [16] D. Emadzadeh, W.J. Lau, T. Matsuura, M. Rahbari-Sisakht, A.F. Ismail, A novel thin film composite forward osmosis membrane prepared from PSf-TiO<sub>2</sub> nanocomposite substrate for water desalination, *Chem. Eng. J.* 237 (2014) 70–80.
  - [17] G.S. Lai, W.J. Lau, P.S. Goh, A.F. Ismail, N. Yusof, Y.H. Tan, Graphene oxide incorporated thin film nanocomposite nanofiltration membrane for enhanced salt removal performance, *Desalination*. 387 (2016).
  - [18] J.T. Arena, B. McCloskey, B.D. Freeman, J.R. McCutcheon, Surface modification of thin film composite membrane support layers with polydopamine: Enabling use of reverse osmosis membranes in pressure retarded osmosis, *J. Memb. Sci.* 375 (2011) 55–62.
  - [19] X. Li, T. Cai, T.S. Chung, Anti-Fouling behavior of hyperbranched polyglycerol-grafted poly(ether sulfone) hollow fiber membranes for osmotic power generation, *Environ. Sci. Technol.* 48 (2014) 9898–9907.
  - [20] Z. Zhou, Y. Hu, C. Boo, Z. Liu, J. Li, L. Deng, X. An, High-Performance Thin-Film Composite Membrane with an Ultrathin Spray-Coated Carbon Nanotube Interlayer, *Environ. Sci. Technol. Lett.* 5 (2018) 243–248.
  - [21] N.N. Bui, M.L. Lind, E.M. V Hoek, J.R. McCutcheon, Electrospun nanofiber supported thin film composite membranes for engineered osmosis, *J. Memb. Sci.* 385–386 (2011) 10–19.
  - [22] M.R. Chowdhury, L. Huang, J.R. McCutcheon, Thin film composite membranes for forward osmosis supported by commercial nanofiber nonwovens, *Ind. Eng. Chem. Res.* 56 (2017) 1057–1063.
  - [23] S. Loeb, S. Sourirajan, Sea Water Demineralization by Means of an Osmotic Membrane, University of California, Department of Engineering, 1963.
  - [24] W.M. Kanadys, J. Oleszczuk, Cukrzyca ciezarnych w materiale Poradni dla Kobiet w latach 1994-1998., Springer Netherlands, Dordrecht, 1999.
  - [25] D.H. Reneker, I. Chun, Nanometre diameter fibres of polymer, produced by electrospinning, *Nanotechnology*. 7 (1996) 216–223.
  - [26] Z.M. Huang, Y.Z. Zhang, M. Kotaki, S. Ramakrishna, A review on polymer nanofibers by electrospinning and their applications in nanocomposites, *Compos. Sci. Technol.* 63 (2003) 2223–2253.
  - [27] J.D. Schiffman, C.L. Schauer, A review: Electrospinning of biopolymer nanofibers and their applications, *Polym. Rev.* 48 (2008) 317–352.
  - [28] S.S. Ray, S.S. Chen, C.W. Li, N.C. Nguyen, H.T. Nguyen, A comprehensive review: Electrospinning technique for fabrication and surface modification of membranes for water treatment application, *RSC Adv.* 6 (2016) 85495–85514.
  - [29] E.S. Kim, B. Deng, Fabrication of polyamide thin-film nano-composite (PA-TFN) membrane with hydrophilized ordered mesoporous carbon (H-OMC) for water purifications, *J. Memb. Sci.* 375 (2011) 46–54.
  - [30] D. Hu, Z.L. Xu, C. Chen, Polypiperazine-amide nanofiltration membrane containing silica nanoparticles prepared by interfacial polymerization, *Desalination*. 301 (2012) 75–81.
  - [31] G.S. Lai, W.J. Lau, S.R. Gray, T. Matsuura, R. Jamshidi Gohari, M.N. Subramanian, S.O. Lai, C.S. Ong, A.F. Ismail, D. Emazadah, M. Ghanbari, A practical approach to synthesize polyamide thin film nanocomposite (TFN) membranes with improved



- separation properties for water/wastewater treatment, *J. Mater. Chem. A*. 4 (2016) 4134–4144.
- [32] X. Dong, Q. Zhang, S. Zhang, S. Li, Thin film composite nanofiltration membranes fabricated from quaternized poly(ether ether ketone) with crosslinkable moiety using a benign solvent, *J. Colloid Interface Sci.* 463 (2016) 332–341.
- [33] Z. Zhou, J.Y. Lee, T.S. Chung, Thin film composite forward-osmosis membranes with enhanced internal osmotic pressure for internal concentration polarization reduction, *Chem. Eng. J.* 249 (2014) 236–245.
- [34] Y. Zhang, N.L. Le, T.S. Chung, Y. Wang, Thin-film composite membranes with modified polyvinylidene fluoride substrate for ethanol dehydration via pervaporation, *Chem. Eng. Sci.* 118 (2014) 173–183.
- [35] S.H. Park, S.J. Kwon, M.G. Shin, M.S. Park, J.S. Lee, C.H. Park, H. Park, J.H. Lee, Polyethylene-supported high performance reverse osmosis membranes with enhanced mechanical and chemical durability, *Desalination*. 436 (2018) 28–38.
- [36] Y. Hai, J. Zhang, C. Shi, A. Zhou, C. Bian, W. Li, Thin film composite nanofiltration membrane prepared by the interfacial polymerization of 1,2,4,5-benzene tetracarbonyl chloride on the mixed amines cross-linked poly(ether imide) support, *J. Memb. Sci.* 520 (2016) 19–28.
- [37] J.S. Lee, J.A. Seo, H.H. Lee, S.K. Jeong, H.S. Park, B.R. Min, Simple method for preparing thin film composite polyamide nanofiltration membrane based on hydrophobic polyvinylidene fluoride support membrane, *Thin Solid Films*. 624 (2017) 136–143.
- [38] Y. Ji, W. Qian, Y. Yu, Q. An, L. Liu, Y. Zhou, C. Gao, Recent developments in nanofiltration membranes based on nanomaterials, *Chinese J. Chem. Eng.* 25 (2017) 1639–1652.
- [39] M. Yasukawa, S. Mishima, Y. Tanaka, T. Takahashi, H. Matsuyama, Thin-film composite forward osmosis membrane with high water flux and high pressure resistance using a thicker void-free polyketone porous support, *Desalination*. 402 (2017) 1–9.
- [40] N. Misdan, W.J. Lau, A.F. Ismail, T. Matsuura, Formation of thin film composite nanofiltration membrane: Effect of polysulfone substrate characteristics, *Desalination*. 329 (2013).
- [41] P.S. Singh, S. V. Joshi, J.J. Trivedi, C. V. Devmurari, A.P. Rao, P.K. Ghosh, Probing the structural variations of thin film composite RO membranes obtained by coating polyamide over polysulfone membranes of different pore dimensions, *J. Memb. Sci.* 278 (2006) 19–25.
- [42] A.K. Ghosh, E.M.V. Hoek, Impacts of support membrane structure and chemistry on polyamide-polysulfone interfacial composite membranes, *J. Memb. Sci.* 336 (2009) 140–148.
- [43] Q. Zhang, Z. Zhang, L. Dai, H. Wang, S. Li, S. Zhang, Novel insights into the interplay between support and active layer in the thin film composite polyamide membranes, *J. Memb. Sci.* 537 (2017) 372–383.
- [44] L. Huang, J.R. McCutcheon, Impact of support layer pore size on performance of thin film composite membranes for forward osmosis, *J. Memb. Sci.* 483 (2015) 25–33.
- [45] N. Misdan, W.J. Lau, A.F. Ismail, T. Matsuura, D. Rana, Study on the thin film composite poly(piperazine-amide) nanofiltration membrane: Impacts of physicochemical properties of substrate on interfacial polymerization formation, *Desalination*. 344 (2014).
- [46] M. Chen, C. Xiao, C. Wang, H. Liu, N. Huang, Preparation and characterization of a novel thermally stable thin film composite nanofiltration membrane with poly (m-

- phenyleneisophthalamide) (PMIA) substrate, *J. Memb. Sci.* 550 (2018) 36–44.
- [47] C. Wu, S. Zhang, D. Yang, X. Jian, Preparation, characterization and application of a novel thermal stable composite nanofiltration membrane, *J. Memb. Sci.* 326 (2009) 429–434.
  - [48] J. Wei, X. Jian, C. Wu, S. Zhang, C. Yan, Influence of polymer structure on thermal stability of composite membranes, *J. Memb. Sci.* 256 (2005) 116–121.
  - [49] J.H. Kim, S.J. Moon, S.H. Park, M. Cook, A.G. Livingston, Y.M. Lee, A robust thin film composite membrane incorporating thermally rearranged polymer support for organic solvent nanofiltration and pressure retarded osmosis, *J. Memb. Sci.* 550 (2018) 322–331.
  - [50] G. Szekely, M.F. Jimenez-Solomon, P. Marchetti, J.F. Kim, A.G. Livingston, Sustainability assessment of organic solvent nanofiltration: From fabrication to application, *Green Chem.* 16 (2014) 4440–4473.
  - [51] B. Chu, K. Yoon, B.S. Hsiao, High flux nanofiltration membranes based on interfacially polymerized polyamide barrier layer on polyacrylonitrile nanofibrous scaffolds, *J. Memb. Sci.* 326 (2009) 484–492.
  - [52] X.Y. Chi, P.Y. Zhang, X.J. Guo, Z.L. Xu, A novel TFC forward osmosis (FO) membrane supported by polyimide (PI) microporous nanofiber membrane, *Appl. Surf. Sci.* 427 (2018) 1–9.
  - [53] M.J. Park, R.R. Gonzales, A. Abdel-Wahab, S. Phuntsho, H.K. Shon, Hydrophilic polyvinyl alcohol coating on hydrophobic electrospun nanofiber membrane for high performance thin film composite forward osmosis membrane, *Desalination.* 426 (2018) 50–59.
  - [54] H.Q. Liang, W.S. Hung, H.H. Yu, C.C. Hu, K.R. Lee, J.Y. Lai, Z.K. Xu, Forward osmosis membranes with unprecedented water flux, *J. Memb. Sci.* 529 (2017) 47–54.
  - [55] S. Zhang, P. Sukitpaneenit, T.S. Chung, Design of robust hollow fiber membranes with high power density for osmotic energy production, *Chem. Eng. J.* 241 (2014) 457–465.
  - [56] S.E. Skilhagen, J.E. Dugstad, R.J. Aaberg, Osmotic power - power production based on the osmotic pressure difference between waters with varying salt gradients, *Desalination.* 220 (2008) 476–482.
  - [57] S. Chou, R. Wang, A.G. Fane, Robust and High performance hollow fiber membranes for energy harvesting from salinity gradients by pressure retarded osmosis, *J. Memb. Sci.* 448 (2013) 44–54.
  - [58] S. Chou, L. Shi, R. Wang, C.Y. Tang, C. Qiu, A.G. Fane, Characteristics and potential applications of a novel forward osmosis hollow fiber membrane, *Desalination.* 261 (2010) 365–372.
  - [59] S. Chou, R. Wang, L. Shi, Q. She, C. Tang, A.G. Fane, Thin-film composite hollow fiber membranes for pressure retarded osmosis (PRO) process with high power density, *J. Memb. Sci.* 389 (2012) 25–33.
  - [60] M. Shibuya, M. Yasukawa, S. Mishima, Y. Tanaka, T. Takahashi, H. Matsuyama, A thin-film composite-hollow fiber forward osmosis membrane with a polyketone hollow fiber membrane as a support, *Desalination.* 402 (2017) 33–41.
  - [61] X. Li, T.S. Chung, Thin-film composite P84 co-polyimide hollow fiber membranes for osmotic power generation, *Appl. Energy.* 114 (2014) 600–610.
  - [62] G. Han, T.S. Chung, Robust and high performance pressure retarded osmosis hollow fiber membranes for osmotic power generation, *AIChE J.* 60 (2014) 1107–1119.
  - [63] Z.L. Cheng, X. Li, Y. Feng, C.F. Wan, T.S. Chung, Tuning water content in polymer dopes to boost the performance of outer-selective thin-film composite (TFC) hollow fiber membranes for osmotic power generation, *J. Memb. Sci.* 524 (2017) 97–107.
  - [64] S. Shokrollahzadeh, S. Tajik, Fabrication of thin film composite forward osmosis

- membrane using electrospun polysulfone/polyacrylonitrile blend nanofibers as porous substrate, *Desalination*. 425 (2018) 68–76.
- [65] R.M. Boom, I.M. Wienk, T. van den Boomgaard, C.A. Smolders, Microstructures in phase inversion membranes. Part 2. The role of a polymeric additive, *J. Memb. Sci.* 73 (1992) 277–292.
- [66] S.H. Yoo, J.H. Kim, J.Y. Jho, J. Won, Y.S. Kang, Influence of the addition of PVP on the morphology of asymmetric polyimide phase inversion membranes: Effect of PVP molecular weight, *J. Memb. Sci.* 236 (2004) 203–207.
- [67] M. Fathizadeh, A. Aroujalian, A. Raisi, Effect of lag time in interfacial polymerization on polyamide composite membrane with different hydrophilic sub layers, *Desalination*. 284 (2012) 32–41.
- [68] A. Idris, N.M. Zain, M.Y. Noordin, Synthesis, characterization and performance of asymmetric polyethersulfone (PES) ultrafiltration membranes with polyethylene glycol of different molecular weights as additives, *Desalination*. 207 (2007) 324–339.
- [69] S. Zhu, S. Zhao, Z. Wang, X. Tian, M. Shi, J. Wang, S. Wang, Improved performance of polyamide thin-film composite nanofiltration membrane by using polyethersulfone/polyaniline membrane as the substrate, *J. Memb. Sci.* 493 (2015) 263–274.
- [70] S. Zhao, Z. Wang, X. Wei, B. Zhao, J. Wang, S. Yang, S. Wang, Performance improvement of polysulfone ultrafiltration membrane using well-dispersed polyaniline-poly(vinylpyrrolidone) nanocomposite as the additive, *Ind. Eng. Chem. Res.* 51 (2012) 4661–4672.
- [71] S. Zhao, Z. Wang, J. Wang, S. Wang, Poly(ether sulfone)/polyaniline nanocomposite membranes: Effect of nanofiber size on membrane morphology and properties, *Ind. Eng. Chem. Res.* 53 (2014) 11468–11477.
- [72] M. Peyravi, A. Rahimpour, M. Jahanshahi, Thin film composite membranes with modified polysulfone supports for organic solvent nanofiltration, *J. Memb. Sci.* 423–424 (2012) 225–237.
- [73] X. Zhang, J. Tian, Z. Ren, W. Shi, Z. Zhang, Y. Xu, S. Gao, F. Cui, High performance thin-film composite (TFC) forward osmosis (FO) membrane fabricated on novel hydrophilic disulfonated poly(arylene ether sulfone) multiblock copolymer/polysulfone substrate, *J. Memb. Sci.* 520 (2016) 529–539.
- [74] E.L. Tian, H. Zhou, Y.W. Ren, Z. a. mirza, X.Z. Wang, S.W. Xiong, Novel design of hydrophobic/hydrophilic interpenetrating network composite nanofibers for the support layer of forward osmosis membrane, *Desalination*. 347 (2014) 207–214.
- [75] L. Huang, J.T. Arena, M.T. Meyering, T.J. Hamlin, J.R. McCutcheon, Tailored multi-zoned nylon 6,6 supported thin film composite membranes for pressure retarded osmosis, *Desalination*. 399 (2016) 96–104.
- [76] K.Y. Wang, T.S. Chung, G. Amy, Developing thin-film-composite forward osmosis membranes on the PES/SPSf substrate through interfacial polymerization, *AIChE J.* 58 (2012) 770–781.
- [77] N. Widjojo, T.S. Chung, M. Weber, C. Maletzko, V. Warzelhan, The role of sulphonated polymer and macrovoid-free structure in the support layer for thin-film composite (TFC) forward osmosis (FO) membranes, *J. Memb. Sci.* 383 (2011) 214–223.
- [78] J. Yin, B. Deng, Polymer-matrix nanocomposite membranes for water treatment, 479 (2015) 256–275.
- [79] C.S. Ong, W.J. Lau, P.S. Goh, B.C. Ng, A.F. Ismail, Preparation and characterization of PVDF–PVP–TiO<sub>2</sub> composite hollow fiber membranes for oily wastewater treatment using submerged membrane system, *Desalin. Water Treat.* 53 (2013) 1–11.

- [80] N.A.A. Hamid, A.F. Ismail, T. Matsuura, A.W. Zularisam, W.J. Lau, E. Yuliwati, M.S. Abdullah, Morphological and separation performance study of polysulfone/titanium dioxide (PSF/TiO<sub>2</sub>) ultrafiltration membranes for humic acid removal, *Desalination*. 273 (2011).
- [81] S. Simone, F. Galiano, M. Faccini, M. Boerrigter, C. Chaumette, E. Drioli, A. Figoli, Preparation and Characterization of Polymeric-Hybrid PES/TiO<sub>2</sub> Hollow Fiber Membranes for Potential Applications in Water Treatment, *Fibers*. 5 (2017) 14.
- [82] J. Li, Y. Hu, W. Liu, X. Weng, X. Dong, X. Zhang, W. Zhou, High Flux and Hydrophilic Fibrous Ultrafiltration Membranes Based on Electrospun Titanium Dioxide Nanoparticles/Polyethylene Oxide/Poly(vinylidene fluoride) Composite Scaffolds, *J. Nanosci. Nanotechnol.* 17 (2017) 9042–9049.
- [83] H. Rabiee, M. Farahani, V.V.-J. of M. Science, U. 2014, Preparation and characterization of emulsion poly (vinyl chloride)(EPVC)/TiO<sub>2</sub> nanocomposite ultrafiltration membrane, *J. Memb. Sci.* 472 (2014) 185–193.
- [84] A. Mollahosseini, A. Rahimpour, Interfacially polymerized thin film nanofiltration membranes on TiO<sub>2</sub>coated polysulfone substrate, *J. Ind. Eng. Chem.* 20 (2014) 1261–1268.
- [85] M.T.M. Pendergast, J.M. Nygaard, A.K. Ghosh, E.M.V. Hoek, Using nanocomposite materials technology to understand and control reverse osmosis membrane compaction, *Desalination*. 261 (2010) 255–263.
- [86] D. Emadzadeh, W.J. Lau, T. Matsuura, A.F. Ismail, M. Rahbari-Sisakht, Synthesis and characterization of thin film nanocomposite forward osmosis membrane with hydrophilic nanocomposite support to reduce internal concentration polarization, *J. Memb. Sci.* 449 (2014) 74–85.
- [87] D. Emadzadeh, W.J. Lau, T. Matsuura, N. Hilal, A.F. Ismail, The potential of thin film nanocomposite membrane in reducing organic fouling in forward osmosis process, *Desalination*. 348 (2014).
- [88] D. Emadzadeh, W.J. Lau, M. Rahbari-Sisakht, H. Ilbeygi, D. Rana, T. Matsuura, A.F. Ismail, Synthesis, modification and optimization of titanate nanotubes-polyamide thin film nanocomposite (TFN) membrane for forward osmosis (FO) application, *Chem. Eng. J.* 281 (2015) 243–251.
- [89] M. Jun, S. Phuntsho, T. He, G.M. Nisola, L.D. Tijning, X. Li, G. Chen, W. Chung, H. Kyong, Graphene oxide incorporated polysulfone substrate for the fabrication of flat-sheet thin-film composite forward osmosis membranes, *J. Memb. Sci.* 493 (2015) 496–507.
- [90] S. Lim, M.J. Park, S. Phuntsho, L.D. Tijning, G.M. Nisola, W.G. Shim, W.J. Chung, H.K. Shon, Dual-layered nanocomposite substrate membrane based on polysulfone/graphene oxide for mitigating internal concentration polarization in forward osmosis, *Polymer (Guildf)*. 110 (2017) 36–48.
- [91] T. Sirinupong, W. Youravong, D. Tirawat, W.J. Lau, G.S. Lai, A.F. Ismail, Synthesis and characterization of thin film composite membranes made of PSF-TiO<sub>2</sub>/GO nanocomposite substrate for forward osmosis applications, *Arab. J. Chem.* (2017).
- [92] F. Li, Y. Qu, M. Zhao, Efficient helium separation of graphitic carbon nitride membrane, *Carbon N. Y.* 95 (2015) 51–57.
- [93] M. Rastgar, A. Shakeri, A. Bozorg, H. Salehi, V. Saadattalab, Impact of nanoparticles surface characteristics on pore structure and performance of forward osmosis membranes, *Desalination*. 421 (2017) 179–189.
- [94] X. Liu, H.Y. Ng, Fabrication of layered silica-polysulfone mixed matrix substrate membrane for enhancing performance of thin-film composite forward osmosis membrane, *J. Memb. Sci.* 481 (2015) 148–163.

- [95] P. Lu, S. Liang, L. Qiu, Y. Gao, Q. Wang, Thin film nanocomposite forward osmosis membranes based on layered double hydroxide nanoparticles blended substrates, *J. Memb. Sci.* 504 (2016) 196–205.
- [96] P.M. Pardeshi, A.K. Mungray, A.A. Mungray, Polyvinyl chloride and layered double hydroxide composite as a novel substrate material for the forward osmosis membrane, *Desalination*. 421 (2017) 149–159.
- [97] M. Tian, Y.N. Wang, R. Wang, A.G. Fane, Synthesis and characterization of thin film nanocomposite forward osmosis membranes supported by silica nanoparticle incorporated nanofibrous substrate, *Desalination*. 401 (2017) 142–150.
- [98] C. Zhang, M. Huang, L. Meng, B. Li, T. Cai, Electrospun polysulfone (PSf)/titanium dioxide (TiO<sub>2</sub>) nanocomposite fibers as substrates to prepare thin film forward osmosis membranes, *J. Chem. Technol. Biotechnol.* 92 (2017) 2090–2097.
- [99] M.T.M. Pendergast, A.K. Ghosh, E.M.V. Hoek, Separation performance and interfacial properties of nanocomposite reverse osmosis membranes, *Desalination*. 308 (2013) 180–185.
- [100] M. Son, H. gyu Choi, L. Liu, E. Celik, H. Park, H. Choi, Efficacy of carbon nanotube positioning in the polyethersulfone support layer on the performance of thin-film composite membrane for desalination, *Chem. Eng. J.* 266 (2015) 376–384.
- [101] E.S. Kim, G. Hwang, M. Gamal El-Din, Y. Liu, Development of nanosilver and multi-walled carbon nanotubes thin-film nanocomposite membrane for enhanced water treatment, *J. Memb. Sci.* 394–395 (2012) 37–48.
- [102] M. Tian, R. Wang, K. Goh, Y. Liao, A.G. Fane, Synthesis and characterization of high-performance novel thin film nanocomposite PRO membranes with tiered nanofiber support reinforced by functionalized carbon nanotubes, *J. Memb. Sci.* 486 (2015) 151–160.
- [103] N.N. Bui, J.R. McCutcheon, Nanoparticle-embedded nanofibers in highly permselective thin-film nanocomposite membranes for forward osmosis, *J. Memb. Sci.* 518 (2016) 338–346.
- [104] N. Ma, J. Wei, S. Qi, Y. Zhao, Y. Gao, C.Y. Tang, Nanocomposite substrates for controlling internal concentration polarization in forward osmosis membranes, *J. Memb. Sci.* 441 (2013) 54–62.
- [105] M. Ghanbari, D. Emadzadeh, W.J. Lau, H. Riazi, D. Almasi, A.F. Ismail, Minimizing structural parameter of thin film composite forward osmosis membranes using polysulfone/halloysite nanotubes as membrane substrates, *Desalination*. 377 (2016).
- [106] Y.H. Pan, Q.Y. Zhao, L. Gu, Q.Y. Wu, Thin film nanocomposite membranes based on imolomite nanotubes blended substrates for forward osmosis desalination, *Desalination*. 421 (2017) 160–168.
- [107] Y. Wang, R. Ou, Q. Ge, H. Wang, T. Xu, Preparation of polyethersulfone/carbon nanotube substrate for high-performance forward osmosis membrane, *Desalination*. 330 (2013) 70–78.
- [108] W.J. Lau, C.S. Ong, N.A.H. Nordin, N.A.A. Sani, N.M. Mokhtar, R.J. Gohari, D. Emadzadeh, A.F. Ismail, Surface Modification of Polymeric Membranes of Various Separation Processes, *Surf. Treat. Biol. Chem. Phys. Appl.* (2017) 115–180.
- [109] X. Zhang, Y. Lv, H.C. Yang, Y. Du, Z.K. Xu, Polyphenol coating as an interlayer for thin-film composite membranes with enhanced nanofiltration performance, *ACS Appl. Mater. Interfaces*. 8 (2016) 32512–32519.
- [110] J.J. Wang, H.C. Yang, M.B. Wu, X. Zhang, Z.K. Xu, Nanofiltration membranes with cellulose nanocrystals as an interlayer for unprecedented performance, *J. Mater. Chem. A*. 5 (2017) 16289–16295.
- [111] G. Han, S. Zhang, X. Li, N. Widjojo, T.S. Chung, Thin film composite forward

- osmosis membranes based on polydopamine modified polysulfone substrates with enhancements in both water flux and salt rejection, *Chem. Eng. Sci.* 80 (2012) 219–231.
- [112] Y. Li, Y. Su, J. Li, X. Zhao, R. Zhang, X. Fan, J. Zhu, Y. Ma, Y. Liu, Z. Jiang, Preparation of thin film composite nanofiltration membrane with improved structural stability through the mediation of polydopamine, *J. Memb. Sci.* 476 (2015) 10–19.
  - [113] J. Zhu, S. Yuan, A. Uliana, J. Hou, J. Li, X. Li, M. Tian, Y. Chen, A. Volodin, B. Van der Bruggen, High-flux thin film composite membranes for nanofiltration mediated by a rapid co-deposition of polydopamine/piperazine, *J. Memb. Sci.* 554 (2018) 97–108.
  - [114] K.Y. Wang, R.C. Ong, T.S. Chung, Double-skinned forward osmosis membranes for reducing internal concentration polarization within the porous sublayer, *Ind. Eng. Chem. Res.* 49 (2010) 4824–4831.
  - [115] W.A. Suwaileh, D.J. Johnson, S. Sarp, N. Hilal, Advances in forward osmosis membranes: Altering the sub-layer structure via recent fabrication and chemical modification approaches, *Desalination*. 436 (2018) 176–201.
  - [116] A. Saraf, K. Johnson, M.L. Lind, Poly(vinyl) alcohol coating of the support layer of reverse osmosis membranes to enhance performance in forward osmosis, *Desalination*. 333 (2014) 1–9.
  - [117] H.H.P. Duong, T. Chung, Highly Permeable Double-skinned Forward Osmosis Membrane for Anti-fouling in the Emulsified Oil-water Separation Process, *Environ. Sci. Technol.* 48 (2015) 0–14.
  - [118] C.S. Ong, B. Al-Anzi, W.J. Lau, P.S. Goh, G.S. Lai, A.F. Ismail, Y.S. Ong, Anti-Fouling Double-Skinned Forward Osmosis Membrane with Zwitterionic Brush for Oily Wastewater Treatment, *Sci. Rep.* 7 (2017) 1–11.
  - [119] X. Liu, S.L. Ong, H.Y. Ng, Fabrication of mesh-embedded double-skinned substrate membrane and enhancement of its surface hydrophilicity to improve anti-fouling performance of resultant thin-film composite forward osmosis membrane, *J. Memb. Sci.* 511 (2016) 40–53.
  - [120] W. Fang, C. Liu, L. Shi, R. Wang, Composite forward osmosis hollow fiber membranes: Integration of RO- and NF-like selective layers for enhanced organic fouling resistance, *J. Memb. Sci.* 492 (2015) 147–155.
  - [121] D. Zhao, G. Qiu, X. Li, C. Wan, K. Lu, T.S. Chung, Zwitterions coated hollow fiber membranes with enhanced antifouling properties for osmotic power generation from municipal wastewater, *Water Res.* 104 (2016) 389–396.
  - [122] T. Cai, X. Li, C. Wan, T.S. Chung, Zwitterionic polymers grafted poly(ether sulfone) hollow fiber membranes and their antifouling behaviors for osmotic power generation, *J. Memb. Sci.* 497 (2016) 142–152.
  - [123] P.W. Morgan, S.L. Kwolek, Interfacial polycondensation. II. Fundamentals of polymer formation at liquid interfaces, *J. Polym. Sci.* 40 (1959) 299–327.
  - [124] J.E. Cadotte, R.S. King, R.J. Majerle, R.J. Petersen, Interfacial Synthesis in the Preparation of Reverse Osmosis Membranes, *J. Macromol. Sci. Part A - Chem.* 15 (1981) 727–755.
  - [125] S. Karan, Z. Jiang, A.G. Livingston, Sub-10 nm polyamide nanofilms with ultrafast solvent transport for molecular separation, *Science* (80-. ). 348 (2015) 1347–1351.
  - [126] C. Wu, S. Liu, Z. Wang, J. Zhang, X. Wang, X. Lu, Y. Jia, W.S. Hung, K.R. Lee, Nanofiltration membranes with dually charged composite layer exhibiting super-high multivalent-salt rejection, *J. Memb. Sci.* 517 (2016) 64–72.
  - [127] Y. Zhu, W. Xie, S. Gao, F. Zhang, W. Zhang, Z. Liu, J. Jin, Single-Walled Carbon Nanotube Film Supported Nanofiltration Membrane with a Nearly 10 nm Thick Polyamide Selective Layer for High-Flux and High-Rejection Desalination, *Small*. 12



- (2016) 5034–5041.
- [128] X. Yang, Y. Du, X. Zhang, A. He, Z.K. Xu, Nanofiltration Membrane with a Mussel-Inspired Interlayer for Improved Permeation Performance, *Langmuir*. 33 (2017) 2318–2324.
  - [129] Z. Yang, Z.W. Zhou, H. Guo, Z. Yao, X.H. Ma, X. Song, S.P. Feng, C.Y. Tang, Tannic Acid/Fe<sup>3+</sup>+Nanoscaffold for Interfacial Polymerization: Toward Enhanced Nanofiltration Performance, *Environ. Sci. Technol.* 52 (2018) 9341–9349.
  - [130] Q. Liu, J. Li, Z. Zhou, J. Xie, J.Y. Lee, Hydrophilic Mineral Coating of Membrane Substrate for Reducing Internal Concentration Polarization (ICP) in Forward Osmosis, *Sci. Rep.* 6 (2016) 19593.
  - [131] Q. Liu, J. Li, Z. Zhou, G. Qiu, J. Xie, J.Y. Lee, Dual-Functional Coating of Forward Osmosis Membranes for Hydrophilization and Antimicrobial Resistance, *Adv. Mater. Interfaces*. 3 (2016) 1–8.
  - [132] H. Il Kim, S.S. Kim, Fabrication of reverse osmosis membrane via low temperature plasma polymerization, *J. Memb. Sci.* 190 (2001) 21–33.
  - [133] H. Il Kim, S.S. Kim, Plasma treatment of polypropylene and polysulfone supports for thin film composite reverse osmosis membrane, *J. Memb. Sci.* 286 (2006) 193–201.
  - [134] E.S. Kim, Y.J. Kim, Q. Yu, B. Deng, Preparation and characterization of polyamide thin-film composite (TFC) membranes on plasma-modified polyvinylidene fluoride (PVDF), *J. Memb. Sci.* 344 (2009) 71–81.
  - [135] A.P. Korikov, P.B. Kosaraju, K.K. Sirkar, Interfacially polymerized hydrophilic microporous thin film composite membranes on porous polypropylene hollow fibers and flat films, *J. Memb. Sci.* 279 (2006) 588–600.
  - [136] N. Oh, J. Jegal, K. Lee, Preparation and Characterization of Nanofiltration Composite Membranes Using Polyacrylonitrile ( PAN ). I . Preparation and Modification of PAN Supports, *J. Appl. Polym. Sci.* 80 (2001) 1854–1862.
  - [137] L. Pérez-Manríquez, J. Aburabi'e, P. Neelakanda, K.-V. Peinemann, Cross-linked PAN-based thin-film composite membranes for non-aqueous nanofiltration, *React. Funct. Polym.* 86 (2015) 243–247.
  - [138] L. Pérez-Manríquez, P. Neelakanda, K.V. Peinemann, Tannin-based thin-film composite membranes for solvent nanofiltration, *J. Memb. Sci.* 541 (2017) 137–142.
  - [139] S.H. Maruf, A.R. Greenberg, J. Pellegrino, Y. Ding, Fabrication and characterization of a surface-patterned thin film composite membrane, *J. Memb. Sci.* 452 (2014) 11–19.
  - [140] S.H. Maruf, A.R. Greenberg, Y. Ding, Influence of substrate processing and interfacial polymerization conditions on the surface topography and permselective properties of surface-patterned thin-film composite membranes, *J. Memb. Sci.* 512 (2016) 50–60.
  - [141] I.M.A. ElSherbiny, A.S.G. Khalil, M. Ulbricht, Surface micro-patterning as a promising platform towards novel polyamide thin-film composite membranes of superior performance, *J. Memb. Sci.* 529 (2017) 11–22.
  - [142] M. Rickman, S. Maruf, E. Kujundzic, R.H. Davis, A. Greenberg, Y. Ding, J. Pellegrino, Fractionation and flux decline studies of surface-patterned nanofiltration membranes using NaCl-glycerol-BSA solutions, *J. Memb. Sci.* 527 (2017) 102–110.
  - [143] M. Tian, C. Qiu, Y. Liao, S. Chou, R. Wang, Preparation of polyamide thin film composite forward osmosis membranes using electrospun polyvinylidene fluoride (PVDF) nanofibers as substrates, *Sep. Purif. Technol.* 118 (2013) 727–736.
  - [144] M. Son, J. Bae, H. Park, H. Choi, Continuous thermal-rolling of electrospun nanofiber for polyamide layer deposition and its detection by engineered osmosis, *Polymer (Guildf)*. 145 (2018) 281–285.